The effect of glucagon-like peptide-1 (GLP-1) receptor agonists on cell viability, ADAM10 maturation and the proteolysis of ADAM10 substrates in SH-SY5Y cells.

Sophie Marie Holmes BSc

Supervisor: Dr. Edward Parkin

This thesis is submitted in fulfilment of the degree of MSc (Research) Biomedical Science.

The work in this thesis is entirely my own, and has not been submitted in any form for the award of a higher degree at any other institution.

March 2018

Abstract

Arguably the causative agent of Alzheimer's disease (AD), amyloid beta (Aβ)-peptides, are generated by sequential proteolysis of the amyloid precursor protein (APP) by β– and γ–secretase activities. Alternatively, APP can be processed non-amyloidogenically by an α-secretase activity that cleaves within the Aβ-domain, precluding the formation of intact Aβ-peptides and liberating a neuroprotective fragment, sAPPα. This latter proteolytic event is catalysed by a disintegrin and metalloproteinase (ADAM) 10.

Recent research has suggested that glucagon-like peptide-1 (GLP-1) analogues; Lixisenatide, Dulaglutide, Liraglutide, and Exenatide (Exendin-4), currently used to treat diabetes, may also be beneficial in the treatment of neurodegenerative conditions such as AD, as they have been shown to exert neuroprotective properties. Research has also suggested that one of these compounds, exendin-4, can enhance the amount of membrane-associated ADAM10.

The current study, therefore, aims to determine firstly; whether GLP-1 analogues can protect neuroblastoma, SH-SY5Y cells, against chemical stressors of relevance to AD and, secondly, whether these compounds alter ADAM10 maturation/activity and the proteolysis of the enzyme's substrates, APP, prion protein (PrP) and neuroligin1 (NLGN-1). Cells treated with hydrogen peroxide (as an oxidative stressor), cobalt chloride (as a hypoxic mimic), methylglyoxal (MG) or thapsigargin (TG) (as Endoplasmic Reticulum stressors) were co-treated with or without GLP-1 analogues and cell viability was subsequently monitored along with the expression and proteolysis of ADAM10 and its substrates. The results of the study showed that the GLP-1 analogue, liraglutide, had no major effect in terms of protecting SH-SY5Y cells against any of the afore-mentioned chemical stressors. However, a second compound, exendin-4, was protective against TG-induced cytotoxicity. Thapsigargin impaired the proteolytic maturation of ADAM10 suggesting a decrease in the activity of the enzyme but exendin-4 was unable to reverse this effect. Nonetheless, exendin-4 was able to partly reverse the inhibitory effect of TG on the expression of endogenous APP, and shedding of over-expressed NLGN1, and sAPPα in cells over-expressing APP_{695}. Interestingly, TG caused an increase in expression of $APP_{695,}$ and an intracellular accumulation of PrP and, subsequently, did not alter the cell surface ADAM-mediated shedding of this protein.

Collectively, these data indicate that liraglutide was ineffective in the protection of SH-SY5Y cells against the chemical stressors employed. However, exendin-4, is mildly protective against thapsigargin-mediated oxidative stress and is able to partly restore the TG-induced decrease in expression of endogenous APP, and

shedding of APP_{695} and NLGN1. Unusually though, this latter effect was not associated with restored proteolytic maturation of ADAM10.

Key words: Exendin-4, ADAM-10, Thapsigargin, APP, PrP, NLGN-1, Alzheimer's disease.

Abbreviations:

Aβ – Amyloid Beta

ACh - Acetylcholine

AD – Alzheimer's Disease

AICD – APP Intracellular Domain

APP – Amyloid Precursor Protein

ADAM10 – A Disintegrin And Metalloproteinase 10

BACE1 – β-site amyloid precursor protein cleaving enzyme 1

ChAT – Choline Acetyltransferase

$CoCl_2$ – Cobalt Chloride

ER – Endoplasmic Reticulum

GLP-1 – Glucagon-Like Peptide-1

H_2O_2 – Hydrogen Peroxide

IDE – Insulin Degrading Enzyme

MG – Methylglyoxal

NFTs – Neurofibrillary tangles

NLGN1 – Neuroligin-1

NMDA – N-Methyl-D-Aspartate

OS – Oxidative Stress

PHFs – Paired Helical Filaments

PrP – Prion Protein

PS1/PS2 – Presenilin-1/Presenilin-2

sAPPα - soluble APP alpha

sAPPβ – soluble APP beta

TG – Thapsigargin

TSEs – Transmissible Spongiform Encephalopathies

Acknowledgements.

I would firstly like to thank my thesis supervisor Dr. Edward Parkin of Lancaster University, for providing invaluable knowledge and continuous motivation throughout my research and thesis writing. Dr. Parkin always made himself available whenever I had a question or just needed some support, and for this I am extremely grateful.

I would also like to acknowledge Professor David Allsop and Professor Patrick Kehoe as the readers of this thesis, and I am sincerely thankful to them for their valuable comments.

Finally, I must express my heartfelt thanks to my family and to my partner, as without their continued support and encouragement, this accomplishment would have been near impossible.

Thank you.

Contents:

Chapter 1: Literature review.

1.1. Introduction.

The purpose of the current study was to characterise the neuroprotective effects of a group of diabetes drugs, known as glucagon-like peptide-1 (GLP-1) analogues, against stress-inducing agents relevant to the neurodegenerative condition, Alzheimer's disease (AD). In addition, the study attempted to determine whether GLP-1 analogues might exert their cytoprotective effects by altering the processing of substrates of the enzyme, a disintegrin and metalloprotease 10 (ADAM10), particularly the amyloid precursor protein (APP), which has direct relevance to the pathogenesis of AD.

1.2. Alzheimer's disease.

Dementia is a term used to describe a set of symptoms associated with cognitive impairment and degeneration of the brain (nhs.uk, 2018). Alzheimer's disease was first described in 1906, by Alois Alzheimer. It is the most common cause of dementia and can be a consequence of brain tissue atrophy causing symptoms such as memory loss, speech impairment and aggression (nhs.uk, 2018) AD is a progressive degenerative disease, meaning symptoms worsen over time with no prospect of reversal, dictating a poor prognosis for AD patients.

1.2.1. Onset of Alzheimer's Disease.

Depending on the age of the patient at the time of onset, AD can be classified into two categories; sporadic and familial (SAD and FAD). Sporadic AD tends to occur over the age of 60-65 years and is caused by a combination of environmental and genetic risk factors. Whilst SAD represents some 95% of all cases (Bali et al., 2012), FAD constitutes only 5% of cases and is directly linked to the inheritance of genetic mutations.

1.2.2. Epidemiology.

Dementia affects approximately 5% of the global population and has been recognised by the World Health Organisation (WHO) as a public health priority (World Health Organization, 2016). The WHO estimated that 60-70% of all dementia cases could be caused by Alzheimer's disease. The region with the highest absolute number of dementia sufferers is Asia but the regions with the highest disease prevalence are the Americas and Europe, with 6.4% and 5.9% prevalence, respectively (Prince *et al.*, 2015; Table 1.1.). However, the same report shows that the projected number of cases in Europe by 2050 increases at a lower rate than in other regions, with numbers in Africa estimated to rise by around 300%. This is most likely the result of anticipated economic growth and improved healthcare in developing countries leading to a higher life expectancy and an associated increase in the prevalence of dementia in this more aged population. The study also predicts that there will be 9.9 million new cases of dementia per year, which equates to the development of a new case every 3.2 seconds. The WHO lists Alzheimer's disease and other similar dementias, collectively, as the seventh leading cause of death in upper-middle income economies (19.5% of total deaths) and the third leading cause of death in high income economies (60.1% of total deaths) in 2015 (World Health Organization, 2015).

Table 1.1. The number and prevalence of dementia cases and predicted increases in case numbers in different regions of the world. Data adapted from source (Prince *et al.,* 2015).

World Region	Population of over 60's (millions)	Crude estimated prevalence (%)	Number of people with Dementia (millions)			Proportionate increases (%)	
			2015	2030	2050	2015-2030	2015-2050
ASIA	485.83	4.7	22.85	38.53	67.18	69.00	194.00
EUROPE	176.61	5.9	10.46	13.42	18.66	28.00	78.00
AMERICAS	147.51	6.4	9.44	15.75	29.86	67.00	216.00
AFRICA	87.19	4.6	4.03	6.99	15.76	74.00	291.00
WORLD	897.14	5.2	46.78	74.69	131.45	60.00	181.00

A report from the Alzheimer's Association claimed that there are approximately 476,000 new cases of the disease per year. It stated that roughly 1 in 9 people aged over 65 and 1 in 3 people over 85 years old have AD, and that two thirds of the people with the condition in America are women (Alzheimer's Association, 2016).

Further studies have suggested that the number of dementia cases can also differ between ethnicities. Meyeda *et al*. (2016) reported that the incidence of dementia in America was highest in African Americans and Native Americans with Latinos, Pacific Islanders and Whites having a mid-range incidence and Asian-Americans displaying the lowest incidence. The results suggested that African Americans were the most at risk of developing Dementia in the next 25 years, with a cumulative incidence of 38%.

1.2.3. Current treatments.

There are currently four main drug treatments for AD available commercially; donepezil, galantamine, rivastigmine, and memantine. The first three drugs are acetylcholinesterase inhibitors and work by reducing the amount of acetylcholine degradation by acetylcholinesterase. The fourth is an N-methyl-D-aspartate (NMDA) receptor antagonist that targets glutamatergic transmission and, consequently, the exposure of cells to calcium (Alzheimer's Association, 2017). However, all of these treatments are only able to alleviate the symptoms of the disease; they cannot cure or prevent its onset. Drugs and therapies that could potentially do this are known as 'disease-modifying' as they aim to either stop or alter the progression (Yiannopoulou & Papageorgiou, 2012). Many of these drugs are currently in clinical trials and target proposed earlier stages of the disease, such as the formation of neurofibrillary tangles and the generation of amyloid-beta (Aβ) peptides. Various other therapies have also been tested including vaccinations, and drugs targeting risk factors such as high cholesterol (Yiannopoulou & Papageorgiou, 2012).

1.2.4. Aetiology.

Currently, there is no cure for AD, mainly due to the large amount of uncertainty and ambiguity regarding the cause of the disease. A common theory is that AD is a multifactorial disease and can have a plethora of causations. There are many hypotheses associated with this disease, including but not limited to; inflammatory, mitochondrial, vascular, oxidative stress, and cholesterol (Mohandas, Rajmohan and Raghunath, 2009). However, arguably the three best known hypotheses for the causation of AD are outlined in the next section of this study.

1.3. Biochemical causation of Alzheimer's Disease.

1.3.1. The cholinergic hypothesis.

The cholinergic hypothesis as a potential cause of AD was first introduced by Bowen *et al.* (1976) and is the oldest theory. It suggests that a reduction in choline acetyltransferase (ChAT) activity (the enzyme responsible for combining acetyl-CoA and choline) leads to decreased production of acetylcholine (ACh), which consequently results in a reduction of neurotransmission between neurons. Brown *et al.* (1977) demonstrated a decrease in ChAT in approximately 66% of autopsy and biopsy cortical specimens from AD sufferers. The resultant lack of cholinergic signalling is thought to have an effect on the rapid decline of cognitive ability in AD patients. However this theory has been challenged as it has been suggested that a decline in cholinergic activity in the cortex can be caused by ageing (Smith *et al*., 1999) and therefore does not necessarily indicate the onset of AD. In addition, reduced levels of cholinergic molecules are evident in other neurodegenerative diseases such as Parkinson's disease (Perry et al., 1985). Furthermore, it has been shown that ChAT seems only to be reduced in later stages of the disease (Davis et al., 1999), and so is not a useful biomarker for AD.

1.3.2. The neurofibrillary tangle (Tau) hypothesis.

Microtubules play an integral role in the stability of neuronal structure and are particularly significant in axonal and dendritic development in addition to being a key component in molecular transportation and signalling (Baas et al., 2016). Microtubules consist of two isoforms of tubulin, α and β tubulin, that are coupled together to form heterodimers which, in turn, combine to form protofilaments. The latter then combine to form the mature microtubules. Conformational stability of microtubules is maintained through the association of phosphorylated Tau protein binding with tubulin. Tau has six isoforms, all of which are found in the adult brain (Goedert et al., 1989). In Alzheimer's disease and other tauopathies, Tau becomes hyperphosphorylated resulting in the aggregation of Tau monomers to form paired helical filaments (PHFs) (Grundke-Iqbal et al., 1986). In healthy adult brain, approximately 5% of Tau is phosphorylated; this figure rises to 100% of the protein in PHFs (Weidner et al., 2009). The accumulation of PHFs eventually creates neurofibrillary tangles (NFTs); insoluble structures commonly found in the brains of AD patients (Kosik, Joachim and Selkoe, 1986). The formation of NFTs has a detrimental effect on the structure of microtubules and, consequently, on neuronal development and signalling (Alonso et al., 1994). In particular, impaired calcium signalling, often mediated by NFTs, is believed to be related to the short term memory loss characteristic of AD (Green, Smith, and Laferla F., 2007).

1.3.3. The amyloid cascade hypothesis.

Arguably the most well-known theory as to the biochemical causation of AD is based around the proteolysis of the amyloid precursor protein (APP) and the subsequent aggregation of amyloid-beta (Aβ)-peptides in the brain. Furthermore, it is possible that Aβ-peptide accumulation links the three main causation hypotheses, with suggestions that Aβ-peptide accumulation reduces choline uptake and ACh release (Francis *et al*., 1999) and also interferes with the phosphorylation of Tau (Stoothoff & Johnson, 2005). As such, the amyloid cascade hypothesis suggests that the altered proteolysis of APP could be the origin of AD, with a subsequent cascade

of events including the formation of NFTs and reduced neurotransmission resulting in the onset of AD.

1.4. Amyloid precursor protein.

The amyloid precursor protein (APP) is a Type I membrane protein that is coded for by the APP gene located on chromosome 21 in humans (Omim.org, 2017). APP contains 19 exons (Yoshikai *et al*., 1991) and alternate splicing produces various isoforms of the APP protein. There are three main isoforms, APP_{695}, APP_{751}, and APP_{770}. APP_{695} is the most abundant isoform in the brain (Zheng & Koo, 2011) with the three isoforms being present at a ratio of 20:10:1, respectively, in the brain cortex (Nalivaeva & Turner, 2013). As a result of alternate splicing, APP_{751} contains an extra domain known as the Kunitz-type protease inhibitor (KPI) domain and APP_{770} contains both the KPI domain and an OX-2 domain whereas APP_{695} contains neither of these two domains.

The APP protein comprises of a large extracellular region, a short membrane-spanning region and a cytoplasmic domain (Fig. 1.1.). The extracellular region contains the E1 and E2 domains, the former of which can be subdivided into a growth factor-like domain (GFLD) and a copper binding domain (CuBD). C-terminal to the CuBD are the extension domain (ED) and an acidic domain (AcD) the latter of which is made up of 56% acidic amino acids (Coburger *et al.,* 2013). The E2 domain, also known as the central APP domain (CAPPD), contains the RERMS sequence thought to have a role in mediating the trophic properties of APP (Reinhard *et al*., 2005). The juxtamembrane region (JMR) connects the E2 domain to the transmembrane helix located in the plasma membrane which, in turn, links the extracellular region to the APP intracellular domain (AICD).

APP is post-translationally subject to N-glycosylation, O-glycosylation and sialylation in the Golgi (Schedin-Weiss *et al*., 2013). The majority of APP degradation

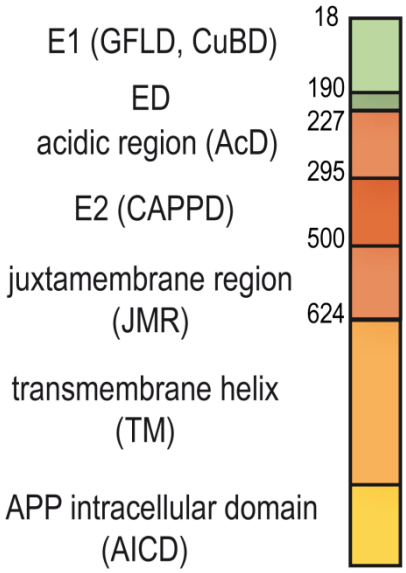

Figure 1.1. The structure of amyloid precursor protein (Coburger *et al*., 2013).

occurs in lysosomes due to a YENPTY sequence in the AICD, which-+ encodes a signal promoting endocytosis (El Ayadi *et al*., 2012). The remaining APP is subject to proteolysis by α, β, and γ-secretases (section 1.5.).

Although APP is ubiquitously expressed in the human body, it is particularly abundant in the brain. Whilst the exact physiological function of the protein remains unclear, APP could play a role as a cell surface receptor, displaying similarities to Notch (Zheng & Koo, 2011) or in the regulation of cell adhesion (Reinhard *et al*., 2005). Specific APP domains have also been associated with neurotrophic and synaptotrophic properties (Thinakaran & Koo, 2008).

1.5. APP proteolysis.

As previously mentioned, full-length APP can be subject to proteolytic processing by α-, β- and γ-secretases and the secretases by which the protein is

processed determine whether the toxic Aβ-peptides associated with AD causation are formed.

1.5.1. The amyloidogenic pathway.

The cleavage of full-length APP by the β- and a γ-secretases constitutes the amyloidogenic proteolytic pathway. The β-secretase, BACE1 (β-site amyloid precursor protein cleaving enzyme 1), is a type-I integral membrane glycoprotein (Venugopal *et al.*, 2008) that is synthesised in the endoplasmic reticulum (ER) and matures into an active enzyme through the Golgi (Chow *et al*., 2009). The enzyme cleaves full-length APP into two fragments; soluble APPbeta (sAPPβ) and a membrane-associated C-terminal fragment (C99) (Fig. 1.2.). Several studies have suggested possible cellular locations for this cleavage, with evidence of some processing occurring at the cell surface (Chyung & Selkoe, 2003). However, the consensus is that BACE1 has a preference for an acidic environment and that cleavage occurs following re-internalisation into endosomal compartments (Venugopal *et al*., 2008). The biological function of the sAPPβ fragment generated is not clear, although it is has been suggested that it may boast some neurotrophic properties (Chasseigneaux et al., 2011).

γ-secretase is a multi-protein complex consisting of presenilins (presenilin-1 (PS1) or presenilin-2 (PS2)), nicastrin, anterior pharynx defective 1 (APH-1), and presenilin enhancer 2 (PEN-2) (Chow *et al*., 2009). The proteolytic ability of this secretase derives from the aspartyl proteinase activity of the presenilins, with PS1 being the predominant form in brain (Duarte et al., 2013). The complex cleaves the C99 fragment within its intra-membrane domain producing the APP intracellular domain (AICD) and Aβ–peptides (Fig. 1.2.). Various lengths of Aβ-peptides can be formed as a consequence of the relaxed specificity of the γ-secretase complex, ranging from 38-43 amino acids (Chow *et al.*, 2009). $A\beta_{1-42}$ is regarded as the most neurotoxic form and, whilst both $A\beta_{1-40}$ and $A\beta_{1-42}$ spontaneously aggregate, the

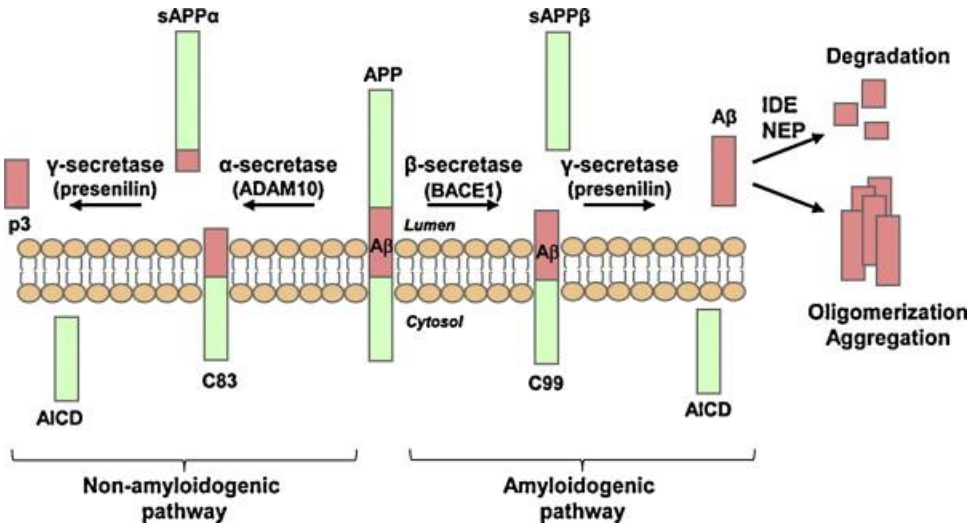

Figure 1.2. The proteolysis of amyloid precursor protein via the amyloidogenic and non-amyloidogenic pathways (Salminen *et al*., 2013).

latter has a higher affinity for self-association and a faster rate of aggregation and is consequently more pathogenic (Hampel *et al*., 2010).

Aβ-peptides can undergo degradation by various proteases including insulin degrading enzyme (IDE) and neprilysin (NEP) (Dorfman *et al*., 2010). However, they may also aggregate to form toxic oligomers, which then further aggregate to produce protofibrils, fibrils and, ultimately, Aβ (senile) plaques. Once aggregated, little or no degradation of Aβ-peptides can occur (Lajtha and Banik, 2011), resulting in the obstruction of nerve signals and, ultimately, the neuronal death observed in AD.

1.5.2. The non-amyloidogenic pathway.

Cleavage of APP by α- and γ-secretases constitutes the non-amyloidogenic proteolytic pathway that accounts for 90% of the APP processing in healthy adult brains (Plácido et al., 2014). During this process, full-length APP is cleaved by α-secretase between lys16 and leu17 of the Aβ region to produce soluble APP alpha (sAPPα) and C83 (Fig. 1.2). The latter fragment is then further cleaved by γ-secretase creating two products; AICD and p3. The majority of APP that reaches the plasma

membrane is processed non-amyloidogenically with only that re-internalised into endosomes being subsequently cleaved by β-secretase (Chow *et al*., 2009). However, it has also been suggested that α-secretase cleavage can occur within intracellular structures such as the Golgi where it could potentially compete with β-secretase activity (Skovronsky *et al*., 2000).

The fact that non-amyloidogenic processing precludes the formation of intact Aβ-peptides has made the up-regulation of this pathway an attractive target as a therapy for AD (Lichtenthaler, 2010). Another benefit of the pathway is that the sAPPα generated by α-secretase has several important roles. Specifically in the brain, there is evidence that sAPPα plays a role in neuritogenesis in chicks and mice, with the RERMS region believed to be involved in this function (Chasseigneaux & Allinquant, 2012). Furthermore, the fragment has been shown to increase the effect of growth factors on the number of adult neuroblasts (Caille´ *et al*., 2004) and to promote the proliferation of neuronal embryonic stem cells (Hayashi *et al*., 1994). In addition, sAPPα has been shown to have a role in repairing neuronal damage in APP knock-out mice helping to enhance spatial learning and long term potentiation (LTP) (Ring *et al*., 2007). Finally, sAPPα has been shown to be protective against neurotoxicity caused by glutamate, glucose deprivation, and oxidative stress induced by Aβ (Chasseigneaux & Allinquant, 2012).

The majority of α-secretase activity is associated with a family of proteolytic enzymes known as a disintegrin and metalloproteinases (ADAMs). Although a number of ADAMs have been shown to possess α-secretase-like activity *in vitro* (Gough, Parr-Sturgess and Parkin, 2011), ADAM10 is thought to be the major physiological α-secretase (Postina *et al*., 2004). The enzyme is a type-I transmembrane glycoprotein and consists of 748 amino acids in its immature form (Tousseyn *et al*., 2006). Its role is specifically as a protease rather than in cell adhesion as is the case for some members of the ADAM family (Tousseyn *et al*., 2006). The ADAMs have a common modular domain structure and the ectodomain of ADAM10 specifically consists of a 19 amino acid N-terminal signal peptide followed by a prodomain, a zinc-binding metalloproteinase domain, a disintegrin domain, and

a cysteine-rich region (Tousseyn *et al*., 2006). However, ADAM10 differs slightly from other members of the ADAM family in that it lacks an epidermal growth factor-like domain (Lichtenthaler, 2010). At the C-terminal end of the ectodomain is a transmembrane (TM) domain and, finally, a cytoplasmic region. The prodomain of ADAM10 is removed by the action of proprotein convertases (furin and PC7) in the Golgi to form the catalytically active form of the enzyme (Lichtenthaler, 2010).

1.6. ADAM10 substrates.

ADAM10 has over forty different transmembrane substrates (Noy *et al*., 2015) many of which are of direct relevance to normal brain function or disease. However, in addition to APP, the shedding of two additional substrates will be examined in the current study; neuroligin-1 and the prion protein.

1.6.1. Neuroligin-1.

Neuroligin-1 (NLGN-1) is a type-I transmembrane protein comprised of a large N-terminal ectodomain (consisting of an N-terminal signal peptide, a cholinesterase-like domain and a carbohydrate attachment region), a transmembrane domain and an intracellular cytosolic region (Lisé & El-Husseini, 2006). It is expressed on the post-synaptic membrane of glutamatergic excitatory neurons in contrast to NLGN-2 that is localised to GABAergic synapses (Suzuki *et al.,* 2012). NLGN-1 has an extremely important function in cell adhesion between neurons facilitating intercellular communication and is also thought to have roles in neuronal morphology, synaptogenesis and functioning, and cell signalling (Zhang *et al*., 2015). Some of these functions are mediated through the interaction of NLGN-1 with a presynaptic cell adhesion protein called neurexin-1β (NRX-1β). NLGN-1 forms a dimer with two NRX-1β molecules binding to identical positions on opposite sides of the dimerised extracellular domains to form a heterotetramer (Araç *et al*., 2007) (Fig. 1.3).

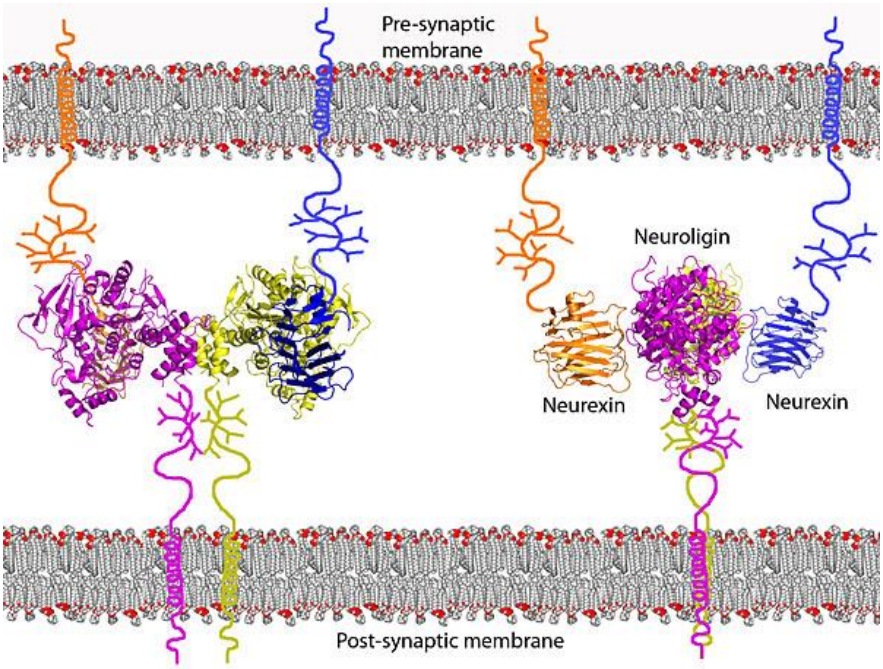

Figure 1.3. Association between NLGN-1 and NRX-1β at the synapse. Right: In the unbound state NLGN-1 exists as a dimer whereas NRX-1β is monomeric. Left: Two NRX-1β molecules bind to opposing sides of the NLGN-1 dimer causing conformational changes. (Www-ssrl.slac.stanford.edu, 2018)

As well as binding to NRX-1β, NLGN-1 also binds to the glutamatergic N-methyl-D-aspartate (NMDA) receptor via a transmembrane, PDZ-containing protein (PSD-95), which binds to the C-terminal tail of NLGN-1 (Song *et al*., 1999). Some studies suggest that increased glutamatergic activity is present in the early stages of Schizophrenia (Théberge *et al*., 2002). For this reason, potential therapy for the condition might involve the regulation of glutamatergic neuronal activity in the brain possibly by reducing levels of NLGN-1 expressed on the neuronal surface. Indeed, the over-expression of NLGN-1 on the surface of neurons has been shown to result in elevated levels of glutamate at both the pre- and post-synapses and, similarly, that proteolysis of the protein reduces glutamatergic neurotransmission (Suzuki *et al*., 2012). The same study suggested that NLGN-1 is in fact cleaved from the neuronal membrane by ADAM10 to produce soluble NLGN-1 (sNLGN-1) and a C-terminal fragment, the latter of which is then cleaved by γ-secretase to release an intracellular domain. Furthermore, it was suggested that proteolysis occurs in the juxtamembrane stalk region of NLGN-1 at Gln^{680} or Gln^{681}.

1.6.2. Prion protein.

The cellular isoform of the prion protein (PrP^C) is highly abundant in adult neurons where it is attached to the plasma membrane via a glycosyl-phosphatidylinositol (GPI)-anchor at the C-terminal end of the protein (Westergard *et al.,* 2007). Furthermore the protein is thought to have roles in cellular protection against oxidative stress and apoptosis (Westergard *et al*., 2007). However, PrP^c is also associated with the pathogenesis of the transmissible spongiform encephalopathies (TSEs), which include Creutzfeld-Jakob disease (CJD) and Kuru in humans, mad cow disease, and scrapie in sheep. These diseases occur when the scrapie-associated isoform of prion protein (PrP^{Sc}) corrupts the endogenous cellular isoform causing a conformational change of the latter from a predominantly α-helical to predominantly β-sheet structure (Fig. 1.4.) (Riesner, 2003). The β-sheet content of PrP^{Sc} inhibits proteolysis of the protein as well as causing it to aggregate to form fibrils similar to those formed by Aβ-peptides (Prusiner et al., 1983). Additionally, Parkin et al. showed that PrP^c can be cleaved by a zinc metalloprotease, in a similar mechanism to that of APP (Parkin et al., 2004). It is thought that the neurodegeneration observed in the TSEs is caused either by the detrimental effects of PrP^{Sc} blocking neuronal signalling or the reduced neurotrophic properties of corrupted PrP^C.

PrP^c is subject to cleavage from the membrane by both phospholipase and ADAM activities with the ADAM-cleaved form having a size very close to that of the membrane-associated form suggesting that this proteolytic event occurred very close to the C-terminus of the protein (Parkin *et al*., 2004). In fact it was subsequently shown that ADAM10 is the key protease involved in this event and that it cleaves the protein between Gly^{228} and Arg^{229}, which are located only 3 amino acids away from the GPI-anchor attachment at Ser^{231} (Taylor *et al.,* 2009).

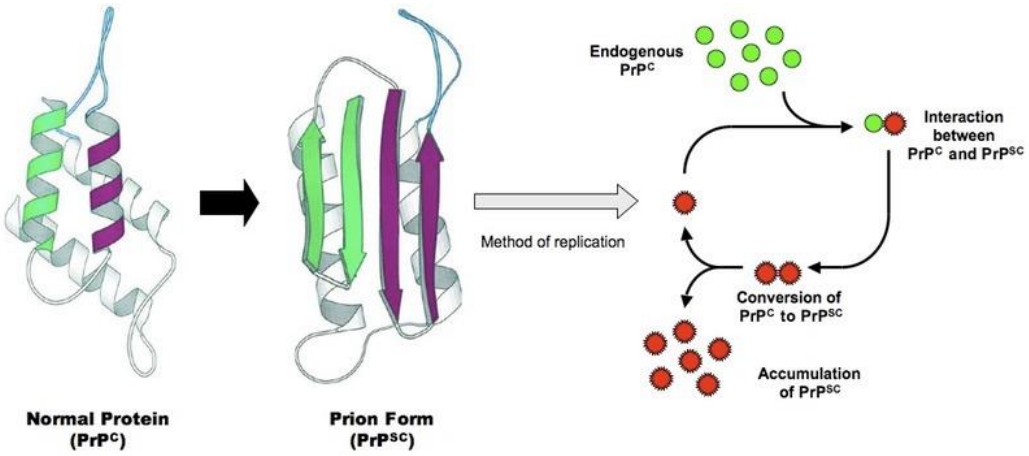

Figure 1.4. The α–helical to β–sheet conformational change induced by PrP^{Sc} in PrP^{c} and the subsequent accumulation/aggregation of PrP^{Sc} (Vce.bioninja.com.au, 2017).

1.7. The effects of cell stress-inducing agents on APP processing.

1.7.1. Hydrogen peroxide and oxidative stress.

Hydrogen peroxide (H_2O_2) is a known to cause oxidative stress (OS) and has been associated with Alzheimer's disease through a disruption in the levels of redox-active transition metals such as Iron (Fe^{2+}) (Smith *et al.*, 2000). The oxidation of aqueous iron to aqueous ferrous iron produces the free radical O_2^-, which further reacts with hydrogen to produce H_2O_2 in the equation $2O_2^- + 2H^+ \longrightarrow H_2O_2 + O_2$. The H_2O_2 then oxidates ferrous iron to produce OH^- and a more reactive free radical, $\cdot OH$ (Lauffer, 1992).

Several studies have reported that secretases involved in APP processing are affected by OS. A positive correlation between elevated levels of oxidative agents and the expression and activity of the β-secretase, BACE1 was found (Tong *et al.*, 2004; Kao *et al.*, 2003), promoting the amyloidogenic pathway. To further the production of Aβ, in 2008, Tamango et al. found that increased oxidative agents also augmented the activity of γ-secretase by over-expressing PS1 (Tamagno et al., 2008).

In addition, a recent study also discovered that ADAM-10 expression was actually significantly reduced when exposed to OS from the ozone (Hernández-Zimbrón and Rivas-Arancibia, 2015), further hindering the non-amyloidogenic pathwayand favouring the production of Aβ.

Furthermore, studies have indicated that there are also numerous feedback loops relating to OS, to enhance and continue the upregulation of the amyloidogenic pathway. Firstly, BACE-1 expression was found to be regulated by the activity of the γ-secretase (Guglielmotto et al., 2010), which coincidentally is also increased by OS. Research has also shown that the production of Aβ also influences the production of additional ROS and oxidative agents. The Aβ residue Tyr^{10} was found to play an essential role in the reduction of Cu^{2+} to further produce H_2O_2 (Barnham et al., 2004); initiating the cycle again.

1.7.2. Cobalt chloride and hypoxia.

Hypoxia occurs when there are reduced levels of oxygen available to cells and, as the brain accounts for approximately 20% of the oxygen requirements in the human body, neurons are particularly susceptible to hypoxia-induced damage (Sun *et al*., 2006). The cellular response to changing oxygen levels is linked to levels of hypoxia inducible factor-1α (HIF-1α) that is quickly degraded under normoxic conditions (Sun *et al*., 2006). Cobalt Chloride ($CoCl_2$) is commonly used in research experiments as a hypoxia-inducing stressor (Wartenberg et al., 2003), as it blocks the degradation of HIF-1α and, consequently, invokes a hypoxic response in cells (Fukuda et al., 2002).

A history of stroke is a risk factor for the development of AD and can approximately double the chance of developing the disease (Sun *et al*., 2006). This is thought to be because stroke and other vascular risk factors cause a lack of blood flow to organs or tissues (known as hypoperfusion) leading to hypoxia. In turn, hypoxia upregulates the production and aggregation of Aβ-peptides as well as impairing memory and causing the destruction of neurons (Daulatzai, 2013). One

possible mechanism for the enhanced production of Aβ-peptides lies in the fact that the exposure of APP_{SWE695} SH-SY5Y cells to hypoxia has been shown to increase the activity and expression of BACE1 leading to enhanced production of C99 and, subsequently, Aβ-peptides (Sun *et al*., 2006). Furthermore, hypoxia has also been shown to reduce the expression of neprilysin (NEP) and endothelin converting enzyme-1 (ECE-1), both of which are responsible for the breakdown of Aβ-peptides (Nalivaeva & Turner, 2013). Additional studies have found that hypoxia also downregulates α-secretase activity (Nalivaevaa *et al*., 2004). Webster *et al.* (2002) showed that hypoxia reduced sAPPα production in SH-SY5Y cells by approximately 60% and that levels of ADAM10 expression were concomitantly reduced by 50%.

1.7.3. Methylglyoxal, thapsigargin and endoplasmic reticulum stress.

Methylglyoxal (MG) and thapsigargin (TG) have been used in numerous research experiments as inducers of endoplasmic reticulum (ER) stress (Bronner et al., 2015, Palsamy et al., 2014). MG is a reactive aldehyde that accumulates in the body as a result of hyperglycaemia and is believed to cause ER stress by phosphorylating PERK, a protein located in the ER membrane that is involved in the unfolded protein response (UPR) (Palsamy *et al*., 2014). MG can also increase ROS levels, enhance the production of advanced glycation end products (AGEs) (Angeloni *et al*., 2014) and induce the release of ER calcium stores into the cytosol (Palsamy *et al*., 2014). Thapsigargin originates from the plant *Thapsia garganica* and is believed to induce ER stress by inhibition of the sarcoplasmic or endoplasmic reticulum Ca-ATPase (SERCA) calcium pumps (Lytton *et al.,* 1991). These pumps usually regulate calcium homeostasis and their inhibition results in a release of ER calcium into the cytoplasm.

It has recently been suggested that ER stress could be linked to neuronal death and AD with elevated calcium levels being found in the neurons of AD patients (Murray *et al*., 1992). A mutation in the *PS1* gene present in a number of FAD cases has been shown to downregulate the UPR and consequently increases ER stress that can result in apoptosis and neuronal death (Katayama *et al*., 2014). Additionally a

variant of the *PS2* gene (PS2V), created by alternate splicing, has also been linked to ER stress (Chadwick *et al.,* 2012). The authors found that cells expressing PS2V demonstrated a vulnerability to ER stress similar to that of cells expressing FAD PS1 mutants. This was thought to be due to PS2V hindering the UPR by inhibiting phosphorylation of the ER stress transducer, IRE1.

A number of studies have also indicated that ER stress can have an impact on the transport and processing of APP. PS2V has been shown to inhibit the transit of APP from the ER to the Golgi thereby impairing maturation of the protein (Chadwick *et al*., 2012). In addition, APP expression is elevated by AGEs (Angeloni *et al*., 2014) and APP proteolysis is altered by disruptions in cellular calcium homeostasis, which itself can be affected by presenilins (Chadwick *et al*., 2012; Jung *et al*., 2015). Furthermore, the expression of BACE-1 is also increased by ER stress (Salminen *et al*., 2009). It was also found that the Aβ-peptide aggregation can be enhanced by MG and that Aβ-peptides glycated by AGEs are more toxic than normal Aβ (Angeloni *et al*., 2014).

In healthy brain tissue, sAPPα exhibits neurotrophic properties in response to ER stress and elevated sAPPα is protective against TG-induced apoptosis (Endres & Reinhardt, 2013). However, when cytosolic calcium is increased, α-secretase activity is impaired and sAPPα generation is concomitantly reduced (Chadwick *et al.,* 2012). It is also notable that the expression of seladin-1/DHCR24, an ER enzyme that modulates APP processing and also exhibits neuroprotective properties especially against the neurotoxicity produced by Aβ, is decreased in AD (Salminen *et al*., 2009).

1.8. Glucagon-like peptide-1 analogues.

Glucagon-like peptide-1 receptor (GLP-1R) agonists (or GLP-1 analogues) are currently used as a treatment for type 2 diabetes mellitus. Their function is to mimic the incretin hormones found naturally in the body, which are normally responsible for regulating blood sugar. They work by increasing the release of insulin, inhibiting the release of glucagon and reducing the speed at which the stomach contents are

emptied; which consequently slows the process of glucose absorption (Diabetes.co.uk, 2017). There are four types of GLP-1 agonists currently administered to diabetic patients with the generic names Lixisenatide, Dulaglutide, Liraglutide, and Exenatide (Exendin-4). The current study focuses on Liraglutide and Exendin-4.

Exendin-4 is a naturally occurring 34 amino acid homologue of human GLP-1 and is found in the saliva of the Gila monster, *Heloderma suspectum* (Donnelly, 2012). It boasts many similarities to GLP-1 but, with a homology of only 53%, it also exhibits many differences. The second N-terminal amino acid of GLP-1, alanine, is replaced by glycine in Exendin-4. As this alanine residue harbours the site for proteolytic inactivation of GLP-1 by dipeptidyl-peptidase-4 (DPP-4), Exendin-4 is resistant to this cleavage (Gupta, 2013).

Liraglutide is a synthetic analogue of human GLP-1 (Donnelly, 2012). It bears 97% sequence homology to human GLP-1 as it only has a single lysine to arginine substitution at residue 34. The only other variation is that of a C-16 acyl group addition to lysine26 in Liraglutide, which increases the binding of albumin thereby protecting the molecule from DPP-4 cleavage and inactivation. The acylation also downregulates renal clearance and therefore, the excretion of Liraglutide (Gupta, 2013). Collectively, these changes extend the half-life of GLP-1 from approximately 2 min to 13 h in the case of Liraglutide (Agersø et al., 2002).

There are some links between type 2 diabetes and AD and the former is certainly a risk factor for the latter (Peila, Rodriguez and Launer, 2002). In addition, insulin may also have neuroprotective properties (Tanaka et al., 1995) and has roles in neurogenesis and proliferation, as well as in elevating activity at synapses and enhancing the formation and storage of memories (Kremerskothen et al., 2002). It has also been reported that insulin affects γ-secretase activity and upregulates the transportation of Aβ to the plasma membrane (Gasparini *et al.,* 2001) reducing the levels in the ER and, therefore, possibly preventing ER stress.

In diabetes the function of insulin is impaired either due to decreased levels or signaling dysfunction, which result in hyperinsulinemia. This is believed to inactivate the insulin receptors located in the blood brain barrier (BBB), which

consequently reduces the amount of insulin reaching the brain, causing a number of defects in brain activity and cognitive abilities (Schwartz et al., 1990). One study reported that, when compared with type 1 diabetes mellitus (which results from depleted levels of insulin), the neuronal degeneration and defective proteolysis of APP were more apparent in cases of type 2 diabetes mellitus (Li *et al*., 2007). This indicates that the neurodegenerative effects associated with diabetes are most likely a result of insulin resistance and the subsequent deficit of insulin, rather than inadequate levels of insulin alone. Furthermore, hyperinsulinemia has also been associated with elevated Aβ-peptide accumulation as the probable result of direct substrate competition between insulin and Aβ-peptides for the insulin degrading enzyme (IDE) (Qiu & Folstein, 2006). Hyperinsulinemia is also associated with the generation of ROS and AGEs that may contribute to the development of AD (Vincent et al., 2005).

Recently, it has been reported that GLP-1 agonists might possess therapeutic properties against neurodegeneration and, therefore, could be a potential target for the treatment of neurodegenerative diseases (Shimoda *et al.*, 2011, Chen *et al*., 2012). They have been reported to enhance cognitive abilities and improve LTP, as well as increasing synaptic plasticity (Hölscher, 2010). Furthermore, they are able to traverse the BBB and display neurotrophic and neuroprotective properties in the central nervous system (CNS) (Kastin & Akerstrom, 2003). GLP-1 agonists have also been reported to exhibit neuroprotective abilities in retaliation to hypoxia and oxidative stress, both of which are involved in AD, and to protect the brain against damage in a number of neurological conditions such as stroke and Parkinson's disease (Li et al., 2009).

Liraglutide, specifically, has been shown to elevate synaptic plasticity, improve cognitive function and memory formation, and to reduce the formation of Aβ plaques in an APP/PS1 transgenic mouse model of AD (McClean et al., 2011).

Exendin-4, specifically, exerts neuroprotective properties against oxidative stress (Chen *et al*., 2012) and glutamate excitotoxicity (Perry *et al*., 2002) and reduces Aβ-peptide levels in neurons *in vitro* and in female mice treated with

streptozotocin (Li et al., 2010). It was recently reported that Exendin-4 increased membrane protein levels of the postsynaptic density protein-95 (PSD-95) and the AMPA receptor GluR1, as well as expression levels of brain-derived neurotrophic factor (BDNF) in the mouse neocortex, all of which play a role in the generation and plasticity of synapses (Ohtake *et al*., 2014). The same report showed that Exendin-4 also enhanced levels of ADAM10 in the cell membrane fraction suggesting that the GLP-1 agonist promotes trafficking of the enzyme to the plasma membrane.

1.9. Summary.

It is clear from the literature that GLP-1 agonists, including Exendin-4 and Liraglutide, exhibit neuroprotective effects. Their ability to combat oxidative damage and neurodegeneration, as well as their existing clinical use in the treatment of diabetes, makes them ideal candidates for repurposing for the treatment of neurodegenerative diseases, especially Alzheimer's disease. The recent observation that Exendin-4 promotes the trafficking of ADAM10 could also represent a mechanism by which the drugs reduce Aβ-peptide production i.e. by enhancing the reciprocal non-amyloidogenic pathway of APP proteolysis. ADAM10 also has many other substrates and its activation is, therefore, potentially relevant to other conditions such as the TSEs and schizophrenia.

The aim of the current investigation is to characterise the protective effects of the GLP-1 agonists, Exendin-4 and Liraglutide, against various chemical stressors used to treat the neuroblastoma cell line, SH-SY5Y. Furthermore, the effect of GLP-1 agonists on the ADAM10-mediated proteolysis of APP, PrP and NLGN-1 will be examined in the same cell line and correlated with any protective effects of the drugs. Studies of this type should aid our understanding of the protective mechanisms of GLP-1 agonists in Alzheimer's disease and other neurological disorders.

Chapter 2: Materials and Methods.

2.1. Materials.

The generation of the human APP_{695} construct in the mammalian expression vector pIREShyg (Clontech-Takara Bio Europe, Saint-Germain-en-Laye, France) and the human prion construct in the mammalian expression vector pIRESneo (Clontech-Takara Bio Europe, Saint-Garmain-en-Laye, France) has been published previously (Parkin *et al*., 2007). Details of the human ADAM10 construct in pIRESneo have also been published (Parkin & Harris, 2009). The human neuroligin-1 construct in pIRESneo was synthesized and sequenced by Epoch Biolabs (Missouri City, USA).

The anti-β-actin monoclonal antibody and the anti-APP-CT polyclonal antibody were from Sigma-Aldrich Co. (Poole, UK). The SAF 32 (anti-prion) monoclonal antibody was purchased from SPI bio/ Bertin Pharma (Montigny le Bretonneux, France). The anti-ADAM10 C-terminal polyclonal antibody was purchased from Merck/Millipore (Temecula, USA). The neuroligin-1 (cytoplasmic domain) polyclonal antibody and neuroligin-1 (extracellular domain) polyclonal antibody were purchased from Synaptic Systems (Göttingen, Germany). The anti-sAPPα (6E10) monoclonal antibody and the anti-sAPPβ polyclonal antibody were purchased from Biolegend (San Diego, USA). The goat anti-rabbit secondary antibody and the rabbit anti-mouse secondary antibody were purchased from Sigma-Aldrich Co. (Poole, UK).

Unless otherwise stated, cell culture reagents were purchased from Scientific Laboratory Supplies (Nottingham, UK) and all other reagents were purchased from Sigma-Aldrich Co. (Poole, UK).

2.2. Methods.

2.2.1. Cell culture.

Human neuroblastoma SH-SY5Y cells were cultured in Dulbecco's Modified Eagle's Medium (DMEM) containing 10% (v/v) Foetal Calf Serum (FCS) and a penicillin/streptomycin mixture (10 units/ml penicillin, 10 µg/ml streptomycin).

Cultures were grown at 37°C in a 5% (v/v) CO_2 environment and the medium was replaced every 2-3 days.

For splitting, 2 ml of trypsin was added to the flask and removed to eliminate any residual media, before being replaced with a fresh 2 ml of trypsin and incubated for approximately 5 min. The flask was then tapped gently and viewed under a microscope, to ensure all cells had detached from the bottom of the flask. 20 ml of growth medium was added to the flask containing the trypsinized cells and the trypsin/medium mixture was transferred to a 50 ml Falcon tube. The cells were centrifuged at 800 rpm for 5 min in an Allegra X-22R centrifuge (Beckman Coulter, California, USA) for 3 min before removing the residual medium to leave an undisturbed pellet. The pellets were resuspended in 10 ml of growth medium and 1 ml of resuspension was added to each new flask, containing 10 ml of fresh growth medium.

2.2.2. Treatment of cells with drugs and stressors.

A confluent T75 flask of SH-SY5Y cells was trypsinized and cells were pelleted as described in section 2.2.1. and the cells were resuspended in 30 ml of complete growth medium. Growth medium (150 μl) and resuspended cells (50 μl) were added to the required number of wells in a 96-well microtitre plate. Cells were then cultured until they reached 80-90% confluency at which point the growth medium was removed and the cells were washed *in situ* with 200 μl of UltraMEM followed by the addition of a fresh 200 μl of the same medium to each well of cells. Stressors and drugs were incorporated into this latter volume of UltraMEM.

Thapsigargin (TG) stock was made by dissolving the supplied 5 mg of lyophilized powder in 961.5 μl of dimethyl sulfoxide (DMSO). Adding 2.5 μl of this stock per 200 μl of medium then gave a final concentration of 100 μM. All other dilutions of TG were made by diluting this solution with DMSO such that the same volume of solution (2.5 μl per 200 μl medium) could be added to achieve the desired final concentrations. DMSO was incorporated into control cultures.

Methylglyoxal (MG) was supplied as a 40% (w/v) stock solution which was diluted 1 : 99 (MG : distilled water) to give a final working solution which was then filter-sterilized under aseptic conditions. Adding 4.3 μl of this working solution to 200 μl of growth medium then gave a final MG concentration of 1200 μM. All other MG concentrations were made by diluting the initial solution with filter-sterilized water.

In the case of hydrogen peroxide, a 30% (w/v) stock solution was diluted 1:199 in distilled water. After filter-sterilizing, the addition of 2.3 μl of this dilution to 200 μl of culture medium gave a final concentration H_2O_2 of 1000 μM. All other concentrations were achieved by diluting the 1:199 solution with filter-sterilised distilled water.

For cobalt chloride ($CoCl_2$) treatments 0.1 g was dissolved in 10 ml distilled water and filter-sterilised. The addition of 5 μl of this stock to 200 μl of culture medium gave a final $CoCl_2$ concentration of 1000 μM. All other concentrations were achieved by diluting the stock with filter-sterilized water.

Liraglutide (LG) and Exendin-4 (E-4) were utilised as follows. A LG stock was made up at an 83 mM concentration using distilled water, aliquoted and frozen at -25 ^{o}C. This stock was then diluted 1:1999 with distilled water and filter-sterilized such that adding 3 μl of this solution to 200 μl of growth medium gave a final LG concentration of 500 nM. All other final concentrations were achieved by diluting the 1:1999 solution with filter-sterilized distilled water. E-4 (1 mg) was dissolved in 29.85 ml of distilled water, aliquoted and frozen at -80^{o}C. This stock was then diluted 1:40 in growth medium and this solution was applied directly to cells (after filter-sterilizing) to give a final E-4 concentration of 200 nM. Further dilutions were made by adding filter-sterilized growth medium to the 1:40 solution. Note that medium on control cells was also filter-sterilized. Batimastat was made up as a 10 mM stock in DMSO and 10 μl of this stock was added to every 10 ml of medium to give a final concentration of 10 μM.

2.2.3. MTS (3-(4,5-dimethylthiazol-2-yl)-5-(3-carboxymethoxyphenyl)-2-(4-sulfophenyl)- 2H-tetrazolium) cell proliferation assay.

After stressor and/or drug treatments, 20 µl of CellTiter 96 Aqueous One Solution (Promega Corporation, Madison, USA) was added to each 200 µl of medium in the wells of the 96-well microtitre plate containing the treated cells (along with blank wells containing just medium) and the plate was mixed thoroughly by extensive tapping on the edge of the bench. The plate was then covered in tin foil and incubated at 37^{O}C until the brown colouration had developed sufficiently (10 min -1 h). During this incubation the plate was intermittently tapped on the bench to dissolve the precipitate effectively. The absorbance of the samples was then read at 490 nm using a wallac VICTOR^{2} spectrophotometer. Blank values were then subtracted from the sample readings.

2.2.4. Conditioning medium for analysis of protein shedding.

Once at the appropriate confluence the spent growth medium was removed from cells in T75 flasks and replaced with 10 ml of UltraMEM reduced serum medium. Flasks were gently rocked by hand and the UltraMEM was removed before adding a fresh 10 ml of the same medium and culturing the cells for a further 24 h. The medium was then collected and stored at -80^{O}C pending concentration.

2.2.5. Concentrating conditioned medium samples.

The medium was thawed in a 37°C water bath and then kept on ice. Centrifugal concentrators (Amicon Ultra-4, Merck Millipore Ltd., Cork, Ireland) were first equilibrated by adding 4 ml distilled water and centrifuging at 4000 rpm in a Hettich Rotanta 460R centrifuge (Hettich, Tuttlingen, Germany) until the water had spun through (approximately 10 min). The water was then removed from the base of the concentrator. Cell debris was pelleted from the conditioned medium samples by centrifuging at 4000 rpm for 5 min. A total of exactly 8 ml of supernatant from each sample was then concentrated to 250 µl by spinning for the required amount of time

in the concentrators at 3000 rpm. Concentrated samples were then removed into Eppendorf tubes and stored at -80^{o}C pending further analysis.

2.2.6. Harvesting cells.

Following the removal of conditioned medium from cell cultures (see section 2.2.4.), 10 ml of phosphate-buffered saline (PBS; 1.5 M NaCl, 20 mM NaH_2PO_4 and 200 mM Na_2HPO_4, pH 7.4) was added to each flask and was gently swilled around for approximately 1 min. The PBS was decanted off and a fresh 10 ml of the same buffer was added, into which the cells were scraped. The cell suspension was then transferred into a 50 ml Falcon tube and a fresh 10 ml of PBS was added to the flask to rinse out the remaining cells; this was then combined with the first 10 ml in the same Falcon tube. The tubes were then centrifuged at 500 rpm in a Hettich Rotanta 460R centrifuge (Hettich, Tuttlingen, Germany) for 5 min (4^{o}C) to pellet the cells. The supernatant was decanted and any remaining PBS was removed using a Gilson pipette.

2.2.7. Preparation of cell lysates.

Cell pellets were resuspended in 1.5 ml of lysis buffer (50 mM Tris, 150 mM NaCl, 1% (v/v) Igepal, 0.1% (w/v) Sodium Deoxycholate, 5 mM EDTA (Ethylenediaminetetraacetic acid), pH 7.4) which had previously had a protease inhibitor cocktail (Sigma-Aldrich Co., Poole, UK) added to it at a volume ratio of 100:1 (lysis buffer:cocktail). The cells were then resuspended by pipetting up and down five times. Next, the samples were sonicated using a probe sonicator on half power for 30 s (MSE, Crawley, UK) and then transferred to 1.5 ml Eppendorf tubes before centrifuging at top speed for 10 min in a bench top microfuge. The supernatants (lysates) were then removed into fresh tubes and, after equalizing protein concentrations (section 2.2.8), were aliquoted into 200 μl fractions and stored at -80^{o}C.

2.2.8. Bicinchoninic Acid (BCA) Assay.

In order to quantify the amounts of protein in lysate samples, a BCA protein assay was performed using bovine Serum Albumin (BSA) to generate a standard curve/line. Standards (10 μl) were added, in duplicate, to the wells in the first row of a 96-well microtitre plate in the order described below:

A1+A2: 0.2 mg ml^{-1} BSA

A3+A4: 0.4 mg ml^{-1} BSA

A5+A6: 0.6 mg ml^{-1} BSA

A7+A8: 0.8 mg ml^{-1} BSA

A9+A10: 1.0 mg ml^{-1} BSA

A11+A12: 0 mg ml^{-1} BSA (distilled water)

Lysate samples (10 μl) were then added in duplicate starting in the second row of the plate. A working reagent of 50:1 (v/v) BCA : 4% (w/v) $CuSO_4.5H_2O$ (BCA; Pierce, Rockford, USA) was then prepared and 200 μl was added to each well of the plate (samples and standards). Samples were thoroughly mixed by gentle tapping of the plate on the edge of the bench and any air bubbles were removed using a hypodermic needle before incubating the plate for 30 min at 37°C. The absorbance of samples was measured at 562 nm using a Wallac VICTOR^2 spectrophotometer (Perkin Elmer, Waltham, USA). A standard regression line was generated using the BSA readings and sample protein concentrations determined using the resultant regression equation. All lysate samples were then equalized to the protein concentration of the lowest sample by adding the required volume of lysis buffer calculated using the equation below:

Volume to be added = ((concentration of most concentrated sample/ concentration of most dilute sample) x volume of most concentrated sample) – volume of most concentrated sample.

2.2.9. Sodium dodecylsulphate-polyacrylamide gel electrophoresis (SDS-PAGE).

SDS-PAGE was carried out using 7-20% gradient resolving gels (Table 2.1). N,N,N',N'-Tetramethylethylenediamine (TEMED) (3µl) was added to both the 7% and the 20% solutions before gently inverting to mix. The resolving gels were then poured using a gradient mixer and peristaltic pump and layered with isopropanol in order to exclude oxygen that might otherwise inhibit polymerization. After approximately 30 min the isopropanol was completely removed and the stacking gel (Table 2.2) was poured (after the addition of 15µl of TEMED to the solution) before inserting the well comb. After allowing the stacking gel to set (30 min), the comb was removed and the gels were transferred to the running kit and the electrode reservoirs were filled with running buffer (0.25 M Tris, 1.92 M Glycine and 1% SDS; Geneflow Ltd, Lichfield, UK).

Samples were diluted 2:1 (v:v) with dissociation buffer (3.5 ml 1 M Tris/HCl, pH 6.8, 2.5 g SDS, 0.3085 g dithiothreitol, 5 ml glycerol, 0.05 mg bromophenol blue, made up to 25 ml with distilled water) and gently vortexed. A low molecular weight standard marker ladder (GE Healthcare, Buckinghamshire, UK)) was prepared in the same manner by diluting with dissociation buffer as were blank solutions containing just distilled water and dissociation buffer. All samples, standards and blanks were then boiled for 3 min and 30 µl aliquots were loaded in the gel wells. Gels were run at 35 mA per gel (70 mA for two simultaneously) until the dye reached the bottom of the gel.

Table 2.1. Resolving gel composition.

	% Acrylamide	
Component	**7%**	**20%**
Sucrose	-	0.37 g
1 M Tris/HCl pH 8.8	1.39 ml	-
1.5 M Tris/HCl pH 8.8	-	0.93 ml
30% acrylamide 0.8% Bis (Universal Biologicals, Cambridge, UK)	0.88 ml	2.5 ml
1.5% (w/v) ammonium persulfate	0.1 ml	0.22 ml
Distilled water	1.36 ml	-
10% (w/v) SDS	37 µl	37 µl

Table 2.2. Stacking gel composition.

Component	**Volume**
1 M Tris/HCl pH 6.8	1.89 ml
30% acrylamide 0.8% Bis (Universal Biologicals, Cambridge, UK)	1.5 ml
1.5% (w/v) ammonium sulphate	0.75 ml
Distilled water	11.49 ml
10% (w/v) SDS	150 µl

2.2.10. Immunoblotting.

Polyvinylidene difluoride (PVDF) transfer membranes (Millipore, Billerica, USA) were activated by placing them in methanol for 5 s, distilled water for 2 min and Towbin transfer buffer (20 mM Tris and 150 mM glycine in 20% (v/v) methanol) for at least 10 min. The SDS-PAGE gels were also equilibrated in Towbin buffer for approximately 5 min. Transfer sandwiches were assembled consisting of; 3 x blotting paper, 1 x membrane, 1 x gel, 3 x blotting paper. All blotting paper was soaked in Towbin buffer and layers were rolled with a test-tube to eliminate air bubbles. The sandwiches were placed in the wet blot transfer kit which was filled with Tobin buffer and the lid was attached such that the positive electrode was on the membrane side of the sandwich. Proteins were transferred at 115V for 1 h. Following transfer, the PVDF membranes were washed in PBS for 5 min before blocking them for 1 h at room temperature in 5% (w/v) skimmed milk powder in PBS + 0.1% (v/v) Tween-20 (PBS-Tween) on a rotating platform. The blocking buffer was then removed and the membranes were washed in PBS for a further 5 min. Primary antibodies were then added to the membranes which were incubated either on a shaking platform or a spiramix overnight at 4^{o}C. All primary antibodies (Table 2.3) were made up in PBS-Tween containing 2% (w/v) BSA. The next morning, the primary antibody solution was removed and the membranes were washed for 1 x 1 min and 2 x 15 min in PBS-Tween. Secondary antibody (made up in the same solution as the primary antibody) (Table 2.3) was then incubated with the membranes for 1 h at room temperature on a rotating platform. The membranes were then washed for a further 1 x 1 min and 2 x 15 min with PBS and developed as described in section 2.2.11.

Table 2.3. Primary and secondary antibodies used for immunoblotting.

Primary Antibody	Species	Working Concentration	Secondary Antibody	Working Concentration
Anti-β-Actin	Mouse monoclonal	1/5000	Rabbit anti-mouse	1/4000
Anti-APP C-Terminal	Rabbit polyclonal	1/5000	Goat anti-rabbit	1/4000
SAF 32 (anti-prion)	Mouse monoclonal	1/2000	Rabbit anti-mouse	1/4000
Neuroligin-1 (Cytoplasmic domain)	Rabbit polyclonal	1/1000	Goat anti-rabbit	1/4000
Neuroligin-1 (Extracellular domain)	Rabbit polyclonal	1/1000	Goat anti-rabbit	1/4000
Anti-sAPPβ	Rabbit polyclonal	1/1000	Goat anti-rabbit	1/4000
Anti-sAPPα (6E10)	Mouse monoclonal	1/4000	Rabbit anti-mouse	1/4000
Anti-ADAM10 C-terminal	Rabbit polyclonal	1/1000	Goat anti-rabbit	1/4000

2.2.11. Immunoblot Development.

The PBS from the final membrane wash was discarded and Enhanced Chemiluminescence (ECL) reagent (Pierce, Rockford, USA). 6 ml was incubated on the membrane for 2 min with thorough manual mixing. The membrane was then placed between two sheets of acetate in a developing cassette and a sheet of X-ray film was placed on top before closing the cassette. Exposures were performed for between 2 min and 1 h before developing and fixing the films.

2.2.12. Amido black staining.

The membranes were removed from the acetate sheets and placed in Amido Black solution (0.1% (w/v) amido black, 1% (v/v) acetic acid, 40% (v/v) methanol) for approximately 1 minute, until the bands appeared. They were then rinsed under cold

water until the excess Amido Black was removed from the background and the bands were clearly prominent.

2.2.13. Bacterial DNA transformation.

XL1-blue *E.Coli* (20 μl) (Agilent Technologies LDA UK Ltd, Stockport, UK) were aliquoted into Eppendorf tubes and placed on ice. Following the addition of 0.3 μl of β-mercaptoethanol (1.42 M), the bacteria were incubated on ice for 10 min with gentle swirling every 2 min. Stock DNA (1 μl) was then added to each aliquot of bacteria before incubating on ice for a further 30 min. The cells were then heat shocked at 42 ^{o}C for exactly 45 secs before being returned to ice for a further 2 min. LB (0.9 ml; 10g Bacto-tryptone, 5 g Bacto-yeast extract, 5 g NaCl, 1 L d.H_2O, pH 7.5) prewarmed to 37^{o}C was then added to each transformation and the samples were incubated on a shaker for 1 h at 37^{o}C. The bacteria were then pelleted by centrifugation at 2000 rpm for 10 min in a bench top microfuge and 800 μl of the supernatant was removed. The remaining liquid in the tube was then used to resuspend the bacteria and they were plated on agar-ampicillin plates. Plates were made by adding 7.5 g agar to 500 ml LB, autoclaving and cooling to 45 ^{o}C for 1 h prior to the addition of 500 μl of 100 mg/ml filter-sterilized ampicillin and subsequent pooring. The plates were incubated at 37 ^{o}C overnight and then a single colony was selected from the plate and inoculated into 5 ml of LB/penicillin. These mini-suspension cultures were grown overnight at 37 ^{o}C with shaking before inoculating 0.5 ml of the culture into a 50 ml midi-suspension culture and growing again overnight.

2.2.14. DNA purification.

The bacterial cells from the suspension cultures (section 2.2.13) were harvested by centrifuging at 6000 *g* for 15 min at 4°C. The DNA was then prepared using the QIAGEN Plasmid Midi Kit according to the manufacturer's instructions. The

final DNA pellet was air-dried for 5-10 min and resuspended in 200 μl of distilled water followed by heating to 60 ^{o}C for 10 min and repeated pipetting.

2.2.15. Restriction enzyme digests.

Purified plasmid DNA was linearized by restriction digest prior to stable transfections being performed. Digest incubations consisted of the following components:

5 μl of 10x restriction enzyme buffer (NEB buffer 4 for Ahd1, and CutSmart Buffer for Xho1)

0.5 μl acetylated BSA (10 g/ l stock?)

0.5 μl Ahd1 or Xho1 (the latter for the Neuroligin1 plasmid) restriction enzyme

15-30 μg of plasmid DNA

RNAase-free distilled water to make up to 50 μl

Digests were then incubated overnight at 37°C

2.2.16. Ethanol precipitation of digested plasmids.

Filter-sterilised sodium acetate (3M, p.H 5.2) (1/10 volume) was added to the restriction digests along with cold absolute ethanol (2 volumes) before mixing and incubating the solutions at -20°C for 1 h. The samples were then centrifuged at 11,600 *g* for 20 min at 4°C and the supernatant was removed. Cold 80% (v/v) ethanol (300 μl) was added to the pellet without resuspension followed by centrifugation as before but for just for 5 min. The supernatant was discarded and the pellet was resuspended, under aseptic conditions, in 30 μl of filter-sterilized distilled water.

2.2.17. Stable transfection of mammalian cells.

A T75 flask of 70% confluent SH-SY5Y cells was trypsinized and pelleted as described in section 2.2.1. The cell pellet was resuspended in 0.8 ml of growth medium before being transferred to an electroporation cuvette (Bio-rad, 0.4cm Gene Pulser/Micropulser). The plasmid resuspension (20 μl) was added to the cuvette and the sample was mixed by repeated pipetting. The cuvette was then electroporated using an ECM630 electroporator (Bio-rad, square wave, 120 V, 25 ms, 2 mm path width). The cells were resuspended in 5 ml of growth medium and transferred to a T75 flask containing 20 ml growth medium. The next morning, the growth medium was changed for a fresh 20 ml and the cells were grown to approximately 60% confluence, with the medium being changed every other day. At this point, the cells were treated with antibiotic (50 μl per 10 ml of medium of 0.1 g ml^{-1} neomycin stock or 30μl per 10 ml medium of 50 mg ml^{-1} Hygromycin stock) until the selection control cells (i.e. no plasmid transfections) had completely died off.

2.2.18. Statistical analysis.

Results are expressed as means +/- S.D. or S.E.M. (as indicated in Figure legends) with the number of repeats indicated in the relevant Figure legends. Significance was tested using Student's *t-test* and the level of significance is indicated on Figures and in Figure legends.

Chapter 3: Results.

3.1. The effects of GLP-1 analogues on SH-SY5Y cell viability under stress conditions.

GLP-1 analogues have previously been shown to protect cells against various stressors (Li et al., 2009, Chen *et al*., 2012). Therefore, in the current study, the ability of liraglutide and exendin-4 to protect SH-SY5Y neuronal cells against various chemical stressors was initially examined.

3.1.1. Determination of cell seeding levels.

In order to achieve a suitable level of confluence within a reasonable time frame it was first necessary to determine the appropriate number of cells to seed into 96 well plates. Unfortunately, SH-SY5Y cells remain in uncountable clumps even after careful trypsinisation. Therefore, cells were allowed to reach confluency in a T75 flask, trypsinised and then resuspended in 10 ml of growth medium. A range of volumes of this resuspension were then added to the wells of 96 well plates together with sufficient growth medium to bring the volumes in all wells to 200 μl. The cells were then cultured until the first wells reached confluency (48 h) and then an MTS assay (see Materials and Methods) was performed in order to determine cell viability. The results (Fig. 3.1.1.) show that, when 100 μl of the cell resuspension was added to each well, confluency was achieved within the 48 h time frame. The remaining volumes of resuspension gave variable levels of confluence within the same time frame. These data enabled the seeding of appropriate volumes of cell resuspensions to achieve the required level of cell confluence in subsequent experiments (experimental plates were always seeded from the cell pellet of a trypsinised confluent T75 flask of cells resuspended every time in the same volume of growth medium).

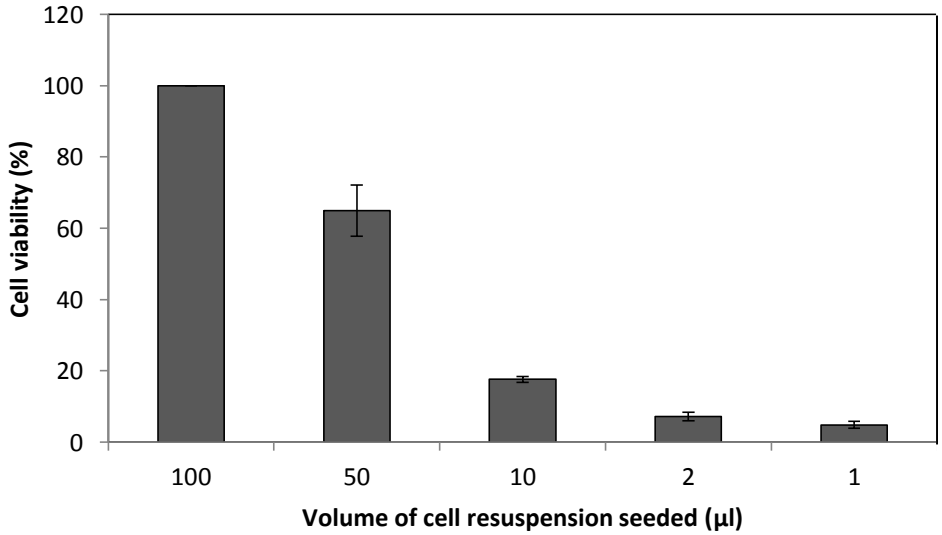

Figure 3.1.1. Determination of SH-SY5Y cell seeding volumes. A confluent T75 flask of cells was trypsinised, pelleted and resuspended in 10 ml of complete growth medium before seeding out 100, 50, 10, 2, and 1 µl of resuspension into the wells of a 96 well plate. All wells in the plate were made up to 200 µl by the addition of further growth medium and the cells were cultured for 48 h. Once the first wells reached confluence an MTS assay was performed as described in the Materials and Methods section. Results are expressed as a percentage of the completely confluent (100 µl cell resuspension) wells and are means ± S.D. (n=3).

3.1.2. GLP-1 analogues and hydrogen peroxide treatment

Hydrogen peroxide was used as an initial stressor as an oxidative stress causative agent. It has previously been reported that hydrogen peroxide induces the production of reactive oxygen species (ROS) (Smith *et al.*, 2000). Initially, hydrogen peroxide toxicity curves were generated. SH-SY5Y cells were seeded into 96 well plates, grown to 80% confluence and then washed *in situ* with complete growth medium. Fresh growth medium containing a range of hydrogen peroxide concentrations was then added to the cells and they were then cultured for a further 24 h before conducting an MTS cell viability assay as described in the Materials and Methods section. The results (Fig. 3.1.2.) show that only the 1000 µM concentration of hydrogen peroxide was cytotoxic when the stressor was added to cells in complete growth medium. It was subsequently hypothesized that components in the complete growth medium might be impacting on the toxicity of the hydrogen peroxide so the experiment was repeated but this time the stressor was added to cells in UltraMEM as opposed to complete growth medium. The results (Fig. 3.1.3.) show that, under these conditions, the stressor was cytotoxic at both 500 µM and 1000 µM

concentrations. Subsequently, the cytotoxicity of additional hydrogen peroxide concentrations between 200 and 500 μM was also examined. Both 300 and 400 μM stressor concentrations resulted in similar toxicity (Fig. 3.1.4.). For future experiments testing the protective effects of GLP-1 analogues it was decided to employ hydrogen peroxide concentrations of 200, 300 and 500 μM.

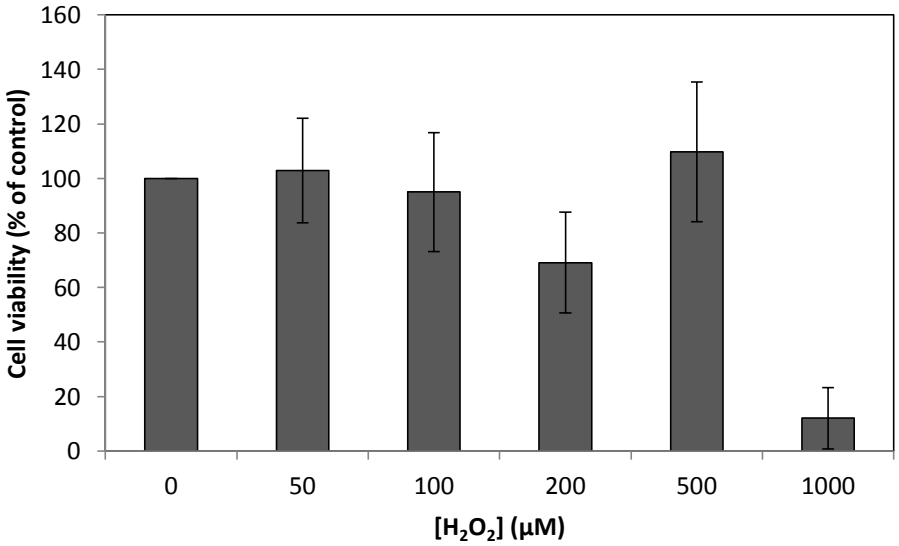

Figure 3.1.2. The effect of hydrogen peroxide on SH-SY5Y cell viability in the presence of complete growth medium. Cells were grown to 80% confluence, washed *in situ* with complete growth medium and then 0, 50, 100, 200, 500, and 1000 μM hydrogen peroxide in complete growth medium was added to the cells. Following a further 24 h culture period, an MTS cell viability was performed as described in the Materials and Methods section. Results are expressed as a percentage of the control viability and are means ± S.D. (n=3).

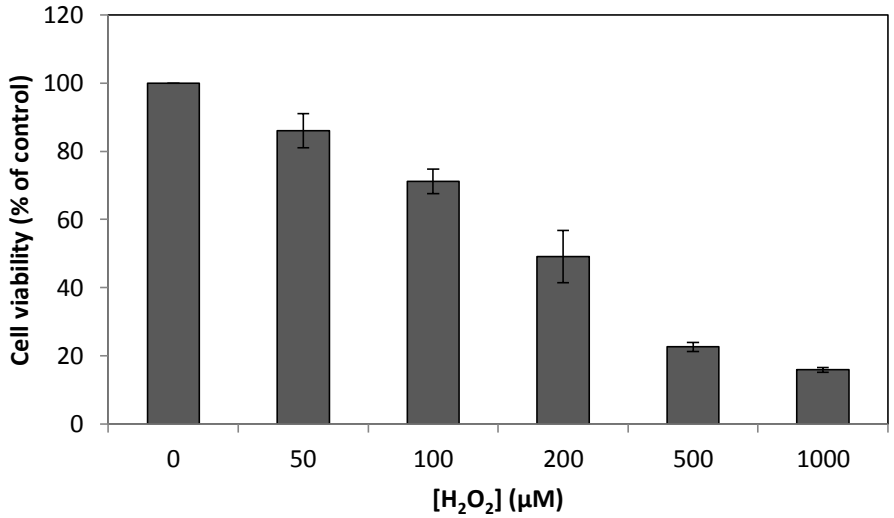

Figure 3.1.3. The effect of hydrogen peroxide on SH-SY5Y cell viability in the presence of UltraMEM. Cells were grown to 80% confluence, washed *in situ* with UltraMEM and then 0, 50, 100, 200, 500, and 1000 µM hydrogen peroxide in UltraMEM was added to the cells. Following a further 24 h culture period, an MTS cell viability was performed as described in the Materials and Methods section. Results are expressed as a percentage of the control viability and are means ± S.D. (n=3).

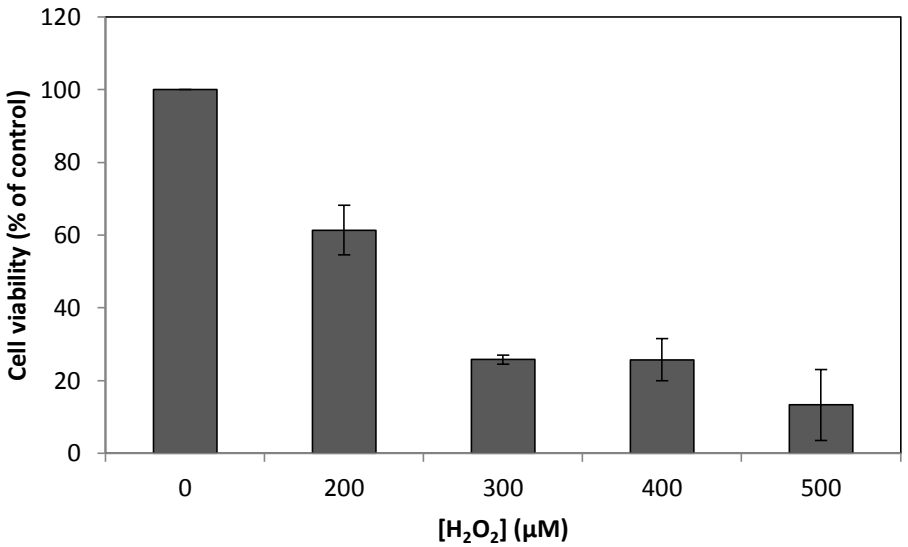

Figure 3.1.4. The effect of hydrogen peroxide on SH-SY5Y cell viability in the presence of UltraMEM. Cells were grown to 80% confluence, washed *in situ* with UltraMEM and then 0, 200, 300, 400, and 500 µM hydrogen peroxide in UltraMEM was added to the cells. Following a further 24 h culture period, an MTS cell viability was performed as described in the Materials and Methods section. Results are expressed as a percentage of the control viability and are means ± S.D. (n=3).

3.1.2.1. Liraglutide and hydrogen peroxide treatment

Next, the ability of liraglutide to protect cells against hydrogen peroxide-mediated toxicity was examined. Cells were once more cultured until they were 80% confluent before being washed in situ with UltraMEM and then being treated with fresh UltraMEM containing 500 μM hydrogen peroxide and/or liraglutide (0, 75, 150, 300 or 750 nM). Following a 48 h incubation, an MTS cell viability assay was performed as described in the Materials and Methods section. The results (Fig. 3.1.5) showed that, whilst 500 μM hydrogen was highly toxic to the cells, liraglutide exerted no protective effect against the stressor. It was hypothesized that the hydrogen peroxide concentration used in this experiment may simply have been too harsh for the liraglutide to show any protective effect. Consequently, the experiment was repeated at lower stressor concentration (300 μM). However, the results from this latter experiment (Fig. 3.1.6.) also failed to demonstrate a protective effect of liraglutide.

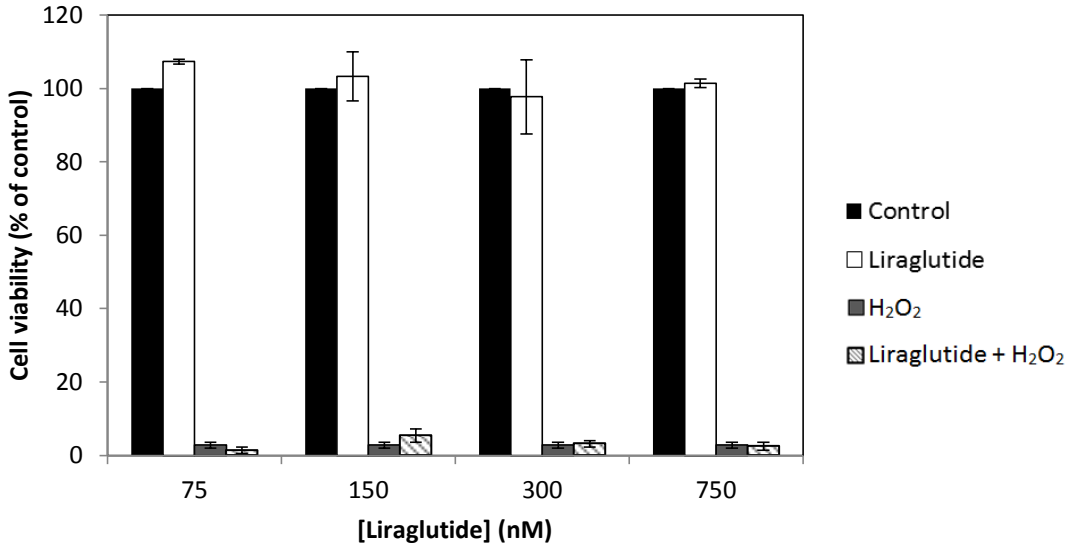

Figure 3.1.5. The effect of liraglutide on the viability of SH-SY5Y cells treated with 500 μM hydrogen peroxide. Cells were grown to 80% confluence, washed *in situ* with UltraMEM and then 500 μM hydrogen peroxide and 75, 150, 300, and 750 nM liraglutide in UltraMEM were added to the cells. Following a further 48 h culture period, an MTS cell viability was performed as described in the Materials and Methods section. Results are expressed as a percentage of the control viability at each liraglutide concentration and are means ± S.D. (n=3) with the exception of 150 nM Liraglutide and 75 nM Liraglutide which are n=2.

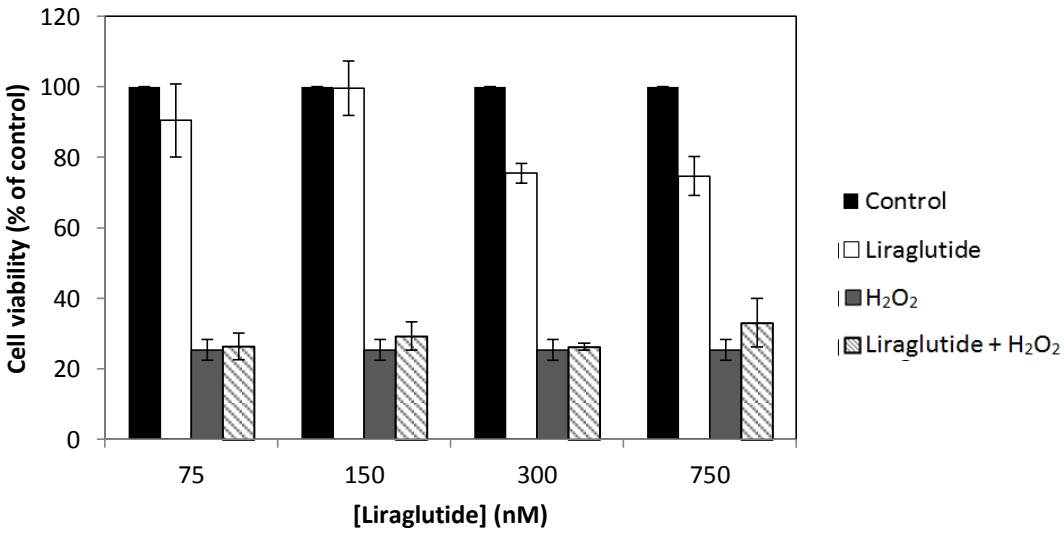

Figure 3.1.6. The effect of liraglutide on the viability of SH-SY5Y cells treated with 300 μM hydrogen peroxide. Cells were grown to 80% confluence, washed *in situ* with UltraMEM and then 300 μM hydrogen peroxide and 75, 150, 300, and 750 nM liraglutide in UltraMEM were added to the cells. Following a further 48 h culture period, an MTS cell viability was performed as described in the Materials and Methods section. Results are expressed as a percentage of the control viability at each liraglutide concentration and are means ± S.D. (n=3).

Given that liraglutide failed to protect against hydrogen peroxide treatment when the stressor and GLP-1 were added to cells concurrently, it was decided to test the effect of pre-treating cells with liraglutide on the toxicity of hydrogen peroxide. To this end, cells were grown to 60% confluency to account for inevitable further growth during pretreatment and a consequent confluency of approximately 80% upon treatment. The cells were then pre-treated with liraglutide for 24 h (in complete growth medium) before washing them *in situ* with UltraMEM and incubating them for an additional 48 h containing hydrogen peroxide and or fresh liraglutide. An MTS viability assay was then performed as described in the Materials and Methods section. Whilst a range of hydrogen peroxide concentrations (200, 300 and 500 μM) were tested, no protective effect of liraglutide was evident against 300 and 500 μM stressor concentrations (Figs. 3.1.7. and 3.1.8.). However, in contrast, when the lower 200 μM hydrogen peroxide concentration was tested (Fig. 3.1.9.), pre-treating the cells with 150 or 750 nM liraglutide resulted in a slight but significant protective effect.

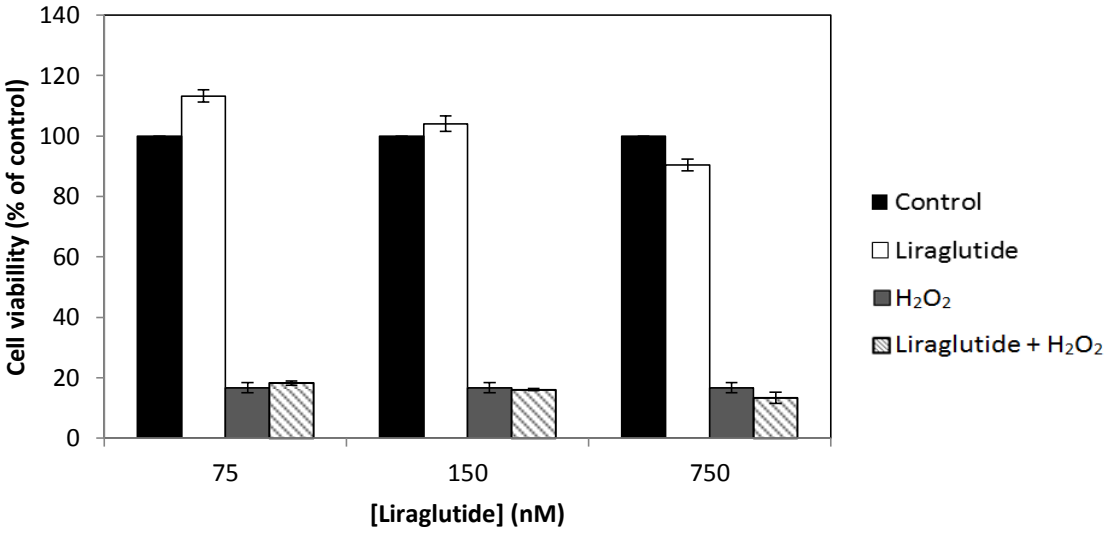

Figure 3.1.7. The effect of liraglutide pre-treatment on the viability of SH-SY5Y cells treated with 500 μM hydrogen peroxide. Cells were grown to 60% confluence and then pre-treated for 24 h with 75, 150, and 750 nM liraglutide in complete growth medium. Next the cells were washed *in situ* with UltraMEM and then 500 μM hydrogen peroxide and 75, 150, and 750 nM fresh liraglutide in UltraMEM were added to the cells. Following a further 48 h culture period, an MTS cell viability was performed as described in the Materials and Methods section. Results are expressed as a percentage of the control viability at each liraglutide concentration and are means ± S.D. (n=3).

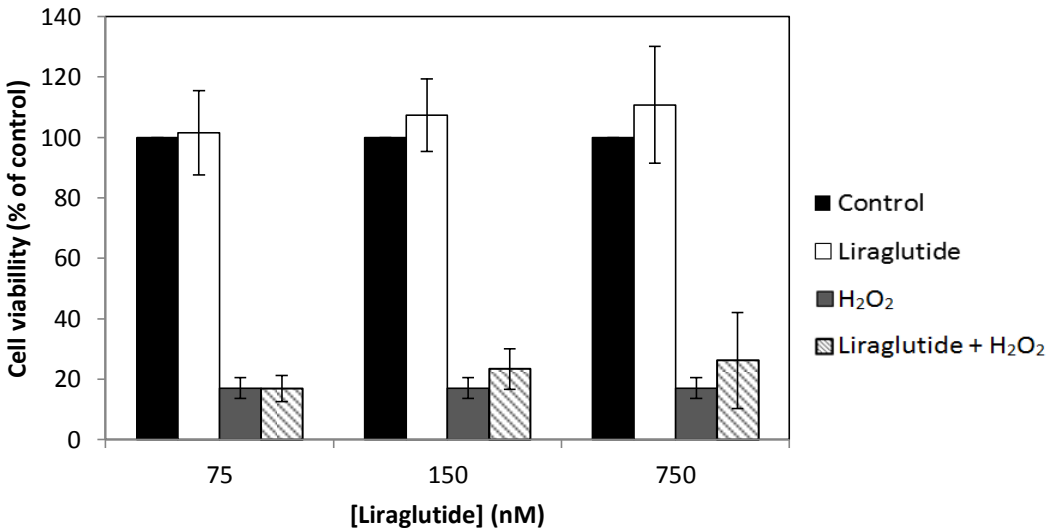

Figure 3.1.8. The effect of liraglutide pre-treatment on the viability of SH-SY5Y cells treated with 300 μM hydrogen peroxide. Cells were grown to 60% confluence and then pre-treated for 24 h with 75, 150, and 750 nM liraglutide in complete growth medium. Next the cells were washed *in situ* with UltraMEM and then 300 μM hydrogen peroxide and 75, 150, and 750 nM fresh liraglutide in UltraMEM were added to the cells. Following a further 48 h culture period, an MTS cell viability was performed as described in the Materials and Methods section. Results are expressed as a percentage of the control viability at each liraglutide concentration and are means ± S.D. (n=3).

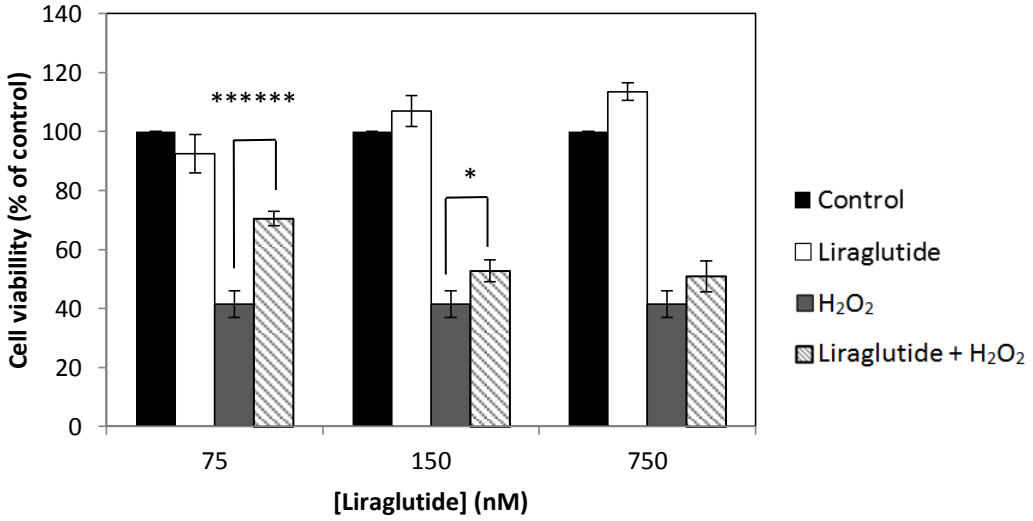

Figure 3.1.9. The effect of liraglutide pre-treatment on the viability of SH-SY5Y cells treated with 200 μM hydrogen peroxide. Cells were grown to 60% confluence and then pre-treated for 24 h with 75, 150, 750 nM liraglutide in complete growth medium. Next the cells were washed *in situ* with UltraMEM and then 200 μM hydrogen peroxide and 75, 150, and 750 nM fresh liraglutide in UltraMEM were added to the cells. Following a further 48 h culture period, an MTS cell viability was performed as described in the Materials and Methods section. Results are expressed as a percentage of the control viability at each liraglutide concentration and are means ± S.D. (n=3). *, significant at $p = 0.05$; ******, significant at $p = 0.001$.

3.1.2.2. Exendin-4 and hydrogen peroxide treatment

The ability of a second GLP-1 analogue, exendin-4, to protect against hydrogen peroxide-mediated cytotoxicity was also examined. Here, the experiments were conducted as described in the preceding section for the liraglutide pre-treatment experiments. The effect of the drug against both 300 and 200 μM stressor concentrations was examined but no protective effect of exendin-4 could be demonstrated at the former hydrogen peroxide concentration (Fig. 3.1.10). However, at the lower, 200 μM, hydrogen peroxide concentration a trend towards a protective effect of exendin-4 could be observed (Fig. 3.1.11.). However, this trend could only be deemed significant at the 100 nM drug concentration.

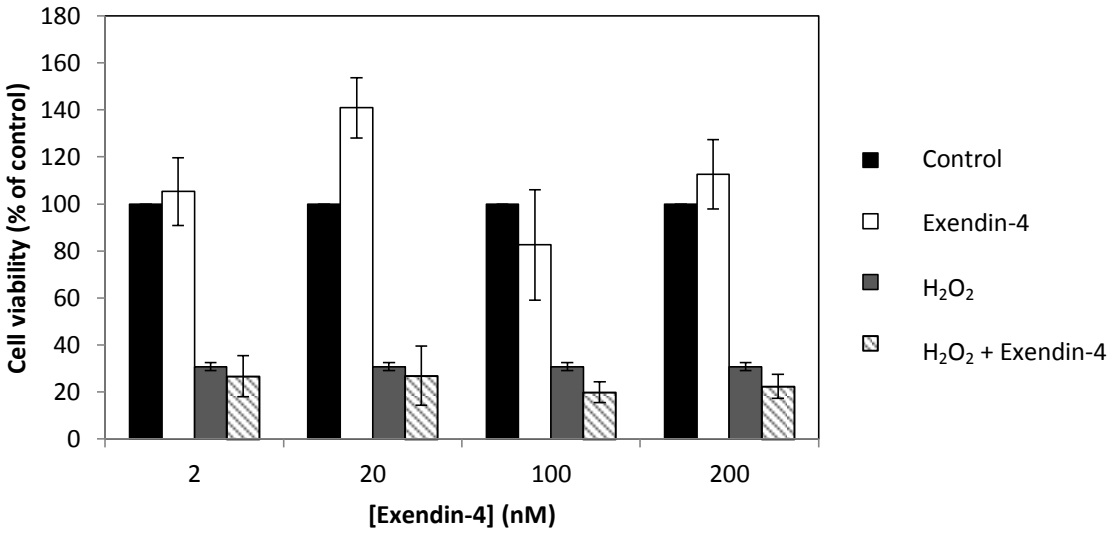

Figure 3.1.10. The effect of exendin-4 pre-treatment on the viability of SH-SY5Y cells treated with 300 μM hydrogen peroxide. Cells were grown to 60% confluence and then pre-treated for 24 h with 2, 20, 100, and 200nM exendin-4 in complete growth medium. Next the cells were washed *in situ* with UltraMEM and then 300 μM hydrogen peroxide and 2, 20, 100, and 200 nM fresh exendin-4 in UltraMEM were added to the cells. Following a further 48 h culture period, an MTS cell viability was performed as described in the Materials and Methods section. Results are expressed as a percentage of the control viability at each exendin-4 concentration and are means ± S.D. (n=3).

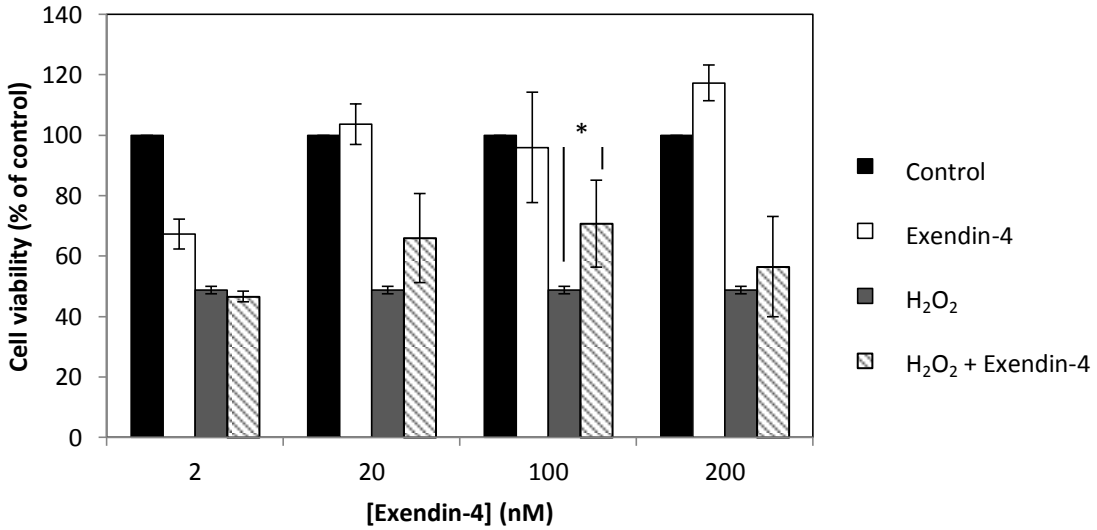

Figure 3.1.11. The effect of exendin-4 pre-treatment on the viability of SH-SY5Y cells treated with 200 μM hydrogen peroxide. Cells were grown to 60% confluence and then pre-treated for 24 h with 2, 20, 100, and 200 nM exendin-4 in complete growth medium. Next the cells were washed *in situ* with UltraMEM and then 200 μM hydrogen peroxide and 2, 20, 100, and200 nM fresh exendin-4 in UltraMEM were added to the cells. Following a further 48 h culture period, an MTS cell viability was performed as described in the Materials and Methods section. Results are expressed as a percentage of the control viability at each exendin-4 concentration and are means ± S.D. (n=3). *, significant at p = 0.05.

3.1.3. GLP-1 analogues and cobalt chloride treatment.

Cobalt chloride was used to mimic hypoxia as it has previously been shown to enhance expression of hypoxia-induced factor-1a (HIF-1a) (Fukuda et al., 2002). As with the hydrogen peroxide previously, a toxicity curve for this stressor was first generated using SH-SY5Y cells. To this end, cells were grown until they were 80% confluent and then washed *in situ* with UltraMEM before replacing this with fresh UltraMEM containing a range of cobalt chloride concentrations (0-1000 μM). The cells were then cultured overnight before conducting an MTS assay (see Materials and Methods section). The results (Fig. 3.1.12.) show that SH-SY5Y were killed in a dose-dependent fashion by cobalt chloride up to a concentration of 300 μM after which the level of viability remained fairly constant. Consequently, it was decided that concentrations between 50 μM and 300 μM would be used in further experiments investigating the potential protective effects of GLP-1 analogues.

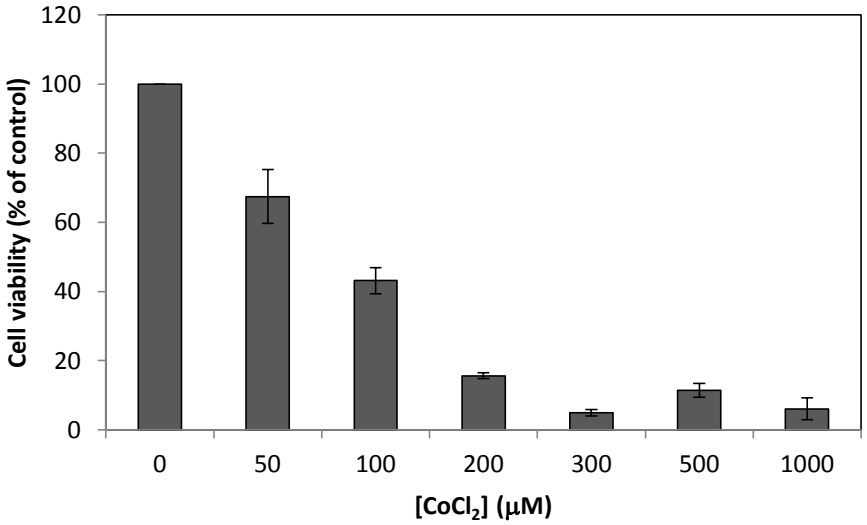

Figure 3.1.12. The effect of cobalt chloride on SH-SY5Y cell viability in the presence of UltraMEM. Cells were grown to 80% confluence, washed *in situ* with UltraMEM and then 0, 50, 100, 200, 300, 500, and 1000 μM cobalt chloride in UltraMEM was added to the cells. Following a further 24 h culture period, an MTS cell viability was performed as described in the Materials and Methods section. Results are expressed as a percentage of the control viability and are means ± S.D. (n=3).

3.1.3.1. Liraglutide and cobalt chloride treatment

Having determined the appropriate concentrations of cobalt chloride to use in the preceding section, the ability of liraglutide to protect against these stressor concentrations was examined. Note that all of these experiments incorporated a pre-treatment step with the GLP-1 analogue. Liraglutide was only tested against a single (200 μM) cobalt chloride concentration but the results (Fig. 3.1.13.) clearly showed a protective effect of the drug against the stressor at this concentration.

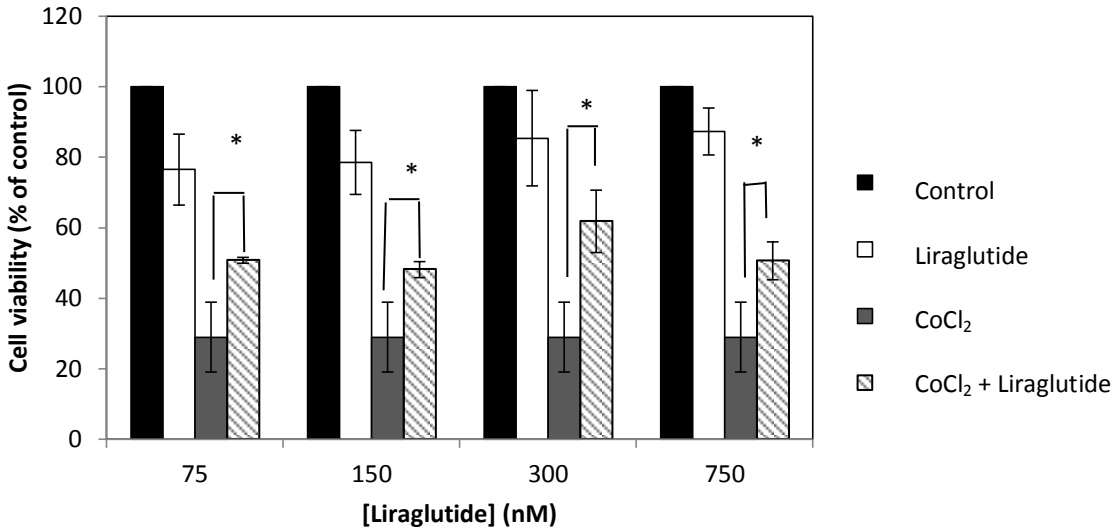

Figure 3.1.13. The effect of liraglutide pre-treatment on the viability of SH-SY5Y cells treated with 200 μM cobalt chloride. Cells were grown to 60% confluence and then pre-treated for 24 h with t75, 150, 300, and 750 nM liraglutide in complete growth medium. Next the cells were washed *in situ* with UltraMEM and then 200 μM cobalt chloride and fresh 75, 150, 300, and 750 nM liraglutide in UltraMEM were added to the cells. Following a further 48 h culture period, an MTS cell viability was performed as described in the Materials and Methods section. Results are expressed as a percentage of the control viability at each liraglutide concentration and are means ± S.D. (n=3). *, significant at $p = 0.05$.

3.1.3.2. Exendin-4 and cobalt chloride treatment

The ability of exendin-4 to protect against cobalt chloride-induced cytotoxicity (this time 50 and 100 μM) was also examined in the same manner. Lower concentrations of the stressor were used in comparison to those used for treatment with Liraglutide in an attempt to increase the effect of exendin-4. However, the results using this GLP-1 analogue failed to show any protective effect against the stressor (Figs. 3.1.14. and 3.1.15.).

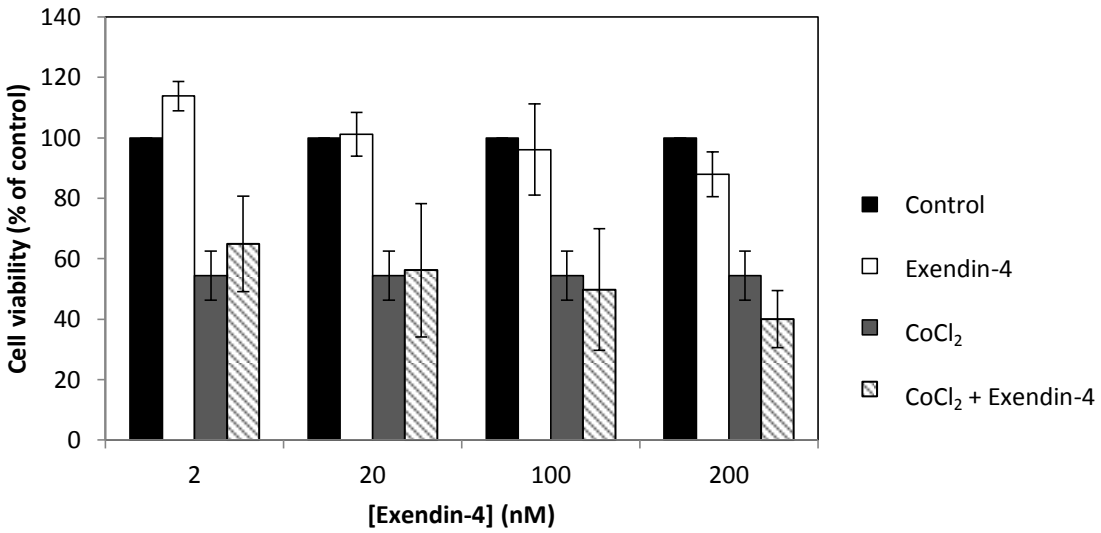

Figure 3.1.14. The effect of exendin-4 pre-treatment on the viability of SH-SY5Y cells treated with 100 μM cobalt chloride. Cells were grown to 60% confluence and then pre-treated for 24 h with 2, 20, 100, and 200 nM exendin-4 in complete growth medium. Next the cells were washed *in situ* with UltraMEM and then 100 μM cobalt chloride and fresh 2, 20, 100, and 200 nM exendin-4 in UltraMEM were added to the cells. Following a further 48 h culture period, an MTS cell viability was performed as described in the Materials and Methods section. Results are expressed as a percentage of the control viability at each exendin-4 concentration and are means ± S.D. (n=3).

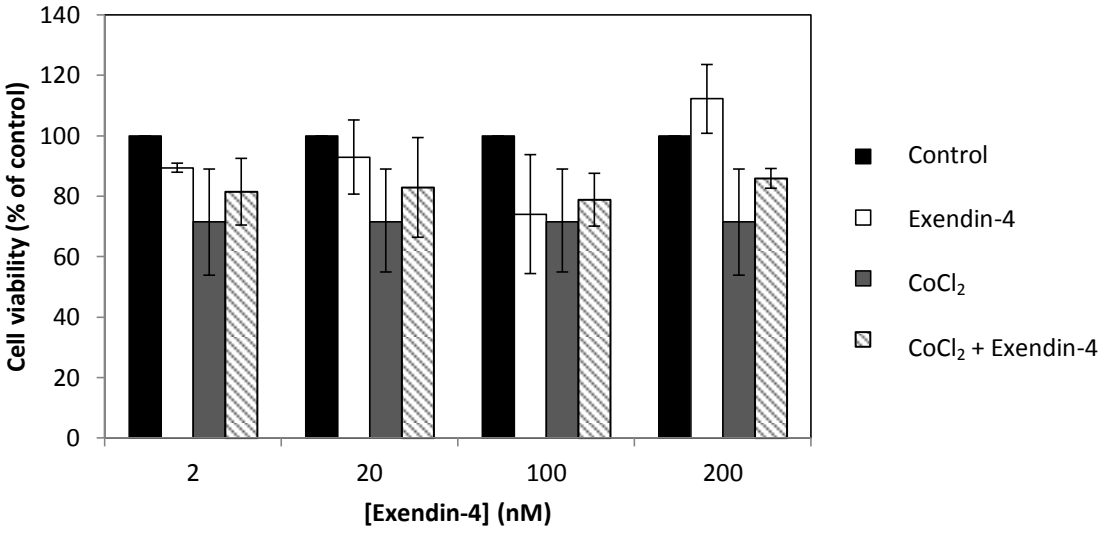

Figure 3.1.15. The effect of exendin-4 pre-treatment on the viability of SH-SY5Y cells treated with 50 μM cobalt chloride. Cells were grown to 60% confluence and then pre-treated for 24 h with 2, 20, 100, and 200 nM exendin-4 in complete growth medium. Next the cells were washed *in situ* with UltraMEM and then 50 μM cobalt chloride and 2, 20, 100, and 200 nM fresh exendin-4 in UltraMEM were added to the cells. Following a further 48 h culture period, an MTS cell viability was performed as described in the Materials and Methods section. Results are expressed as a percentage of the control viability at each exendin-4 concentration and are means ± S.D. (n=3).

3.1.4. GLP-1 analogues and methylglyoxal treatment

Methylglyoxal (MG) is cytotoxic due to its induction of endoplasmic stress-associated reactive oxygen species and associated mitochondrial dysfunction (Palsamy *et al*., 2014, Angeloni *et al*., 2014). In the current study, SH-SY5Y cells were initially exposed to a range of MG concentrations for 24 h and subsequently subjected to an MTS assay in order to determine the appropriate stressor concentrations to use in subsequent GLP-1 analogue experiments. The results (Fig. 3.1.16) showed an intermediate level of cell death of approximately 60-65% at the 2000 μM concentration of MG, with approximately 90% and 5-10% at the 2500 μM and 1500 μM concentrations, respectively. From these results it was determined that MG concentrations of 2000 and 1750 μM would subsequently be used to examine any potential protective effects of GLP-1 analogues against the stressor.

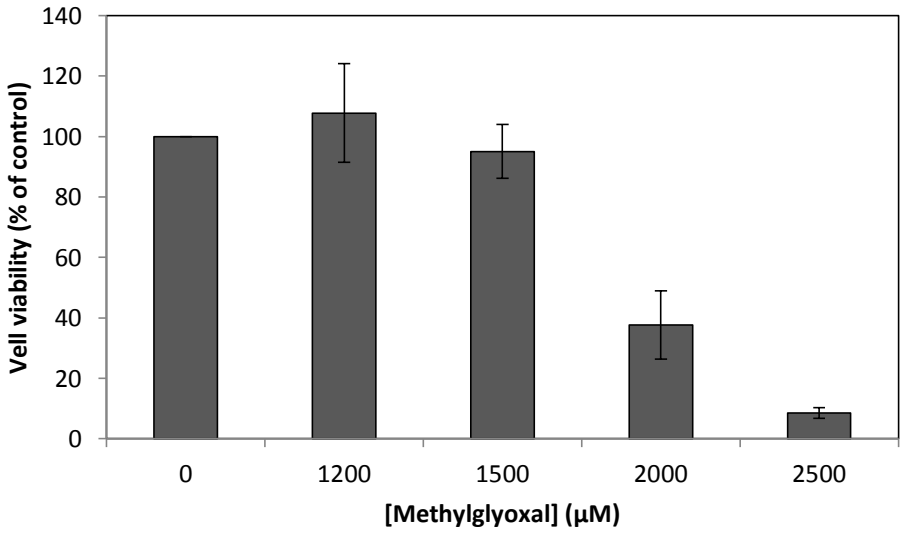

Figure 3.1.16. The effect of methylglyoxal on SH-SY5Y cell viability in the presence of UltraMEM. Cells were grown to 80% confluence, washed *in situ* with UltraMEM and then 0, 1200, 1500, 2000, and 2500 μM methylglyoxal in UltraMEM was added to the cells. Following a further 24 h culture period, an MTS cell viability was performed as described in the Materials and Methods section. Results are expressed as a percentage of the control viability and are means ± S.D. (n=3).

Only the effect of exendin-4 and not liraglutide was tested in relation to MG treatment of SH-SY5Y cells. Note also that here the pre-treatment and treatment steps were reduced to 6 and 17 h, respectively, such that they were more in line with a previous publication (Sharma *et al*., 2014) in which the effect of MG and a GLP-1 analogue on SH-SY5Y cells had been investigated. When the effect of exendin-4 was investigated in relation to 2000 μM MG the results (Fig. 3.1.17.) showed little protective effect of the GLP-1 analogue although, at the lowest exendin-4 concentration (2 nM) there did appear to be a slight but significant effect. However, it is notable that this effect was evident regardless of the presence of MG and so is unlikely to represent a protective effect. Furthermore, no protective effect of exendin-4 was observed when it was tested against a lower MG concentration of 1750 μM (Fig. 3.1.18.).

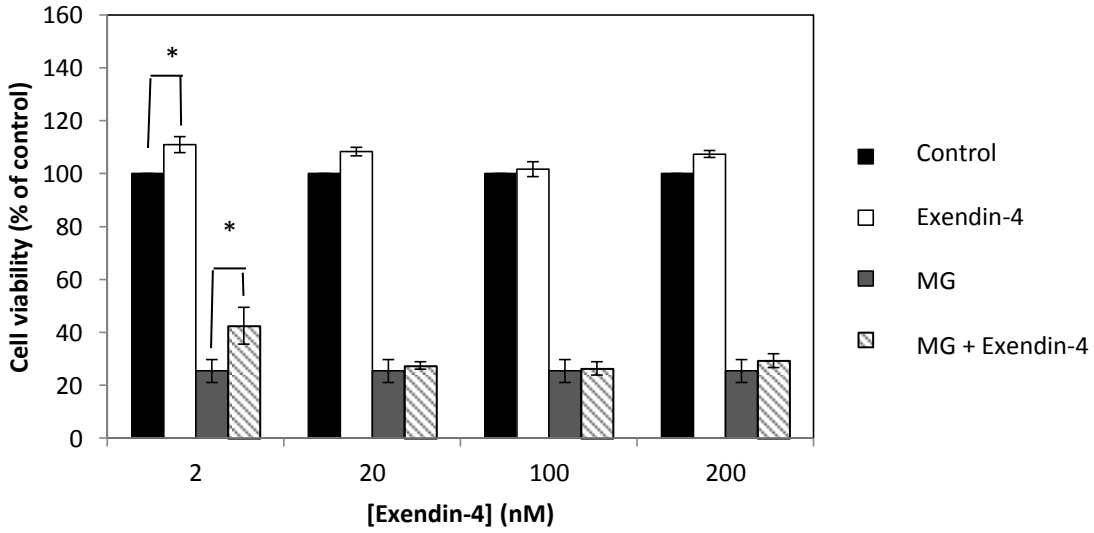

Figure 3.1.17. The effect of exendin-4 pre-treatment on the viability of SH-SY5Y cells treated with 2000 μM methylglyoxal. Cells were grown to 90% confluence and then pre-treated for 6 h with 2, 20, 100, and 200 nM exendin-4 in complete growth medium. Next the cells were washed *in situ* with UltraMEM and then 2000 μM methylglyoxal and 2, 20, 100, and 200 nM fresh exendin-4 in UltraMEM were added to the cells. Following a further 17 h culture period, an MTS cell viability was performed as described in the Materials and Methods section. Results are expressed as a percentage of the control viability at each exendin-4 concentration and are means ± S.D. (n=3). *, significant at $p = 0.05$.

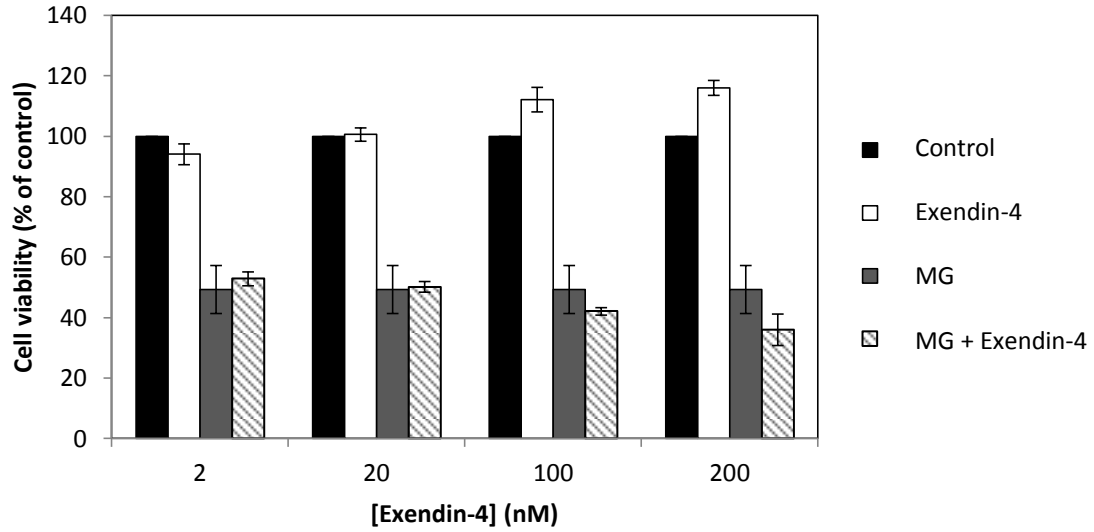

Figure 3.1.18. The effect of exendin-4 pre-treatment on the viability of SH-SY5Y cells treated with 1750 μM methylglyoxal. Cells were grown to 90% confluence and then pre-treated for 6 h with 2, 20, 100, and 200 nM exendin-4 in complete growth medium. Next the cells were washed *in situ* with UltraMEM and then 1750 μM methylglyoxal and 2, 20, 100, and 200 nM fresh exendin-4 in UltraMEM were added to the cells. Following a further 17 h culture period, an MTS cell viability was performed as described in the Materials and Methods section. Results are expressed as a percentage of the control viability at each exendin-4 concentration and are means ± S.D. (n=3).

3.1.5. GLP-1 analogues and thapsigargin treatment

Thapsigargin (TG), an endoplasmic reticulum stressor (Stutzbach *et al*., 2013) was used as it has been shown to cause ER stress which correlates with amyloid-β production in Retinal Ganglion Cells (RGC) (Liu *et al*., 2014). In the current study, suitable concentrations of TG were first determined by treating SH-SY5Y cells for 24 h in the presence of the stressor and then conducting an MTS assay. The results (Fig. 3.1.19.) show that there was a dose-dependent increase in cell death between TG concentrations of 0-100 μM. From these data TG concentrations of 10 and 100 μM were chosen for subsequent GLP-1 analogue experiments.

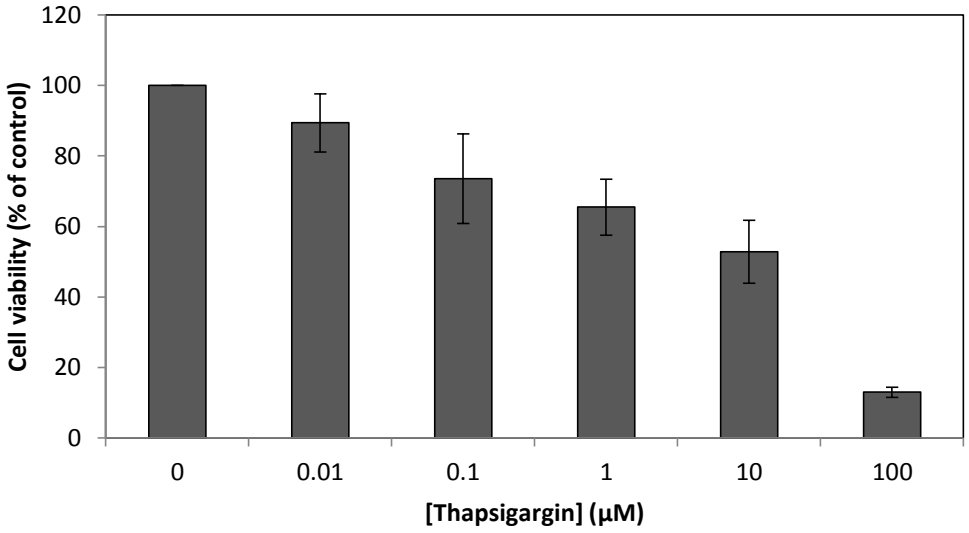

Figure 3.1.19. The effect of thapsigargin on SH-SY5Y cell viability in the presence of UltraMEM. Cells were grown to 80% confluence, washed *in situ* with UltraMEM and then 0, 0.01, 0.1, 1, 10, and 100 μM thapsigargin in UltraMEM was added to the cells. Following a further 24 h culture period, an MTS cell viability was performed as described in the Materials and Methods section. Results are expressed as a percentage of the control viability and are means ± S.D. (n=3).

Next, the ability of exendin-4 to protect SH-SY5Y cells against thapsigargin-induced cytotoxicity was examined. Initially, the GLP-1 analogue showed no protective effect against a 100 μM stressor concentration (Fig. 3.1.20.). However, when a lower (10 μM) thapsigargin concentration was used, there was a significant protective effect of exendin-4 (at 200 nM) against the stressor (Fig. 3.1.21.).

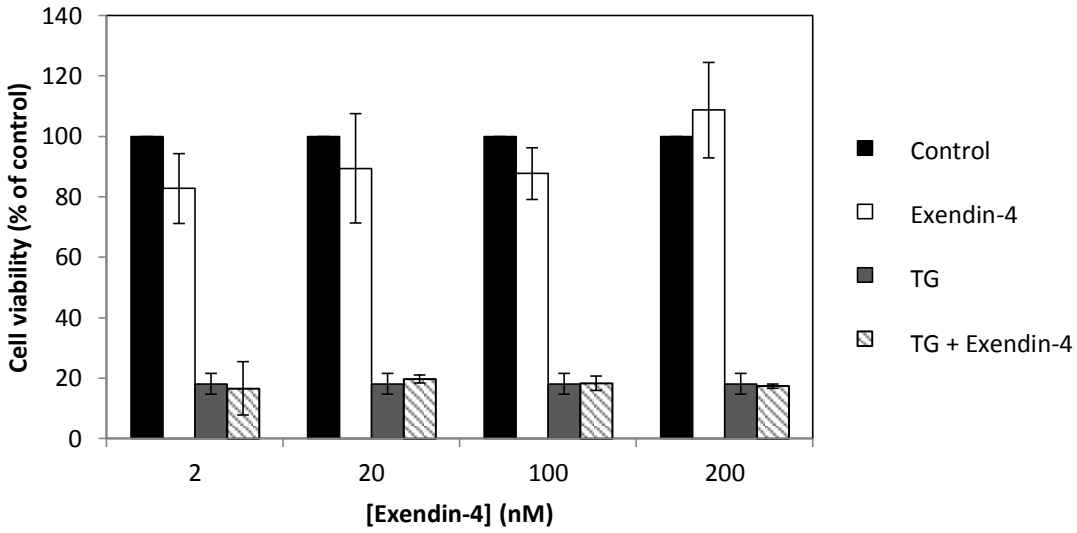

Figure 3.1.20. The effect of exendin-4 pre-treatment on the viability of SH-SY5Y cells treated with 100 μM thapsigargin. Cells were grown to 90% confluence and then pre-treated for 6 h with 2, 20, 100, and 200 nM exendin-4 in complete growth medium. Next the cells were washed *in situ* with UltraMEM and then 100 μM thapsigargin and 2, 20, 100, and 200 nM fresh exendin-4 in UltraMEM were added to the cells. Following a further 17 h culture period, an MTS cell viability was performed as described in the Materials and Methods section. Results are expressed as a percentage of the control viability at each exendin-4 concentration and are means ± S.D. (n=3).

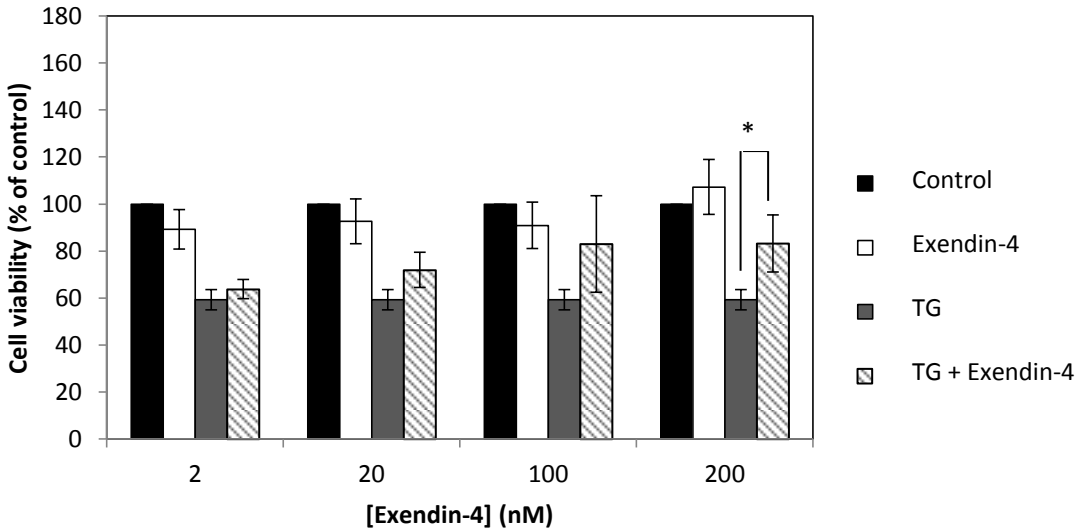

Figure 3.1.21. The effect of exendin-4 pre-treatment on the viability of SH-SY5Y cells treated with 10 μM thapsigargin. Cells were grown to 90% confluence and then pre-treated for 6 h with 2, 20, 100, and 200 nM exendin-4 in complete growth medium. Next the cells were washed *in situ* with UltraMEM and then 10 μM thapsigargin and 2, 20, 100, and 200 nM fresh exendin-4 in UltraMEM were added to the cells. Following a further 17 h culture period, an MTS cell viability was performed as described in the Materials and Methods section. Results are expressed as a percentage of the control viability at each exendin-4 concentration and are means ± S.D. (n=3). *, significant at $p = 0.05$.

3.2. Expression of ADAM10 and ADAM10 substrates in SH-SY5Y cells

In the preceding section it was determined that exendin-4 (200 nM) was able to protect SH-SY5Y cells against the cytotoxic effects of 10 μM thapsigargin. In addition, exendin-4 has previously been shown to alter the amount of mature ADAM10 in the cell membrane fraction (Ohtake *et al*., 2014). As such, the current study next sought to determine whether the protective effect of exendin-4 observed against thapsigargin was linked to changes in the expression/processing of ADAM10 and some of its key substrates (APP, NLGN-1 and PrP). However, before this could be done, it was first necessary to determine the endogenous expression of these proteins and, where necessary, generate stable transfectants over-expressing the same proteins.

3.2.1. Detection of endogenous and over-expressed ADAM10.

In order to characterise endogenous expression of ADAM10 in SH-SY5Y cells, cultures were grown to confluence in T75 flasks and then lysates were prepared, equalized for protein concentration and subjected to PAGE and subsequent immunoblotting with an anti-ADAM10 C-terminal antibody as described in the Materials and Methods section. The results (Fig. 3.2.1.) showed that ADAM10, in addition to some non-specific bands, was detected as bands of approximately 97 and 66 kDa most likely representing the proteolytically immature and mature forms of the protein, respectively.

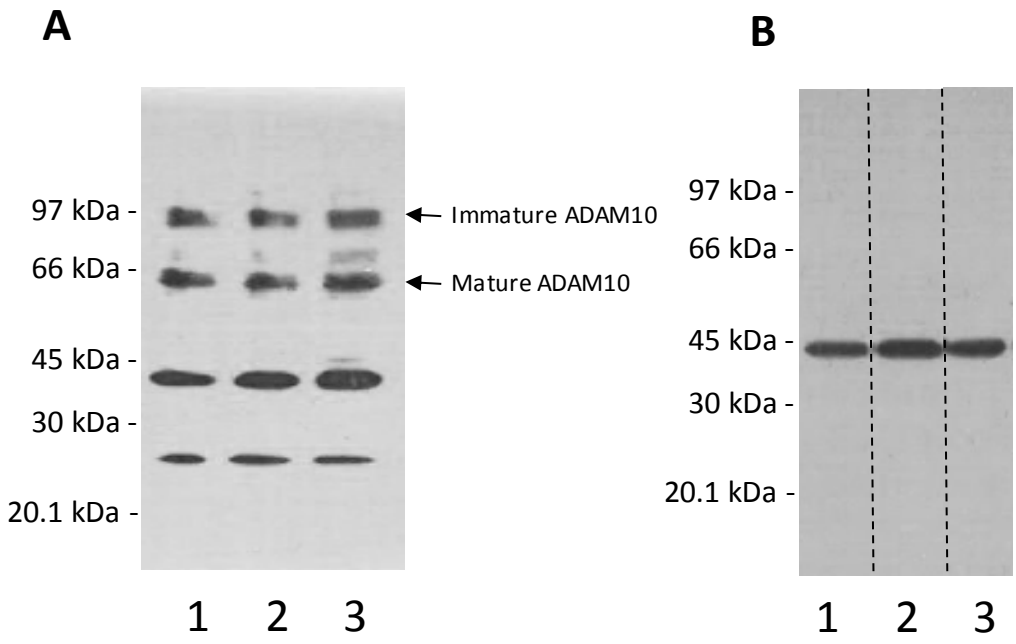

Figure 3.2.1. **Immunodetection of endogenous ADAM10 in SH-SY5Y cell lysates.** Three independent cell cultures (lanes 1-3) were grown to confluence and lysates prepared, equalized in terms of protein and subjected to PAGE and immunoblotting as described in the Materials and Methods section. **A.** Immunodetection using an anti-ADAM10 C-terminal antibody. **B.** Immunodetection using an anti-actin antibody. Dashed lines show where non-adjacent lanes form the same immunoblot were spliced together for the purposes of presentation.

As the exposure times required in order to detect endogenous ADAM10 were extensive it was decided also to generate stable ADAM10 over-expressing SH-SY5Y transfectants. To this end, cells were stably transfected with the pIRESneo-ADAM10 plasmid or empty vector alone (mock transfectants) as described in the Materials and Methods section. Cell lysates were subsequently prepared from both mock- and ADAM-10 stable transfectants and once more immunoblotted with the anti-ADAM10 C-terminal antibody. The results (Fig. 3.2.2.) show the detection of a band at approximately 97 kDa that was more intense in the ADAM10- than the mock-transfectant cell lysates. No increase in a band corresponding to the mature form of ADAM10 was detected. However, interestingly, there was also a very prominent band at around 14.4 kDa in the ADAM10-transfected cell lysates possibly representing the ADAM-cleaved C-terminal fragment of ADAM10 (Tousseyn et al., 2009).

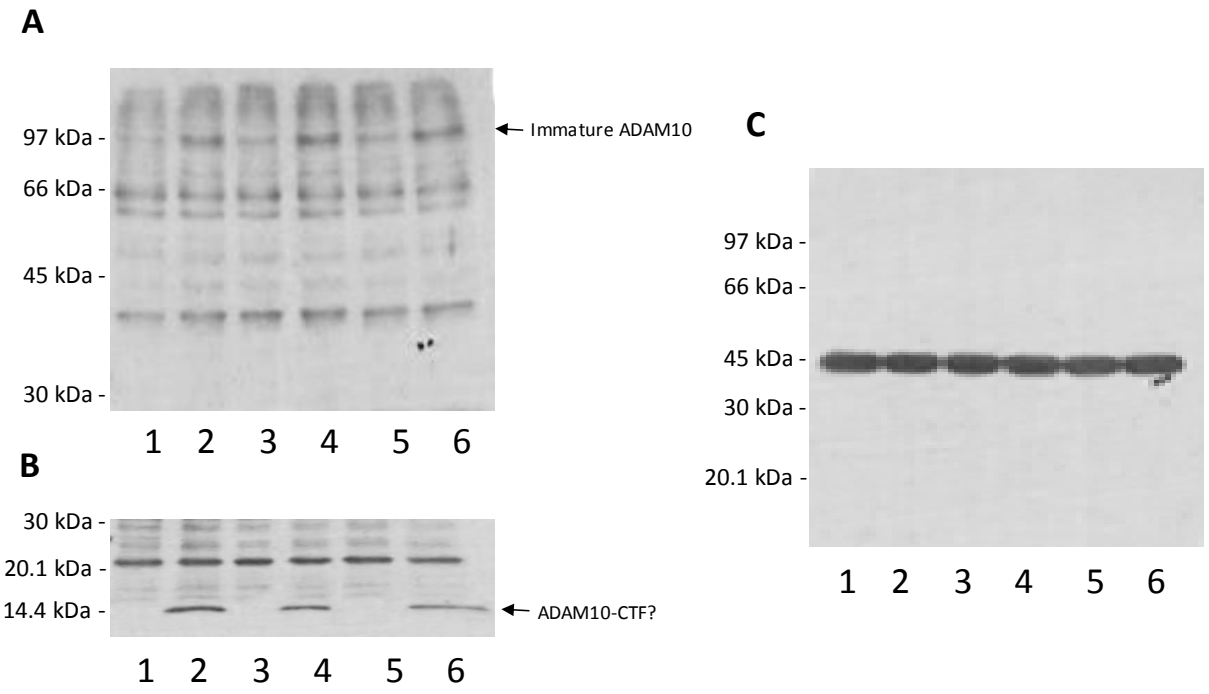

Figure 3.2.2. Immunodetection of over-expressed ADAM10 in SH-SY5Y cell lysates. Three independent cell cultures of mock- (lanes 1,3 and 5) and ADAM10-transfected (lanes 2, 4 and 6) cells were grown to confluence and lysates prepared, equalized in terms of protein and subjected to PAGE and immunoblotting as described in the Materials and Methods section. **A.** Immunodetection using an anti-ADAM10 C-terminal antibody. **B.** Immunodetection using an anti-ADAM10 C-terminal antibody and a lower acrylamide concentration gel in order to show the putative ADAM10-CTF (C-terminal fragment). **C.** Immunodetection using an anti-actin antibody.

3.2.2. Detection of endogenous and over-expressed APP.

APP has previously been shown to be a substrate for ADAM10 by many groups (Gough, Parr-Sturgess and Parkin, 2011, Postina *et al*., 2004). In the current study, the lysate samples used in Fig.3.2.1. were immunoblotted using an anti-APP C-terminal antibody in order to assess endogenous expression of APP. The results (Fig. 3.2.3.) show that APP was detected as a number of bands around 110 kDa consistent with there being multiple APP glycoforms and isoforms in SH-SY5Y cells (Delvaux et al., 2013). In addition, SH-SY5Y cells were stably transfected with an IREShyg- APP_{695} plasmid as described in the Materials and Methods section.

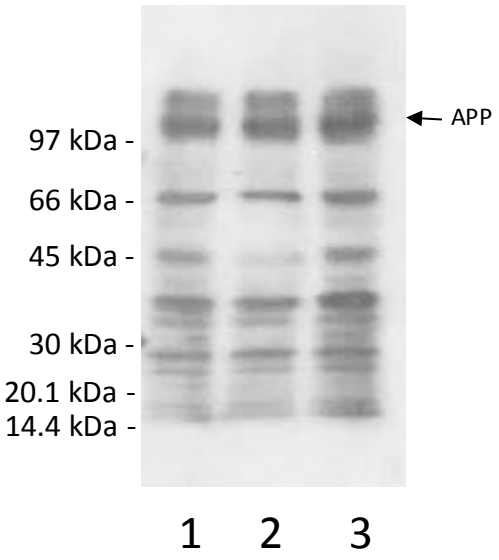

Figure 3.2.3. Immunodetection of endogenous APP in SH-SY5Y cell lysates. Three independent cell cultures (lanes 1-3) were grown to confluence and lysates prepared, equalized in terms of protein and subjected to PAGE and immunoblotting as described in the Materials and Methods section using an anti-APP C-terminal antibody.

Independent T75 flask cultures of both mock- and APP_{695}- transfected cells were grown to confluence and then washed *in situ* with UltraMEM before replacing the wash with 10 ml of the same medium and incubating the cells for a further 24 h. The conditioned medium was then collected and processed and cell lysates prepared as described in the Materials and Methods section. The lysates were then immunoblotted with an anti-APP C-terminal antibody. The results (Fig. 3.2.4.) clearly show that APP_{695} was successfully over-expressed with the protein being so abundant that, at the level of exposure used, endogenous APP was not even detected in the mock-transfected cells.

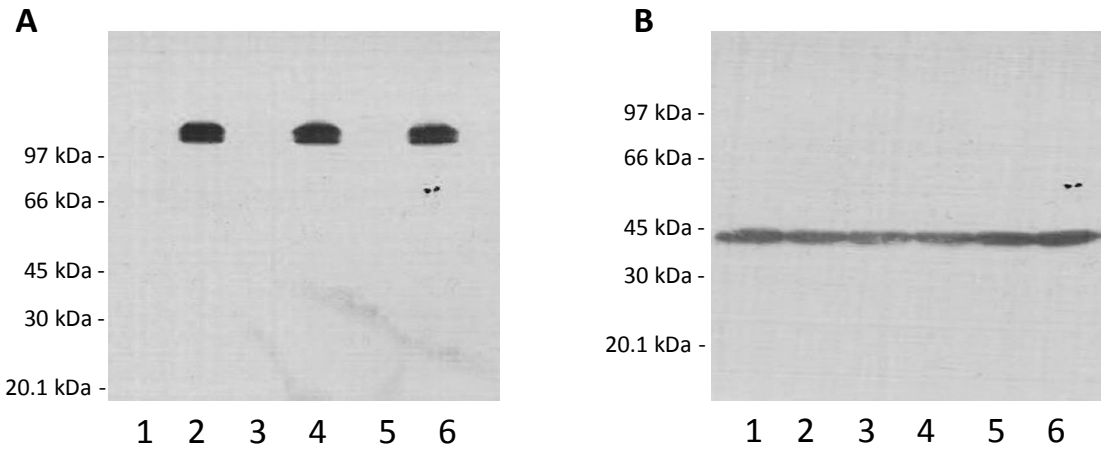

Figure 3.2.4. Immunodetection of over-expressed APP in SH-SY5Y cell lysates. Three independent cell cultures of mock- (lanes 1,3 and 5) and APP_{695}-transfected (lanes 2, 4 and 6) cells were grown to confluence and lysates prepared, equalized in terms of protein and subjected to PAGE and immunoblotting as described in the Materials and Methods section. **A.** Immunodetection using an anti-APP C-terminal antibody. **B.** Immunodetection using an anti-actin antibody.

Next, the 24 h conditioned medium was immunoblotted with antibody 6E10 to detect sAPPα and an anti-sAPPβ antibody. The results show that two bands were detected in conditioned medium using antibody 6E10 (Fig. 3.2.5A); the bottom band corresponded to sAPP695α and the top to a combination of sAPP751/770α. Notably, the lower band was substantially increased in the APP_{695}-transfected cells showing, once again, that the stable transfection had been successful. In contrast, sAPPβ was detected only as a single band and detected only in the APP_{695}-transfected cells (Fig. 3.2.5B).

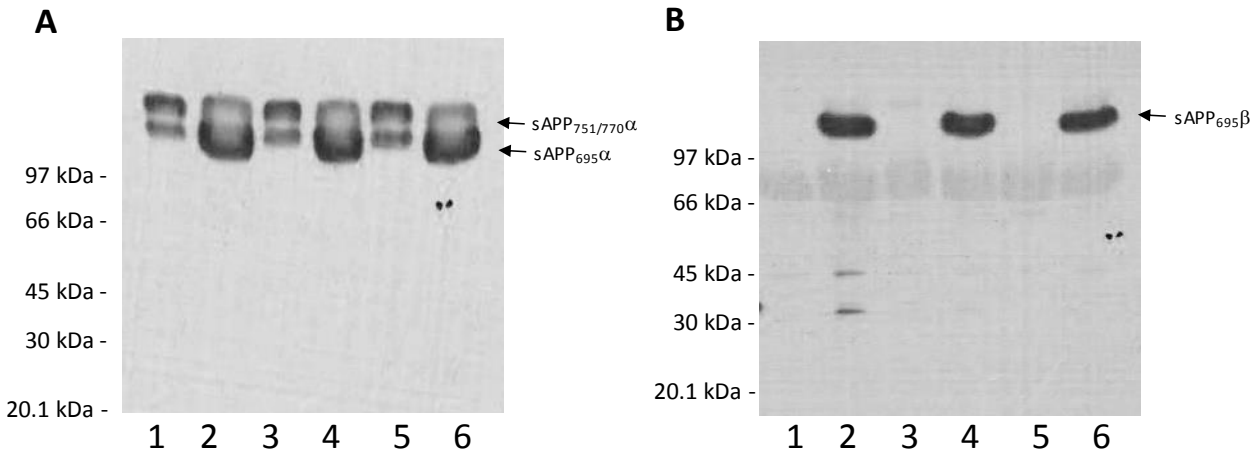

Figure 3.2.5. Immunodetection of over-expressed APP fragments in SH-SY5Y cell conditioned medium. Three independent cell cultures of mock- (lanes 1,3 and 5) and APP_{695}-transfected (lanes 2, 4 and 6) cells were grown to confluence and conditioned medium was prepared and subjected to PAGE and immunoblotting as described in the Materials and Methods section. **A.** Immunodetection of sAPPα using antibody 6E10. **B.** Immunodetection of sAPPβ.

3.2.3. Detection of over-expressed NLGN1.

NLGN1 has also previously been shown to be a substrate for ADAM10 (Suzuki *et al*., 2012). In the current study, the endogenous protein could not be detected in SH-SY5Y cell lysates and so cells were stably transfected with an pIRESneo-NLGN1 plasmid as described in the Materials and Methods section.

Independent T75 flask cultures of both mock- and NLGN1-transfected cells were grown to confluence and then then washed *in situ* with UltraMEM before replacing the wash with 10 ml of the same medium and incubating the cells for a further 24 h. The conditioned medium was then collected and processed and cell lysates prepared as described in the Materials and Methods section. The lysates were then immunoblotted with an anti-NLGN1 N-terminal antibody. The results (Fig. 3.2.6.) showed a band at 110 kDa the intensity of which was enhanced in the NLGN1-transfected cell lysates consistent with previously reported sizes for the protein (Peixoto et al., 2012).

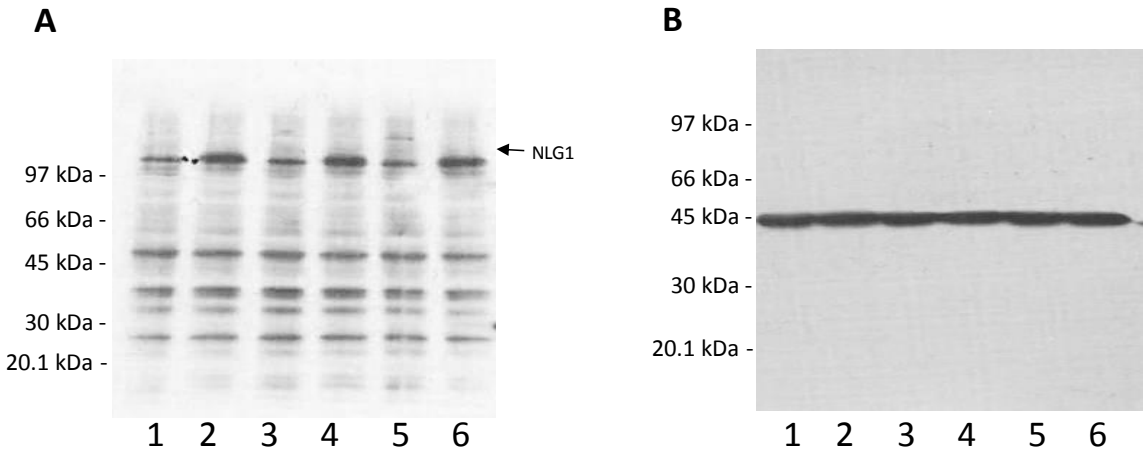

Figure 3.2.6. Immunodetection of over-expressed NLGN1 in SH-SY5Y cell lysates. Three independent cell cultures of mock- (lanes 1,3 and 5) and NLGN1-transfected (lanes 2, 4 and 6) cells were grown to confluence and lysates prepared, equalized in terms of protein and subjected to PAGE and immunoblotting as described in the Materials and Methods section. **A.** Immunodetection using an anti-NLGN1 N-terminal antibody. **B.** Immunodetection using an anti-actin antibody.

Next, the 24 h conditioned medium was immunoblotted with the same anti-NLGN1 N-terminal. The results (Fig. 3.2.7.) showed a very intense band again at around 110 kDa in only the NLGN1-transfected cell lysates proving that the stable transfection had worked and that the protein was shed from cells into conditioned medium.

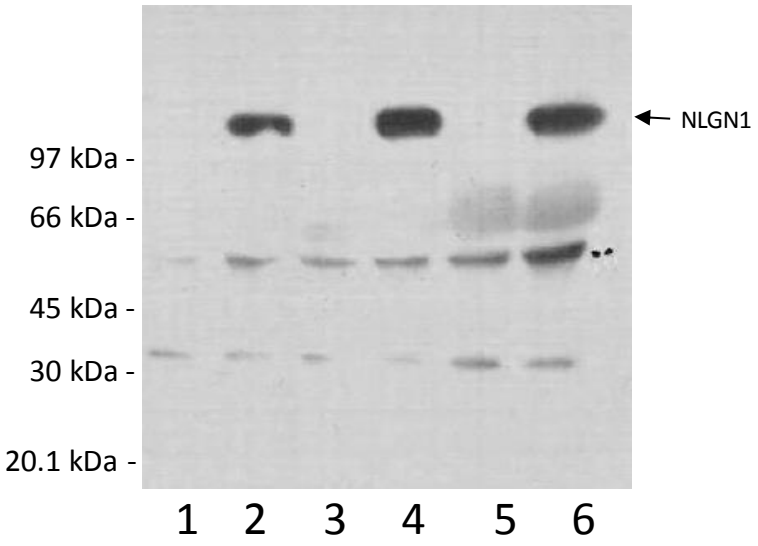

Figure 3.2.7. Immunodetection of over-expressed NLGN1 fragments in SH-SY5Y cell conditioned medium. Three independent cell cultures of mock- (lanes 1,3 and 5) and NLGN1-transfected (lanes 2, 4 and 6) cells were grown to confluence and conditioned medium was prepared and subjected to PAGE and immunoblotting as described in the Materials and Methods section using an anti-NLGN1 N-terminal antibody.

3.2.4. Detection of endogenous and over-expressed PrP.

PrP was originally shown to be shed from the cell surface by the action of both a phospholipase and an ADAM-like activity in a 'dual shedding' manner (Parkin et al., 2004). It was subsequently shown that ADAM10 was the zinc metalloproteinase responsible for this shedding activity (Taylor et al., 2009). In the current study, endogenous PrP was detected in cell lysates using the SAF32 antibody as a typical smear centred around 35 kDa (Fig. 3.2.8A.). Minor amounts of the endogenous protein were also detected in conditioned medium using the same antibody and appeared to exist largely as unglycosylated fragments (Fig. 3.2.8B.).

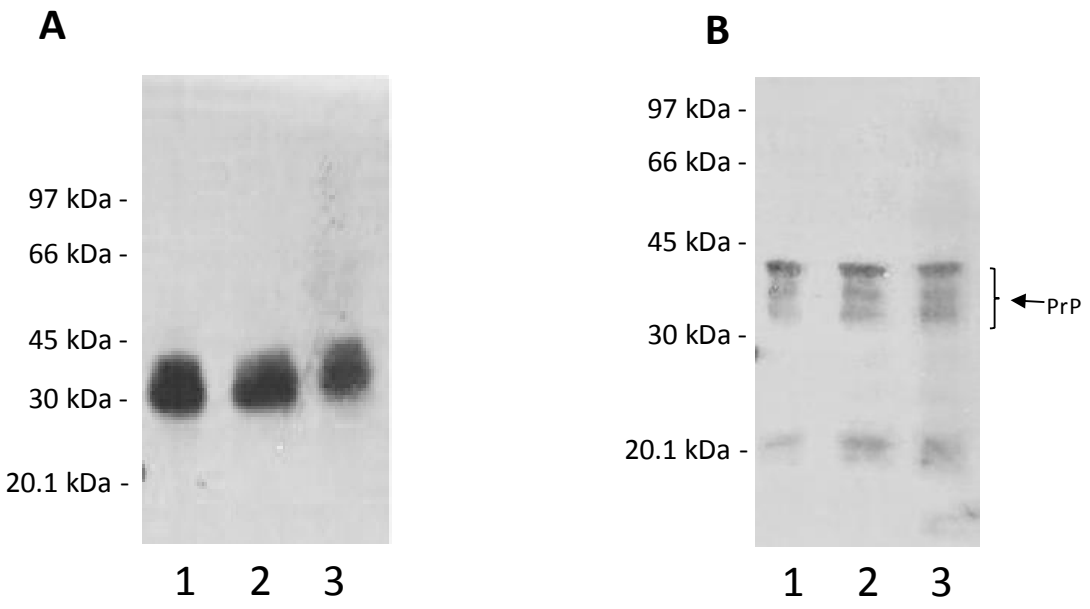

Figure 3.2.8. Immunodetection of endogenous PrP in SH-SY5Y cell lysates and conditioned medium. Three independent cell cultures (lanes 1-3) were grown to confluence and incubated for 24 h with UltraMEM. Cell lysates and conditioned medium samples were then prepared as detailed in the Materials and Methods section. **A.** Immunodetection of PrP in cell lysates using SAF32. **B.** Immunodetection of PrP in conditioned medium using SAF32.

As only very low levels of endogenous PrP were detected in conditioned medium, stable transfectants were also generated using a pIRESneo-PrP plasmid as described in the Materials and Methods section.

Independent T75 flask cultures of both mock- and PrP-transfected cells were grown to confluence and then washed *in situ* with UltraMEM before replacing the wash with 10 ml of the same medium and incubating the cells for a further 24 h. The conditioned medium was then collected and processed and cell lysates prepared as described in the Materials and Methods section. The lysates were then immunoblotted with the SAF32 antibody. The results (Fig. 3.2.9.) clearly show that PrP was successfully over-expressed with the protein being so abundant that, at the level of exposure used, endogenous PrP was barely detected in the mock-transfected cells.

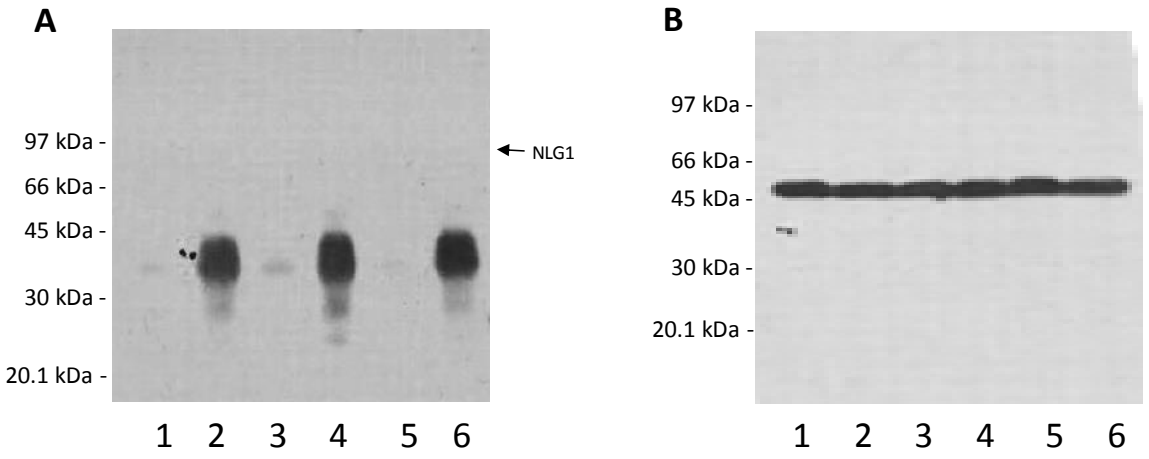

Figure 3.2.9. Immunodetection of over-expressed PrP in SH-SY5Y cell lysates. Three independent cell cultures of mock- (lanes 1,3 and 5) and PrP-transfected (lanes 2, 4 and 6) cells were grown to confluence and lysates prepared, equalized in terms of protein and subjected to PAGE and immunoblotting as described in the Materials and Methods section. **A.** Immunodetection using SAF32. **B.** Immunodetection using an anti-actin antibody.

Next the conditioned medium was also immunoblotted with SAF32 and the results (Fig. 3.2.10.) clearly shed that, not only was PrP successfully over-expressed, it was effectively shed into the conditioned medium of cells.

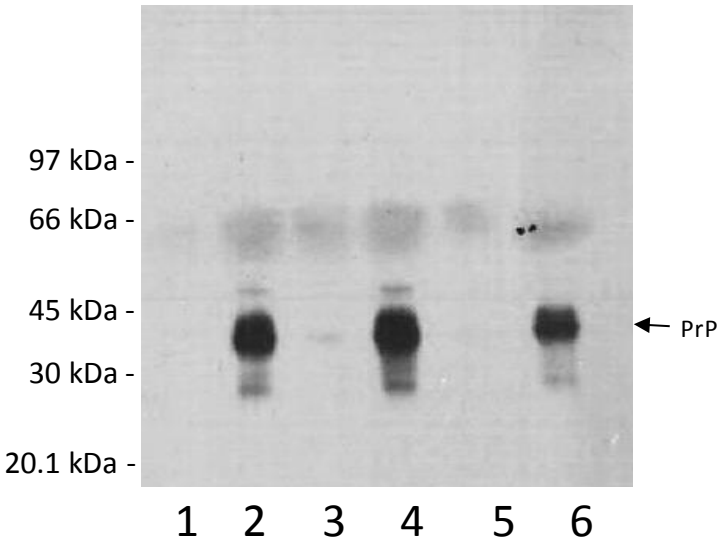

Figure 3.2.10. Immunodetection of over-expressed PrP fragments in SH-SY5Y cell conditioned medium. Three independent cell cultures of mock- (lanes 1,3 and 5) and PrP-transfected (lanes 2, 4 and 6) cells were grown to confluence and conditioned medium was prepared and subjected to PAGE and immunoblotting as described in the Materials and Methods section using the SAF32 antibody.

3.3. The effects of exendin-4 and thapsigargin on the expression and proteolysis of ADAM10 and its substrates.

This study determined that exendin-4 (200 nM) protected SH-SY5Y cells against thapsigargin-mediated toxicity (section 3.1.5.). Having generated stable transfectants over-expressing ADAM10 or its key substrates (section 3.2.), the next step was to examine whether thapsigargin treatment in the absence or presence of exendin-4 altered the expression/proteolysis of the over-expressed proteins.

3.3.1. The effect of exendin-4 and thapsigargin on the expression and proteolytic maturation of over-expressed ADAM10

SH-SY5Y-ADAM10 stable transfectants were grown to 90% confluence in T75 flasks and then pre-treated with 200 nM exendin-4 for 6 h before further incubating the cells in the presence of 10 μM thapsigargin and/or fresh exendin-4 for a further 17 h. The cells were then harvested, processed and immunoblotted with anti-ADAM10 C-terminal antibody as described in the Materials and Methods section. The results (Fig. 3.3.1.A) suggest that treatment with thapsigargin decreases mature ADAM10 and increases immature ADAM10, with figure 3.3.1.C confirming that all protein

levels were equal between samples. Following image processing analysis, figure 3.3.1.B shows a significant increase in the levels of immature ADAM10 in response to thapsigargin treatment with a concomitant decrease in levels of the proteolytically mature form of the enzyme. Exendin-4, in the presence of thapsigargin, had no significant remedial effect on levels of immature and mature protein.

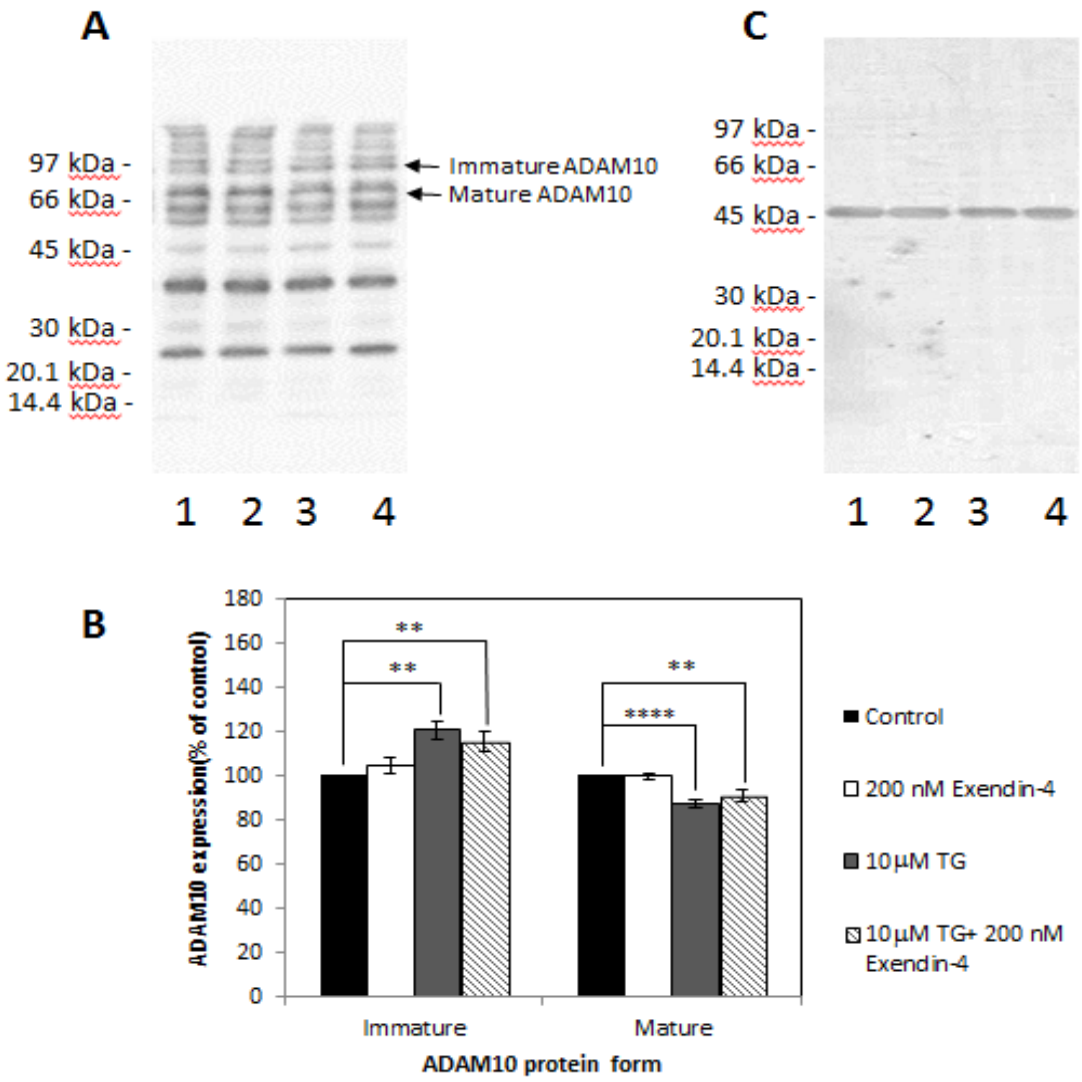

Figure 3.3.1. The effect of exendin-4 and thapsigargin treatments on ADAM10 expression and proteolytic maturation in SH-SY5Y-ADAM10 cells. Cells were grown to confluence in T75 flasks before being pre-treated for 6 h with 200 nM exendin-4 in complete growth medium. Next the cells were washed *in situ* with 10 ml UltraMEM before adding a fresh 10 ml of the same medium containing the relevant treatment (lane 1, control; lane 2, exendin-4; lane 3, thapsigargin (10 µM); lane 4, exendin-4 + thapsigargin (10 µM). The cells were then cultured for a further 17 h before harvesting them, preparing cell lysates and immunoblotting with **A**. Anti-ADAM10 C-terminal antibody and **C**. Anti-actin antibody. Representative blots are shown for each experiment, which was repeated in triplicate and multiple ADAM10 blots were quantified and the relative levels of the immature and proteolytically mature protein are shown in B**.** Results are means ± S.D. (n=3). **, significant at 0.01; ****, significant at p = 0.001.

3.3.2. The effect of exendin-4 and thapsigargin on the expression and proteolytic shedding of endogenous APP

Untransfected SH-SY5Y cells were treated with exendin-4 and/or thapsigargin as described in the preceding section and cells and conditioned medium samples were harvested and processed as described in the Materials and Methods section. Initially, the lysates were immunoblotted with the anti-APP C-terminal antibody and the results (Fig. 3.3.2.) show that thapsigargin treatment reduced APP holoprotein levels by approximately 50% relative to the control cultures. Interestingly, exendin-4 was able to significantly reverse this effect.

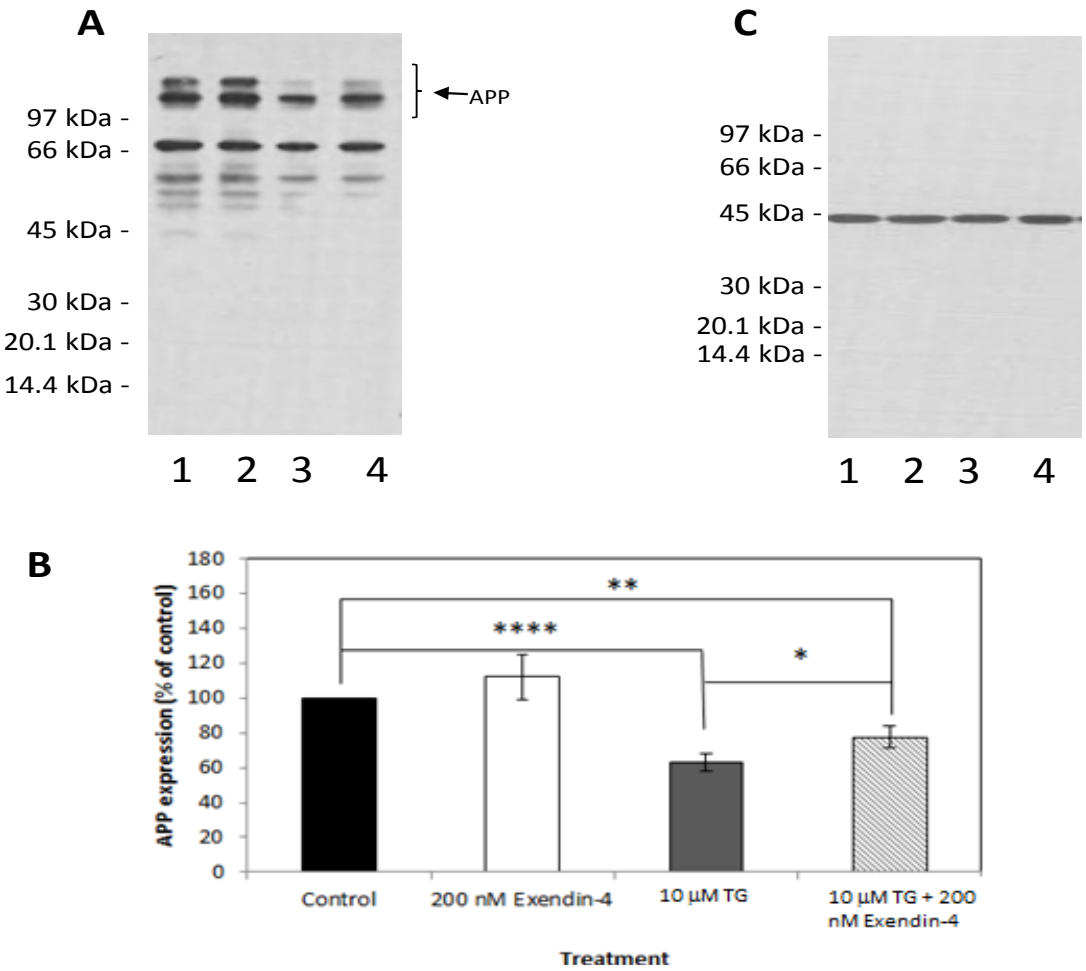

Figure 3.3.2. The effect of exendin-4 and thapsigargin treatments on endogenous APP expression in untransfected SH-SY5Y cells. Cells were grown to confluence in T75 flasks before pre-treatment for 6 h with 200 nM exendin-4 in complete growth medium. The cells were washed *in situ* with 10 ml UltraMEM before adding a fresh 10 ml of the same medium containing the relevant treatment (lane 1, control; lane 2, exendin-4; lane 3, thapsigargin (10 µM); lane 4, exendin-4 + thapsigargin (10 µM). The cells were cultured for a further 17 h before harvesting, preparing cell lysates and immunoblotting with **A**. Anti-APP C-terminal antibody and **C**. Anti-actin antibody. Representative blots are shown for each experiment which was repeated in triplicate and multiple APP blots were quantified and the relative levels of the protein are shown in **B.** Results are means ± S.D. (n=3). *, significant at $p = 0.05$; **, significant at p = 0.01; ****, significant at p = 0.001.

The conditioned medium samples were then immunoblotted with antibody 6E10 to detect sAPPα and the anti-sAPPβ antibody. The results (Fig. 3.3.3.) show that sAPPα was significantly decreased and sAPPβ was dramatically decreased in the conditioned medium from thapsigargin-treated cells; though this could not be deemed significant as n=1 and therefore a statistical 1 tailed, type 2 could not be performed. However, exendin-4 either on its own or in the presence of thapsigargin had no additional significant effect of sAPPα or sAPPβ levels.

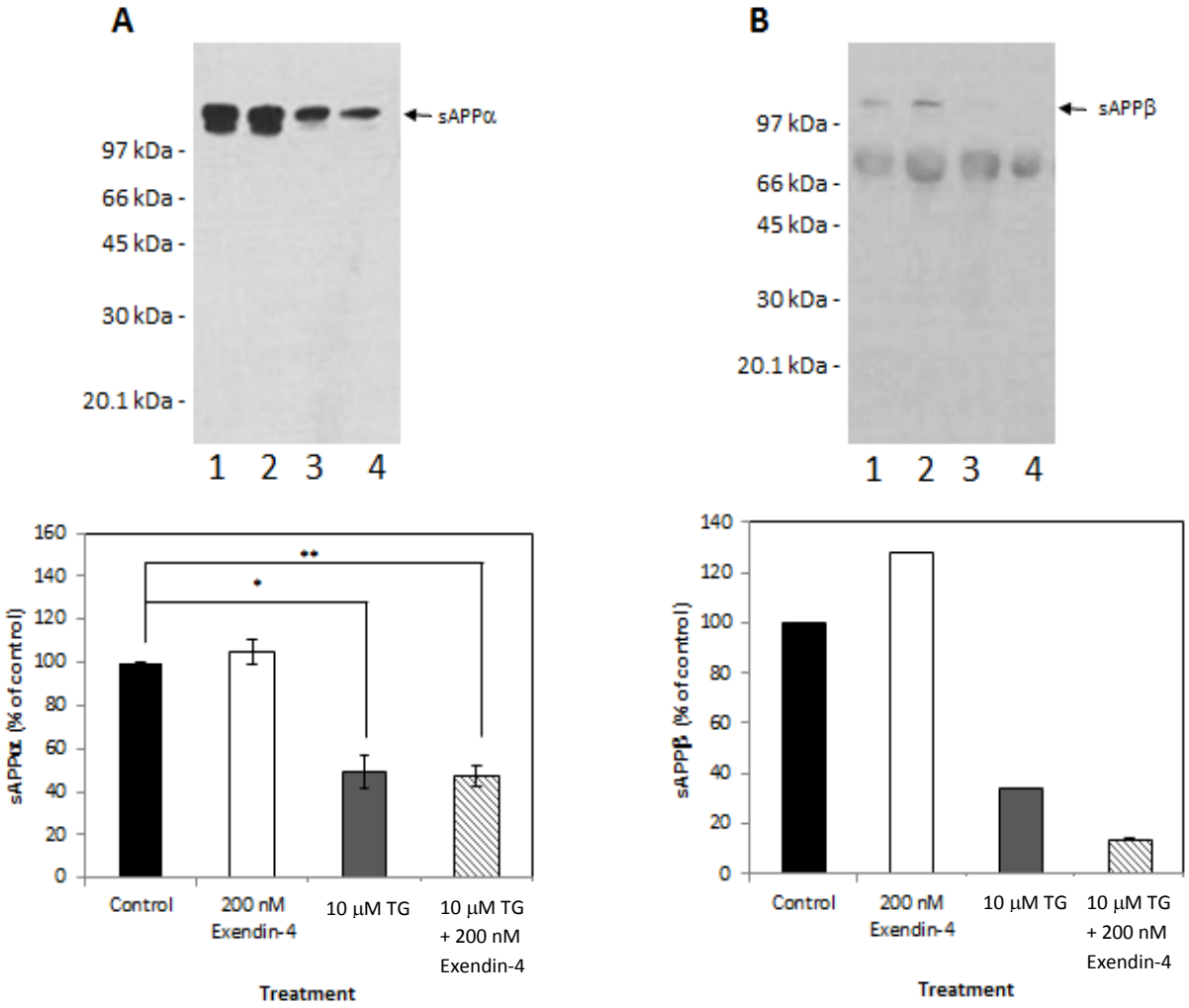

Figure 3.3.3. The effect of exendin-4 and thapsigargin treatments on the levels of soluble APP in conditioned medium from untransfected SH-SY5Y cells. Cells were grown to confluence in T75 flasks before pre-treatment for 6 h with 200 nM exendin-4 in complete growth medium. The cells were washed *in situ* with 10 ml UltraMEM before adding a fresh 10 ml of the same medium containing the relevant treatment (lane 1, control; lane 2, exendin-4; lane 3, thapsigargin (10 μM); lane 4, exendin-4 + thapsigargin (10 μM). The cells were cultured for a further 17 h before harvesting the conditioned medium, processing it as described in the Materials and Methods section and immunoblotting with **A**. Antibody 6E10 and **B**. Anti-sAPPβ antibody. Multiple immunoblots were quantified and the relative amounts of each APP fragment are displayed graphically underneath the corresponding immunoblot. Results are means ± S.D. (n=3 for sAPPα and n=1 for sAPPβ). *, significant at $p = 0.05$; **, significant at p = 0.01.

3.3.3. The effect of exendin-4 and thapsigargin on the expression and proteolytic shedding of over-expressed APP_{695}

The experiments described in the preceding section were also performed using APP_{695} over-expressing SH-SY5Y cells. The results from these latter experiments (Fig. 3.3.4.) showed that thapsigargin enhanced the expression of APP in these cells, both of which were significant at the p = 0.05 threshold. However, exendin-4 had no significant effect on expression either in the absence or presence of thapsigargin.

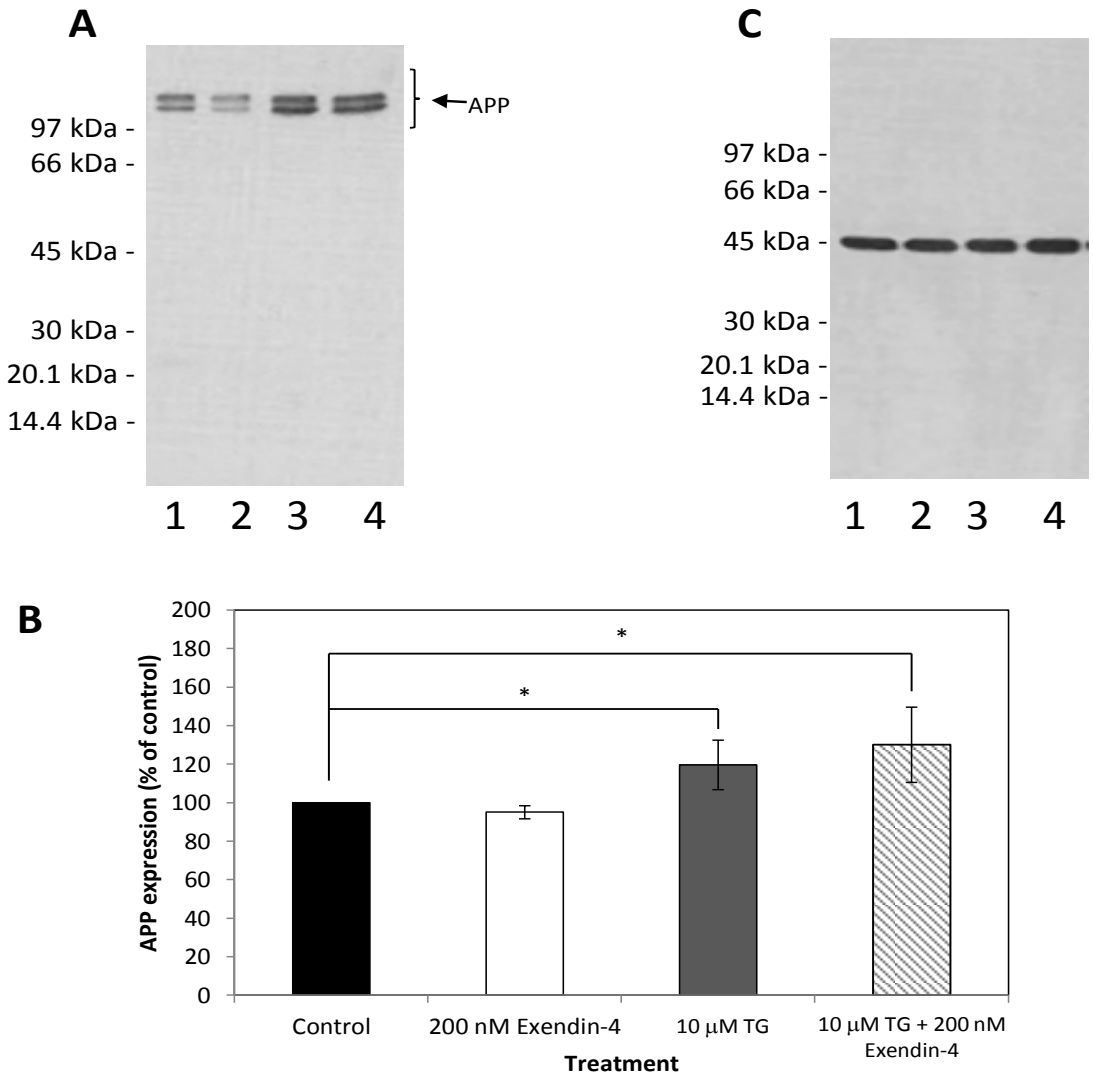

Figure 3.3.4. The effect of exendin-4 and thapsigargin treatments on APP expression in SH-SY5Y-APP_{695} cells. Cells were grown to confluence in T75 flasks before pre-treatment for 6 h with 200 nM exendin-4 in complete growth medium. The cells were washed *in situ* with 10 ml UltraMEM before adding a fresh 10 ml of the same medium containing the relevant treatment (lane 1, control; lane 2, exendin-4; lane 3, thapsigargin (10 μM); lane 4, exendin-4 + thapsigargin (10 μM). The cells were then cultured for a further 17 h before harvesting, preparing cell lysates and immunoblotting with **A**. Anti-APP C-terminal antibody and **C**. Anti-actin antibody. Representative blots are shown for each experiment which was repeated in triplicate and multiple APP blots were quantified and the relative levels of the protein are shown in **B.** Results are means ± S.D. (n=3). *, significant at p = 0.05.

Next the conditioned medium from these cells was immunoblotted with antibody 6E10 and anti-sAPPβ antibody. The results (Fig. 3.3.5A.) showed that thapsigargin alone had no effect on sAPPα generation but that exendin-4, when added in the presence of thapsigargin, resulted in a significant increase in sAPPα shedding. In contrast, neither thapsigargin or exendin-4 had any significant effect of sAPPβ production whether used individually or in combination (Fig. 3.3.5B).

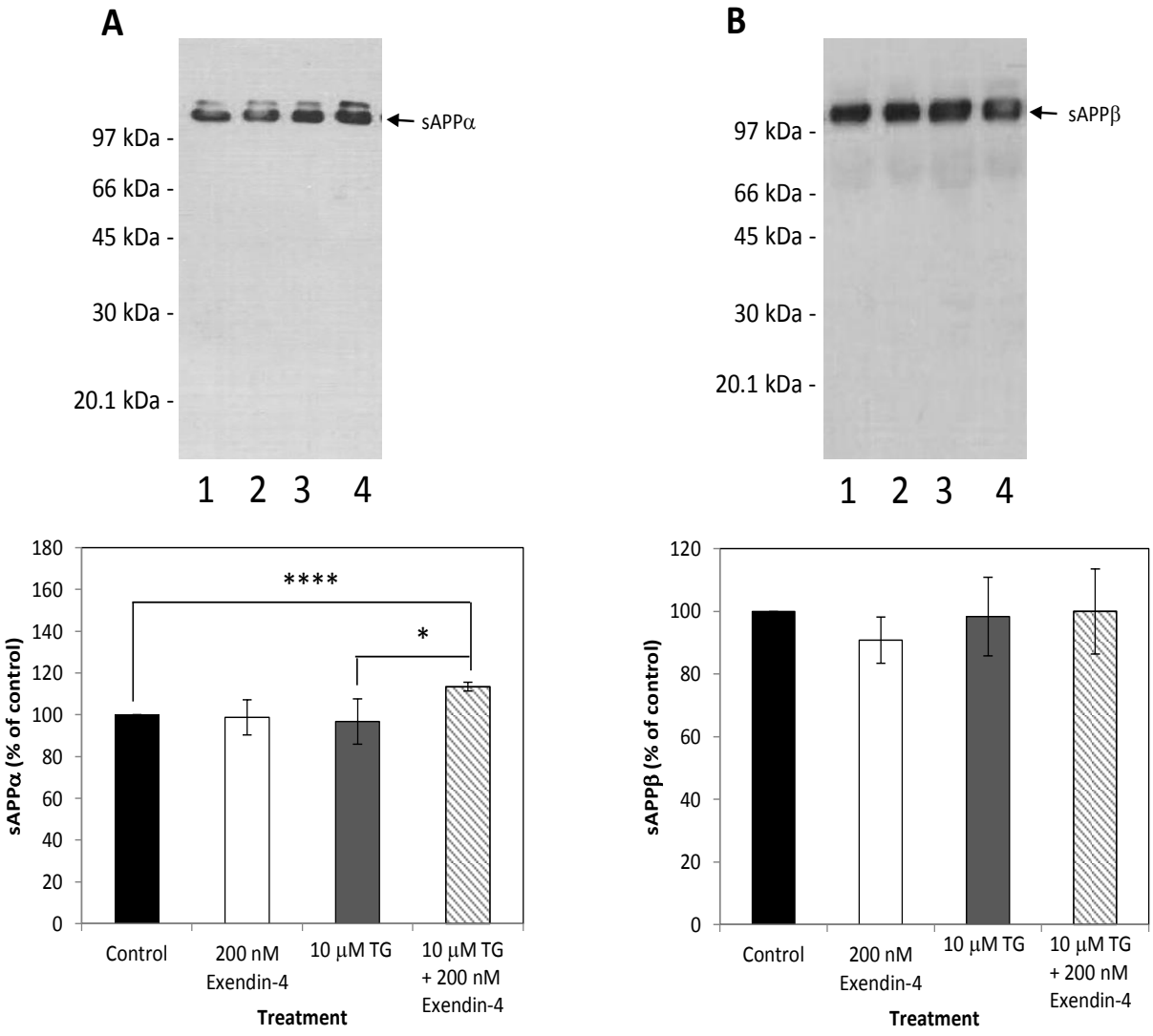

Figure 3.3.5. The effect of exendin-4 and thapsigargin treatments on the levels of soluble APP in conditioned medium from SH-SY5Y-APP$_{695}$ cells. Cells were grown to confluence in T75 flasks before pre-treatment for 6 h with 200 nM exendin-4 in complete growth medium. The cells were washed *in situ* with 10 ml UltraMEM before adding a fresh 10 ml of the same medium containing the relevant treatment (lane 1, control; lane 2, exendin-4; lane 3, thapsigargin (10 μM); lane 4, exendin-4 + thapsigargin (10 μM). The cells were cultured for a further 17 h before harvesting the conditioned medium, processing it as described in the Materials and Methods section and immunoblotting with **A**. Antibody 6E10 and **B**. Anti-sAPPβ antibody. Multiple immunoblots were quantified and the relative amounts of each APP fragment are displayed graphically underneath the corresponding immunoblot. Results are means ± S.D. (n=3). *, significant at *p* = 0.05; ****, significant at p = 0.001.

3.3.4. The effect of exendin-4 and thapsigargin on the expression and proteolytic shedding of over-expressed NLGN1

The experiments described in preceding sections were again repeated but this time using SH-SY5Y-NLGN1 stable transfectants. The results (Fig. 3.3.6.) showed a significant decrease of NLGN1 expression in cells treated with thapsigargin and exendin-4 in comparison to those treated with thapsigargin or exendin-4 alone.

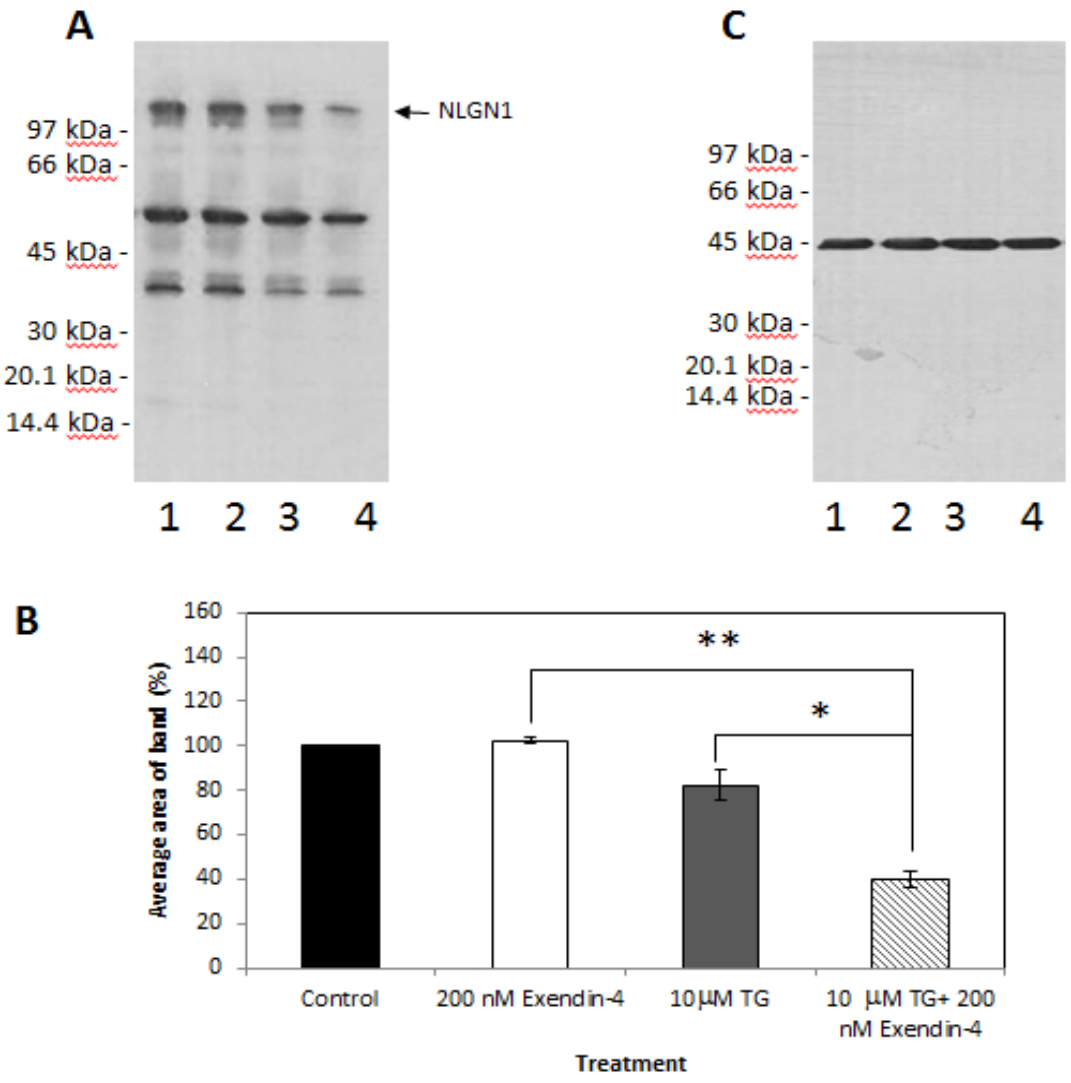

Figure 3.3.6. The effect of exendin-4 and thapsigargin treatments on NLGN1 expression in SH-SY5Y-NLGN1 cells. Cells were grown to confluence in T75 flasks before being pre-treated for 6 h with 200 nM exendin-4 in complete growth medium. Next the cells were washed *in situ* with 10 ml UltraMEM before adding a fresh 10 ml of the same medium containing the relevant treatment (lane 1, control; lane 2, exendin-4; lane 3, thapsigargin (10 µM); lane 4, exendin-4 + thapsigargin (10 µM). The cells were then cultured for a further 17 h before harvesting them, preparing cell lysates and immunoblotting with **A**. Anti-NLGN1 N-terminal antibody and **C**. Anti-actin antibody. Representative blots are shown for each experiment which was repeated in triplicate and multiple NLGN1 blots were quantified and the relative levels of the protein are shown in **B.** Results are means ± S.D. *, significant at p=0.05, **, significant at p=0.01.

Conditioned medium samples from the same experiment were also immunoblotted using the anti-NLGN1 N-terminal antibody and the results (Fig. 3.3.7.) show that, whilst thapsigargin alone did not alter shedding of NLGN1 into conditioned medium in comparison to the control, the co-treatment of thapsigargin-treated cells with exendin-4 did result in an increase in NLGN1 shedding.

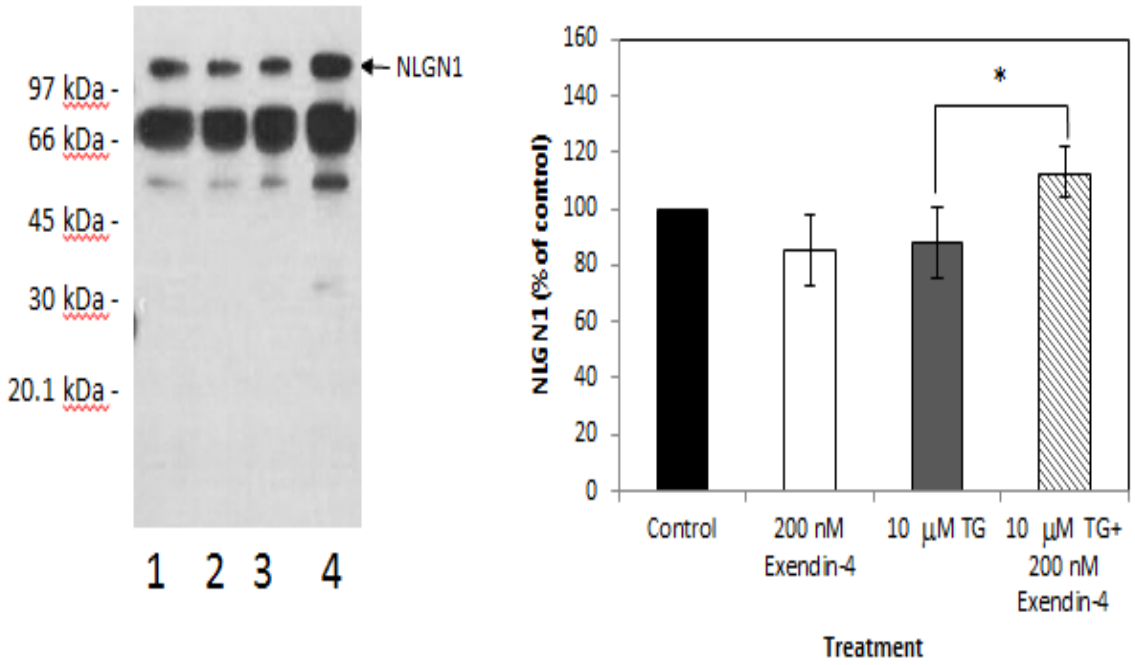

Figure 3.3.7. The effect of exendin-4 and thapsigargin treatments on the levels of soluble NLGN1 in conditioned medium from SH-SY5Y-NLGN1 cells. Cells were grown to confluence in T75 flasks before pre-treatment for 6 h with 200 nM exendin-4 in complete growth medium. The cells were washed *in situ* with 10 ml UltraMEM before adding a fresh 10 ml of the same medium containing the relevant treatment (lane 1, control; lane 2, exendin-4; lane 3, thapsigargin (10 μM); lane 4, exendin-4 + thapsigargin (10 μM). The cells were cultured for a further 17 h before harvesting the conditioned medium, processing it as described in the Materials and Methods section and immunoblotting with an anti-NLGN1 N-terminal antibody. Multiple immunoblots were quantified and the relative amounts of shed NLGN1 fragment are displayed graphically. Results are means ± S.D. (n=3). *, significant at p = 0.05

3.3.5. The effect of exendin-4 and thapsigargin on the expression and proteolytic shedding of over-expressed PrP

Finally, the experiments described in preceding sections were repeated but using SH-SY5Y-PrP stable transfectants. The results (Fig. 3.3.8.) showed that thapsigargin, alone or in the presence of exendin-4 dramatically enhanced levels of PrP in cell lysates. Exendin-4, in contrast had no effect on PrP expression levels.

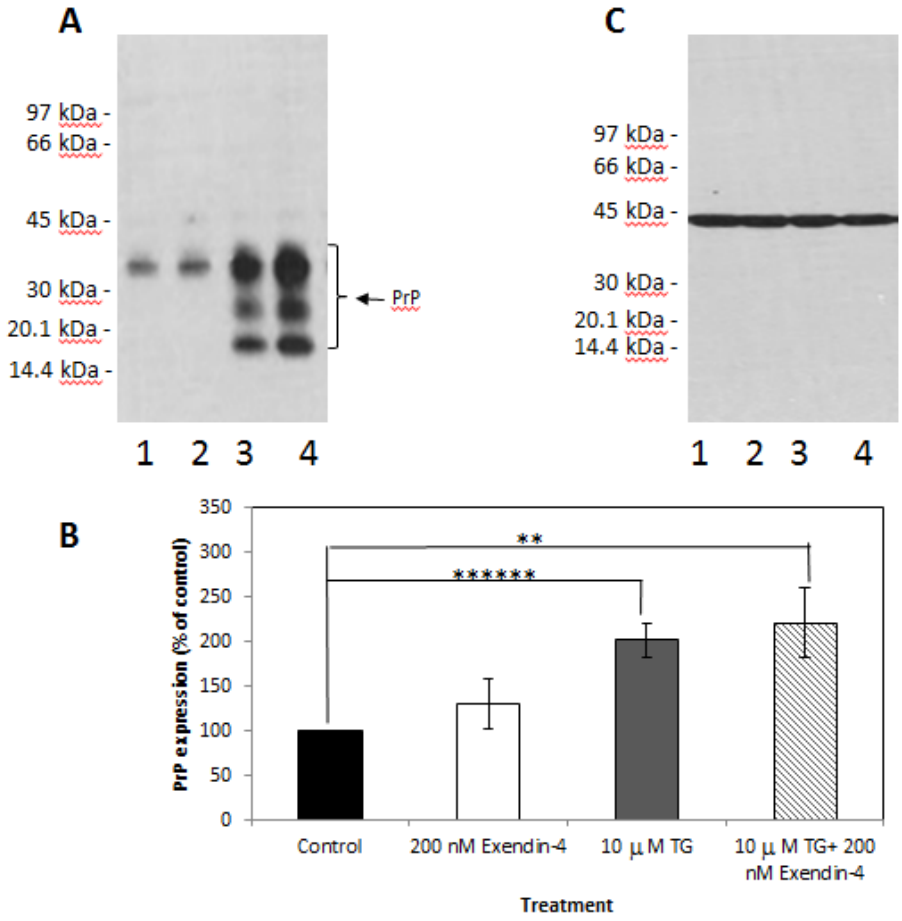

Figure 3.3.8. The effect of exendin-4 and thapsigargin treatments on PrP expression in SH-SY5Y-PrP cells. Cells were grown to confluence in T75 flasks before being pre-treated for 6 h with 200 nM exendin-4 in complete growth medium. Next the cells were washed *in situ* with 10 ml UltraMEM before adding a fresh 10 ml of the same medium containing the relevant treatment (lane 1, control; lane 2, exendin-4; lane 3, thapsigargin (10 μM); lane 4, exendin-4 + thapsigargin (10 μM). The cells were then cultured for a further 17 h before harvesting them, preparing cell lysates and immunoblotting with **A**. SAF32 antibody and **C**. Anti-actin antibody. Representative blots are shown for each experiment which was repeated in triplicate and multiple SAF32 blots were quantified and the relative levels of the protein are shown in **B.** Results are means ± S.D. **, significant at $p = 0.01$; ******, significant at $p = 0.0001$.

Next, the conditioned medium from the same experiments was immunoblotted with the SAF32 antibody in order to detect shed PrP. The results (Fig. 3.3.9.) suggest that thapsigargin enhanced PrP shedding slightly, whilst treatment of cells with exendin-4 enhanced shedding, however none of these increases were significant. Interestingly, the co-treatment of thapsigargin and exendin-4 appeared to have the least shedding function of PrP than either the stressor or the drug alone.

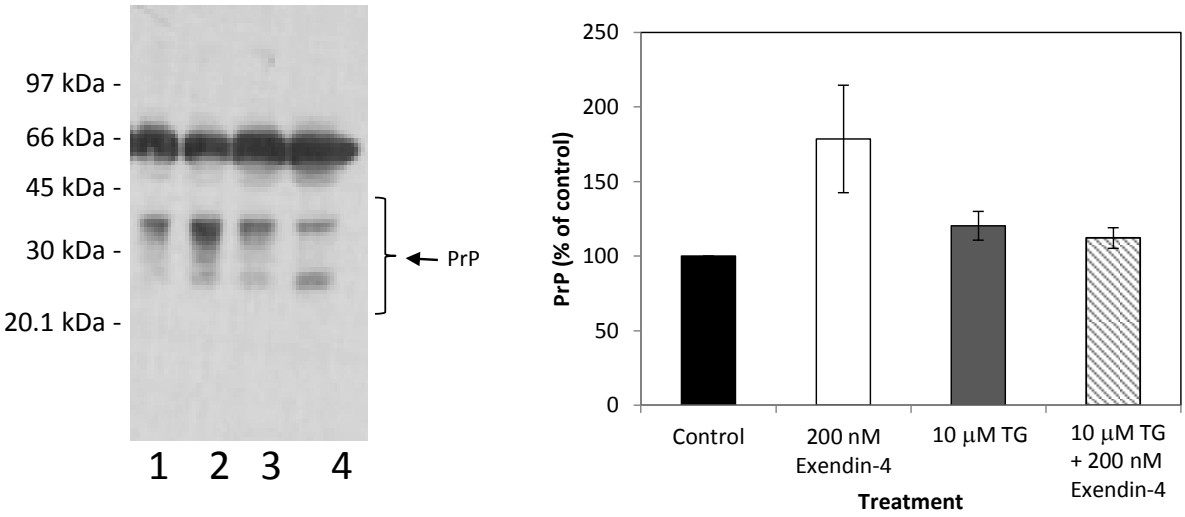

Figure 3.3.9. The effect of exendin-4 and thapsigargin treatments on the levels of soluble PrP in conditioned medium from SH-SY5Y-PrP cells. Cells were grown to confluence in T75 flasks before being pre-treated for 6 h with 200 nM exendin-4 in complete growth medium. Next the cells were washed *in situ* with 10 ml UltraMEM before adding a fresh 10 ml of the same medium containing the relevant treatment (lane 1, control; lane 2, exendin-4; lane 3, thapsigargin (10 μM); lane 4, exendin-4 + thapsigargin (10 μM). The cells were then cultured for a further 17 h before harvesting the conditioned medium, processing it as described in the Materials and Methods section and immunoblotting with the SAF32 antibody. Multiple immunoblots were quantified and the relative amounts of shed PrP fragment are displayed graphically. Results are means ± S.D. (n=2).

3.4. Summary.

The purpose of this study was to investigate the potential protective effects of GLP-1 analogues against various cell stressors and to investigate their effects on the expression and proteolysis of ADAM10 and its substrates.

In terms of cell viability, hydrogen peroxide was found to be cytotoxic in a dose-dependent fashion in the concentration range 0-1000 μM. The protective effect of liraglutide was limited to 200 μM hydrogen peroxide; with higher stressor concentrations there was no protective effect. In contrast, exendin-4 exhibited very /little by the way of protection against hydrogen peroxide-mediated cytotoxicity. Cobalt chloride was also found to be cytotoxic in a dose-dependent fashion in the concentration range of 0-1000 μM. Again, liraglutide proved to have the greater protective effect enhancing cell viability in the presence of 200 μM cobalt chloride at all the concentrations tested (75, 150, 300 and 750 nM). Exendin-4 was not protective against cobalt chloride-induced cytotoxicity. Methylglyoxal was cytotoxic in a dose-dependent fashion over a concentration range of 0-2500 μM. The protective effects of liraglutide were not tested against this stressor, partly due to concerns surrounding the drug's integrity but also because the link between exendin-4 and ADAM10 shifted the focus onto this GLP-1; however exendin-4 was and showed minimal protective effects. Finally, in terms of cell viability, thapsigargin was shown to be cytotoxic in a dose-dependent fashion between 0 and 100 μM. Again, liraglutide was not tested against this stressor but exendin-4 (200 nM) was protective against 10 μM but not 100 μM thapsigargin.

The effects of exendin-4 (200 nM) and/or thapsigargin (10 μM) treatment on the expression and proteolysis of ADAM10 and some of its key substrates were then examined. The proteolytic maturation of over-expressed ADAM10 appeared to be inhibited by thapsigargin, however exendin-4 was unable to modify this effect.

In the case of endogenous APP, thapsigargin decreased expression levels, an effect that was partially restored by exendin-4. Thapsigargin also decreased the generation of both sAPPα and sAPPβ in a manner that was not affected by co-

incubation with thapsigargin and exendin-4. However, the situation was somewhat different when SH-SY5Y-APP_{695} cells were used. Here, thapsigargin appeared to actually enhance APP expression and this corresponded with increased sAPPα shedding upon co-treatment with both the stressor and the drug, but not sAPPβ shedding. No additional significant effects were observed when cells were treated with exendin-4 in the absence or presence of thapsigargin.

In SH-SY5Y-NLGN1 cells, the combination of thapsigargin and exendin-4 significantly decreased the expression of NLGN-1, in comparison to the effects of thapsigargin alone. Similarly, thapsigargin alone did not enhance NLGN-1 shedding but co-treatment with both thapsigargin and exendin-4 did enhance shedding.

Finally, thapsigargin caused a dramatic accumulation of PrP in the lysates of SH-SY5Y-PrP cells. No increase in the shedding of PrP was evident from thapsigargin-treated cells and although there appeared to be PrP shedding caused by treatment with exendin-4 alone, this was not significant.

In summary, the effects of thapsigargin and exendin-4 on the expression of ADAM10 and its substrates were diverse and differed depending on whether proteins were under endogenous promoter control or stably over-expressed. Certainly, whilst thapsigargin alone had dramatic effects on the expression of some proteins there appeared to be no consistent link between exendin-4 treatment and alteration of ADAM10 substrate shedding.

Chapter 4: Discussion.

4.1. Introduction.

Previous research has investigated the potential use of GLP-1 analogues in the treatment of neurodegenerative diseases (Parthsarathy, V. and Hölscher, C., 2013, Chen *et al*., 2012) and some of these compounds are currently in clinical trials because of their apparent neuroprotective properties (NCT01255163- A Pilot Clinical Trial of Exendin-4 in Alzheimer's Disease, NCT03439943 – Study to Evaluate the Effect of Lixisenatide in Patient with Parkinson's Disease) (Clinicaltrials.gov, 2018). In addition, one of these compounds, exendin-4, has been shown to increase levels of the secretase, ADAM10 in the cell membrane fraction and to alter APP processing (Ohtake *et al*., 2014).

The aims of the current project were to determine whether GLP-1 analogues were able to protect human neuroblastoma, SH-SY5Y, cells against toxic insults related to neurodegenerative conditions and to investigate whether any such protective effects were linked to the altered expression/proteolytic maturation of ADAM10 and the proteolysis of some of the enzyme's key substrates.

4.2. The protective effects of GLP-1R agonists against stressors.

4.2.1. Liraglutide

In the current study, liraglutide showed minimal effect against cytotoxicity mediated by hydrogen peroxide or cobalt chloride even when cells were pre-treated with the drug before adding the stressors. Some protection of the drug against hydrogen peroxide and cobalt chloride at a concentration of 200 μM was evident (Fig. 3.1.9, Fig 3.1.13). Liraglutide has previously been shown to enhance neuronal numbers in the brains of $APP_{swe}/PS1_{E9}$ mice (Parthsarathy, V. and Hölscher, C., 2013) although it is notable that, in this study, the drug was administered once daily for 7 days as opposed to the much shorter cell culture treatments in the current study. Shimoda *et al.* (2011) showed that twice daily administration of liraglutide to BKS.Cg-+ $Lepr^{db}$/+ $Lepr^{db}$/Jcl (*db/db*) mice for a period of 2 days increased the expression of gene products involved in cell proliferation and differentiation and in the inhibition

of apoptosis. However, the authors also demonstrated no effect of the drug on gene products associated with the cell response to oxidative or ER stress. The same study showed that an extended course of liraglutide administration (2 weeks) enhanced the expression of these latter gene products again suggesting that prolonged exposure to the drug was necessary to alter cellular response to oxidative insult. In addition, in a study led by Hansen, it was found that liraglutide also showed no neuroprotective effects against varying levels of dopaminergic neuronal loss in the rat 6-OHDA lesion model of Parkinson's Disease (PD) (Hansen et al., 2016).

4.2.2. Exendin-4

Like liraglutide, exendin-4 did not have broad ranging protective effects against the stressors studied in the current report (there was a slight effect against 200 μM hydrogen peroxide and 10 μM thapsigargin (Fig. 1.3.21)). Although these results contradict some literature surrounding the protective effects of exendin-4 (Chen *et al*., 2012, Perry *et al*., 2002), Crutchlow *et al*. (2008) demonstrated that exendin-4 was ineffective in both the promotion of β-cell proliferation and the reduction of β-cell death throughout the first 10 days following a syngeneic islet transplant in mouse recipients (Crutchlow et al., 2008). Similarly, Fan *et al*. (2008) reported that, although exendin-4 improved blood glucose control in young and old C57/DBA mice, this was not correlated with an increase in β-cell proliferation. Additionally, Chen *et al*. (2011) showed that, whilst exendin-4 had a therapeutic effect on lipopolysaccharides (LPS) induced inflammatory response, it did not prevent apoptosis in H9c2 cells.

The current study demonstrates that exendin-4 was protective against low (10 μM) concentrations of the competitive SERCA inhibitor, thapsigargin (Fig. 1.3.21). These data corroborate several other studies (Abe et al., 2013, Younce, Burmeister and Ayala, 2013). Furthermore, Kim *et al.* (2012) showed that exendin-4 inhibited apoptosis in HIT-T15 β-cells treated with glibenclamide. Although glibenclamide is predominantly an inhibitor of ATP-sensitive potassium channels, the authors also reported a reduction in SERCA2 and SERCA3 mRNA following a 48 h cell treatment

with the drug. A similar reduction was observed with TG and, furthermore, SERCA levels along with ER calcium uptake, were replenished when the cells were pre-treated with exendin-4. These observations might explain why, in the current study, exendin-4 had a greater protective effect against TG than other stressors in SH-SY5Y cells.

4.3. The effect of exendin-4 on the expression and proteolysis of ADAM10

In the current study, TG appeared to reduce the serine-protease-mediated removal of the prodomain from ADAM10 resulting in an accumulation of the larger molecular weight proteolytically immature form of the enzyme with a concomitant decrease in the amount of catalytically active proteolytically mature enzyme (Fig. 3.3.1A and B). As TG is known to induce ER stress (Lytton *et al.,* 1991), this might cause retention of ADAM10 in this membrane system and, subsequently, less cleavage of the protein in the Golgi by furin and/or prohormone convertase 7 (PC7) (Lichtenthaler, 2010). Another possible explanation could be that the disrupted calcium homeostasis caused by TG (Lytton *et al.,* 1991) could affect the calcium-dependant activities of the afore mentioned proteases.

The results from this study also demonstrated that in combination with TG, exendin-4 was unable to reverse the detrimental effects of the stressor, displaying no significant effect on the levels of immature ADAM10 and mature ADAM10 (Fig. 3.3.1A and B). This would suggest that the protective effect against TG may not actually result from the increased trafficking and maturation of ADAM10 as first hypothesised, but rather involves another mechanism entirely.

4.4. The effect of exendin-4 on the expression and proteolysis of APP

The results from this study (Fig. 3.3.2A and B) demonstrated that TG significantly decreased the expression of endogenous APP in SH-SY5Y cells, as well as

significantly reduced the shedding of sAPPα (Fig. 3.3.3A). Additionally TG also appeared to reduce the shedding of sAPPβ (Fig. 3.3.3B) although this latter result was somewhat limited by lack of experimental repetition. Jung *et al*. (2015) reported that, in 7w-PSML cells (a Chinese Hamster Ovary cell line, stably transfected to express wild-type APP and mutant presenilin 1), treatment with calcium ionophore A23187 resulted in an intracellular calcium influx not dissimilar to that observed in the case of TG-induced ER stress. The authors also reported concomitantly enhanced degradation of APP by the ubiquitin-proteasome system (UPS) and subsequently impaired generation of both sAPPα, and sAPPβ. It is, therefore, possible in the current study that TG promoted UPS-mediated degradation of APP and a concomitant decrease in shedding of the protein. It was also notable in the current study that exendin-4 partly reversed the TG-mediated reduction in endogenous APP levels (Fig. 3.3.2A and B). This might have resulted from the previously outlined phenomenon whereby exendin-4 might reverse the effect of TG on ER calcium uptake (section 4.2.2).

Interestingly, in the current study, the effects of TG and exendin-4 on APP expression and proteolysis differed substantially between cells expressing endogenous levels of the protein (section 3.3.2.) and stable transfectants over-expressing APP_{695} (section 3.3.3.). In the latter cells TG significantly enhanced APP expression (Fig. 3.3.4. A and B) and in combination with exendin-4, TG also significantly increased shedding of sAPPα. Kögel et al. reported that PC12 cells that over-expressed wild-type APP actually provided protection against neuronal apoptosis induced by two ER stressors; tunicamycin and brefeldin A, in comparison to vector-transfected control cell lines PC12 neo O1 and PC12 neo O3 (Kögel et al., 2003), which could provide a possible explanation for the differences between the endogenous and over-expressed APP.

4.5. The effect of exendin-4 on the expression and proteolysis of NLGN-1

The combination of treatment with exendin-4 and TG showed a significant decline in the expression of NLGN-1 in comparison to TG alone (Fig. 3.3.6). Additionally, the combination of treatment with both the stressor and the drug displayed a significant increase in the shedding of NLGN-1 in comparison to the stressor alone (Fig. 3.3.7). Consequently, the reduction of NLGN-1 after treatment with exendin-4 and TG is accounted for by a significant increase in the shedding of NLGN-1 N-terminal following the same treatment. This indicates that exendin-4 is able to cleave this protein in response to stress, however previous data discussed in this study (section 4.3) implies that this mechanism does not involve the maturation of ADAM-10. Interestingly, Peixoto et al. reported that the proteolytic activity of matrix metalloprotease 9 (MMP9) is involved in the cleavage of NLGN-1 (Peixoto et al., 2012), which could be a possible component in the mechanism enforced by exendin-4. The authors also described that the Ca^{2+}/calmodulin-dependent protein kinase also plays a role in the cleavage of this protein, which is particularly interesting considering the apparent calcium homeostasis restorative effect of exendin-4 reported by studies mentioned in previous sections (4.2.2 and 4.4).

4.6. The effect of exendin-4 on the expression and proteolysis of PrP

The results from this study also showed that thapsigargin-induced ER stress enhanced the levels of cell-associated PrP (Fig. 3.3.8). In this respect, Déry *et al*. (2013) showed that ER stress, as indicated by increased expression of the ER stress marker immunoglobulin heavy chain binding protein BiP, enhanced PrP expression in breast cancer tumours. The authors also demonstrated that PrP expression increased in MCF-7 cells following 18 h treatment with TG. Furthermore, Orsi *et al.* (2006) demonstrated that ER stress, and in particular TG, increased the levels of cytosolic PrP, a form which interestingly retained its N-terminal signal peptide and did not display N-glycans or disulphide bonds, suggesting that it did not enter the ER (Orsi *et*

al. 2006). If the cytosolic PrP in this study is the same or a similar form to that found by Orsi et al, it could imply that TG inhibits the trafficking of the protein. Notably the increase in cell-associated PrP in the current study did not correlate with enhanced shedding of the protein (Fig. 3.3.9). This could be explained by the findings of the afore-mentioned study whereby PrP is retained in intracellular components and, therefore, not present at the cell surface to be subject to shedding.

4.7. Limitations

The main limitation in this study was the uncertainty surrounding the integrity of the Liraglutide. The behaviour of the drug in this study contradicted a large amount of the literature surrounding its neuroprotective effects in cells, and in particular SH-SY5Y cells; however, it was not evident as to why. It was speculated that it could have been associated with the storage conditions or the origin of the drug, as it was not obtained directly from the supplier. To ensure this did not affect the outcomes of this study, Liraglutide was not used in later experiments, with the focus shifting to exendin-4 instead. Exendin-4 was purchased from the supplier and prepared to known concentrations in the laboratory.

4.8. Conclusions

The purpose of this study was to investigate the effects of GLP-1 receptor agonists on the protection of SH-SY5Y cells against various stressors related to neurodegeneration and, in particular, Alzheimer's disease. A further aim was to investigate whether any such neuroprotection might be associated with altered ADAM10 expression/processing and proteolysis of ADAM10 substrates. The results from the study found that neither liraglutide nor exendin-4 had major effects in terms of protecting SH-SY5Y cells against oxidative stress, hypoxia, or endoplasmic reticulum stress. Exendin-4 did show significant protection against thapsigargin-induced ER stress, however it was demonstrated that this drug was unable to reverse

the TG-induced increase of immature ADAM-10, suggesting that its neuroprotective properties were not related to ADAM-10 maturation.

In regards to ADAM10 substrates, exendin-4 was able to increase endogenous APP expression in SH-SY5Y cells in combination with TG, but displayed no significant effect on the shedding of the protein. (Fig. 3.3.2, Fig. 3.3.3). In contrast, in APP over-expressing cells the drug was able to increase the shedding of sAPPα when the cells were co-treated with TG. Similarly, exendin-4 was able to partly restore the shedding of NLGN-1 in TG-treated SH-SY5Y cells (Fig. 3.3.7). However, exendin-4 failed to restore the shedding of PrP in TG-treated cells (Fig. 3.3.9).

In regards to the direction of future research following on from this study, a particularly interesting further experiment would be to examine the mechanism of how Exendin-4 provides protection against TG in neuronal cells and whether calcium, or other metalloproteinases have an involvement. The role of; glial cells, inflammation, insulin, and other factors could also be researched, to investigate whether they have an effect on APP processing, and whether they have any interactions or beneficial relations with GLP-1 receptor agonists. In future studies it might also be pertinent to examine the role of other types of GLP-1 receptor agonists on the proteolysis of APP and NLGN-1 in particular. However to conclude this study, certainly, in terms of APP and NLGN-1 the enhanced shedding of these proteins in TG-treated cells raises the possibility that exendin-4 might have a role to play in the treatment of Alzheimer's disease or schizophrenia.

5.0. Bibliography:

Journals:

Abe, H., Uchida, T., Hara, A., Mizukami, H., Komiya, K., Koike, M., Shigihara, N., Toyofuku, Y., Ogihara, T., Uchiyama, Y., Yagihashi, S., Fujitani, Y. and Watada, H. (2013). Exendin-4 Improves β-Cell Function in Autophagy-Deficient β-Cells. *Endocrinology*, 154(12), pp.4512-4524.

Agersø, H., Jensen, L., Elbrønd, B., Rolan, P. and Zdravkovic, M. (2002). The pharmacokinetics, pharmacodynamics, safety and tolerability of NN2211, a new long-acting GLP-1 derivative, in healthy men. *Diabetologia*, 45(2), pp.195-202.

Allinson, T., Parkin, E., Condon, T., Schwager, S., Sturrock, E., Turner, A. and Hooper, N. (2004). The role of ADAM10 and ADAM17 in the ectodomain shedding of angiotensin converting enzyme and the amyloid precursor protein. *European Journal of Biochemistry*, 271(12), pp.2539-2547.

Alonso, A., Zaidi, T., Grundke-Iqbal, I. and Iqbal, K. (1994). Role of abnormally phosphorylated tau in the breakdown of microtubules in Alzheimer disease. *Proceedings of the National Academy of Sciences*, 91(12), pp.5562-5566.

Angeloni, C., Zambonin, L. and Hrelia, S. (2014). Role of Methylglyoxal in Alzheimer's Disease. *BioMed Research International*, 2014, pp.1-12.

Araç, D., Boucard, A., Özkan, E., Strop, P., Newell, E., Südhof, T. and Brunger, A. (2007). Structures of Neuroligin-1 and the Neuroligin-1/Neurexin-1β Complex Reveal Specific Protein-Protein and Protein-Ca2+ Interactions. *Neuron*, 56(6), pp.992-1003.

Baas, P., Rao, A., Matamoros, A. and Leo, L. (2016). Stability properties of neuronal microtubules. *Cytoskeleton*, 73(9), pp.442-460.

Bali, J., Gheinani, A., Zurbriggen, S. and Rajendran, L. (2012). Role of genes linked to sporadic Alzheimer's disease risk in the production of -amyloid peptides. *Proceedings of the National Academy of Sciences*, 109(38), pp.15307-15311.

Barnham, K., Haeffner, F., Ciccotosto, G., Curtain, C., Tew, D., Mavros, C., Beyreuther, K., Carrington, D., Masters, C., Cherny, R., Cappai, R. and Bush, A. (2004). Tyrosine gated electron transfer is key to the toxic mechanism of Alzheimer's disease -amyloid. *The FASEB Journal*.

Bekris, L., Yu, C., Bird, T. and Tsuang, D. (2010). Review Article: Genetics of Alzheimer Disease. *Journal of Geriatric Psychiatry and Neurology*, 23(4), pp.213-227.

Bowen, D., Smith, C., White, P. and Davison, A. (1976). Neurotransmitter-related enzymes and indices of hypoxia in senile dementia and other abiotrophies. *Brain*, 99(3), pp.459-496.

Bronner, D., Abuaita, B., Chen, X., Fitzgerald, K., Nuñez, G., He, Y., Yin, X. and O'Riordan, M. (2015). Endoplasmic Reticulum Stress Activates the Inflammasome via NLRP3- and Caspase-2-Driven Mitochondrial Damage. *Immunity*, 43(3), pp.451-462.

Caille, I., Allinquant, B., Dupont, E., Bouillot, C., Langer, A., Müller, U. and Prochiantz, A. (2004). Soluble form of amyloid precursor protein regulates proliferation of progenitors in the adult subventricular zone. *Development*, 131(9), pp.2173-2181.

Chadwick, W., Mitchell, N., Martin, B. and Maudsley, S. (2012). Therapeutic Targeting of the Endoplasmic Reticulum in Alzheimers Disease. *Current Alzheimer Research*, 9(1), pp.110-119.

Chasseigneaux, S. and Allinquant, B. (2012). Functions of Aβ, sAPPα and sAPPβ : similarities and differences. *Journal of Neurochemistry*, 120, pp.99-108.

Chasseigneaux, S., Dinc, L., Rose, C., Chabret, C., Coulpier, F., Topilko, P., Mauger, G. and Allinquant, B. (2011). Secreted Amyloid Precursor Protein β and Secreted Amyloid Precursor Protein α Induce Axon Outgrowth In Vitro through Egr1 Signaling Pathway. *PLoS ONE*, 6(1), p.e16301.

Chen, S., Liu, A., An, F., Yao, W. and Gao, X. (2012). Amelioration of neurodegenerative changes in cellular and rat models of diabetes-related Alzheimer's disease by exendin-4. *AGE*, 34(5), pp.1211-1224.

Chen, T., Wo, H., Wu, C., Wang, J., Wang, C., Hsieh, I., Kuo, C. and Liu, C. (2011). Exendin-4 attenuates lipopolysaccharides induced inflammatory response but does not protect H9c2 cells from apoptosis. *Immunopharmacology and Immunotoxicology*, 34(3), pp.484-490.

Cheng, S. and Trombetta, L. (2004). The induction of amyloid precursor protein and α-synuclein in rat hippocampal astrocytes by diethyldithiocarbamate and copper with or without glutathione. *Toxicology Letters*, 146(2), pp.139-149.

Chow, V., Mattson, M., Wong, P. and Gleichmann, M. (2009). An Overview of APP Processing Enzymes and Products. *NeuroMolecular Medicine*, 12(1), pp.1-12.

Chyung, J. and Selkoe, D. (2003). Inhibition of Receptor-mediated Endocytosis Demonstrates Generation of Amyloid β-Protein at the Cell Surface. *Journal of Biological Chemistry*, 278(51), pp.51035-51043.

Coburger, I., Dahms, S., Roeser, D., Gührs, K., Hortschansky, P. and Than, M. (2013). Analysis of the Overall Structure of the Multi-Domain Amyloid Precursor Protein (APP). *PLoS ONE*, 8(12), p.e81926.

Corcoran, C., Mujica-Parodi, L., Yale, S., Leitman, D. and Malaspina, D. (2002). Could Stress Cause Psychosis in Individuals Vulnerable to Schizophrenia?. *CNS Spectrums*, 7(01), pp.33-42.

Crutchlow, M., Yu, M., Bae, Y., Deng, S. and Stoffers, D. (2008). Exendin-4 Does Not Promote Beta-Cell Proliferation or Survival During the Early Post-Islet Transplant Period in Mice. *Transplantation Proceedings*, 40(5), pp.1650-1657.

Daulatzai, M. (2013). Death by a Thousand Cuts in Alzheimer's Disease: Hypoxia—The Prodrome. *Neurotoxicity Research*, 24(2), pp.216-243.

Davis, K., Mohs, R., Marin, D., Purohit, D., Perl, D., Lantz, M., Austin, G. and Haroutunian, V. (1999). Cholinergic Markers in Elderly Patients With Early Signs of Alzheimer Disease. *JAMA*, 281(15), p.1401.

De Strooper, B and Annaert, W (2000). Proteolytic processing and cell biological functions of the amyloid precursor protein. Journal of Cell Science, 113, 1857–1870.

Déry, M., Jodoin, J., Ursini-Siegel, J., Aleynikova, O., Ferrario, C., Hassan, S., Basik, M. and LeBlanc, A. (2013). Endoplasmic reticulum stress induces PRNP prion protein gene expression in breast cancer. *Breast Cancer Research*, 15(2).

Donnelly, D. (2012). The structure and function of the glucagon-like peptide-1 receptor and its ligands. *British Journal of Pharmacology*, 166(1), pp.27-41.

Dorfman, V., Pasquini, L., Riudavets, M., López-Costa, J., Villegas, A., Troncoso, J., Lopera, F., Castaño, E. and Morelli, L. (2010). Differential cerebral deposition of IDE and NEP in sporadic and familial Alzheimer's disease. *Neurobiology of Aging*, 31(10), pp.1743-1757.

Duarte, A., Candeias, E., Correia, S., Santos, R., Carvalho, C., Cardoso, S., Plácido, A., Santos, M., Oliveira, C. and Moreira, P. (2013). Crosstalk between diabetes and brain: Glucagon-like peptide-1 mimetics as a promising therapy against neurodegeneration. *Biochimica et Biophysica Acta (BBA) - Molecular Basis of Disease*, 1832(4), pp.527-541.

El Ayadi, A., Stieren, E., Barral, J. and Boehning, D. (2012). Ubiquilin-1 regulates amyloid precursor protein maturation and degradation by stimulating K63-linked polyubiquitination of lysine 688. *Proceedings of the National Academy of Sciences*, 109(33), pp.13416-13421.

Endres, K. and Reinhardt, S. (2013). ER-stress in Alzheimer's disease: turning the scale? *American Journal of Neurodegenerative Disease*, *2*(4), 247–265.

Fan, R., Kang, Z., He, L., Chan, J. and Xu, G. (2011). Exendin-4 Improves Blood Glucose Control in Both Young and Aging Normal Non-Diabetic Mice, Possible Contribution of Beta Cell Independent Effects. *PLoS ONE*, 6(5), p.e20443.

Francis, P., Palmer, A., Snape, M. and Wilcock, G. (1999). The cholinergic hypothesis of Alzheimer's disease: a review of progress. *Journal of Neurology, Neurosurgery & Psychiatry*, 66(2), pp.137-147.

Fukuda, R., Hirota, K., Fan, F., Jung, Y., Ellis, L. and Semenza, G. (2002). Insulin-like Growth Factor 1 Induces Hypoxia-inducible Factor 1-mediated Vascular Endothelial

Growth Factor Expression, Which is Dependent on MAP Kinase and Phosphatidylinositol 3-Kinase Signaling in Colon Cancer Cells. *Journal of Biological Chemistry*, 277(41), pp.38205-38211.

Gasparini, L., Gouras, G.K., Wang, R., Gross, R.S., Beal, M.F., Greengard, P. and Xu, H. (2001). Stimulation of beta-amyloid precursor protein trafficking by insulin reduces intraneuronal beta-amyloid and requires mitogen-activated protein kinase signalling Journal of Neuroscience, 21, pp. 2561-2570

Goedert, M., Spillantini, M., Jakes, R., Rutherford, D. and Crowther, R. (1989). Multiple isoforms of human microtubule-associated protein tau: sequences and localization in neurofibrillary tangles of Alzheimer's disease. *Neuron*, 3(4), pp.519-526.

Gough, M., Parr-Sturgess, C. and Parkin, E. (2011). Zinc Metalloproteinases and Amyloid Beta-Peptide Metabolism: The Positive Side of Proteolysis in Alzheimer's Disease. *Biochemistry Research International*, 2011, pp.1-13.

GREEN K., SMITH I., LAFERLA F. (2007) Role of Calcium in the Pathogenesis of Alzheimer's Disease and Transgenic Models. In: Carafoli E., Brini M. (eds) Calcium Signalling and Disease. Subcellular Biochemistry, vol 45. Springer, Dordrecht.

Grundke-Iqbal, I., Iqbal, K., Tung, Y., Quinlan, M., Wisniewski, H. and Binder, L. (1986). Abnormal phosphorylation of the microtubule-associated protein tau (tau) in Alzheimer cytoskeletal pathology. *Proceedings of the National Academy of Sciences*, 83(13), pp.4913-4917.

Guglielmotto, M., Giliberto, L., Tamagno, E. and Tabaton, M. (2010). Oxidative stress mediates the pathogenic effect of different Alzheimer's disease risk factors. *Frontiers in Aging Neuroscience*.

Gupta, V. (2013). Glucagon-like peptide-1 analogues: An overview. *Indian Journal of Endocrinology and Metabolism*, 17(3), p.413.

Hampel, H., Shen, Y., Walsh, D., Aisen, P., Shaw, L., Zetterberg, H., Trojanowski, J. and Blennow, K. (2010). Biological markers of amyloid β-related mechanisms in Alzheimer's disease. *Experimental Neurology*, 223(2), pp.334-346.

Hansen, H., Fabricius, K., Barkholt, P., Kongsbak-Wismann, P., Schlumberger, C., Jelsing, J., Terwel, D., Termont, A., Pyke, C., Knudsen, L. and Vrang, N. (2016). Long-Term Treatment with Liraglutide, a Glucagon-Like Peptide-1 (GLP-1) Receptor Agonist, Has No Effect on β-Amyloid Plaque Load in Two Transgenic APP/PS1 Mouse Models of Alzheimer's Disease. *PLOS ONE*, 11(7), p.e0158205.

Hansen, H., Fabricius, K., Barkholt, P., Mikkelsen, J., Jelsing, J., Pyke, C., Knudsen, L. and Vrang, N. (2016). Characterization of liraglutide, a glucagon-like peptide-1 (GLP-1) receptor agonist, in rat partial and full nigral 6-hydroxydopamine lesion models of Parkinson's disease. *Brain Research*, 1646, pp.354-365.

Hayashi, Y., Kashiwagi, K., Ohta, J., Nakajima, M., Kawashima, T. and Yoshikawa, K. (1994). Alzheimer Amyloid Protein Precursor Enhances Proliferation of Neural Stem Cells from Fetal Rat Brain. *Biochemical and Biophysical Research Communications*, 205(1), pp.936-943.

Hernández-Zimbrón, L. and Rivas-Arancibia, S. (2015). Oxidative stress caused by ozone exposure induces β-amyloid 1–42 overproduction and mitochondrial accumulation by activating the amyloidogenic pathway. *Neuroscience*, 304, pp.340-348.

Hölscher, C. (2010). The Role of GLP-1 in Neuronal Activity and Neurodegeneration. *Incretins and Insulin Secretion*, pp.331-354.

Imaizumi, K., Miyoshi, K., Katayama, T., Yoneda, T., Taniguchi, M., Kudo, T. and Tohyama, M. (2001). The unfolded protein response and Alzheimer's disease. *Biochimica et Biophysica Acta (BBA) - Molecular Basis of Disease*, 1536(2-3), pp.85-96.

Jung, E., Hong, H., Kim, C. and Mook-Jung, I. (2015). Acute ER stress regulates amyloid precursor protein processing through ubiquitin-dependent degradation. *Scientific Reports*, 5(1).

Kastin, A. and Akerstrom, V. (2003). Entry of exendin-4 into brain is rapid but may be limited at high doses. *International Journal of Obesity*, 27(3), pp.313-318.

Kao, S., Krichevsky, A., Kosik, K. and Tsai, L. (2003). BACE1 Suppression by RNA Interference in Primary Cortical Neurons. *Journal of Biological Chemistry*, 279(3), pp.1942-1949.

Katayama, T., Imaizumi, K., Manabe, T., Hitomi, J., Kudo, T. and Tohyama, M. (2004). Induction of neuronal death by ER stress in Alzheimer's disease. *Journal of Chemical Neuroanatomy*, 28(1-2), pp.67-78.

Kim, J., Lim, D., Park, H., Moon, C., Choi, K., Lee, S., Baik, H., Park, K. and Kim, B. (2012). Exendin-4 Protects Against Sulfonylurea-Induced β-Cell Apoptosis. *Journal of Pharmacological Sciences*, 118(1), pp.65-74.

Kögel, D., Schomburg, R., Schürmann, T., Reimertz, C., König, H., Poppe, M., Eckert, A., Müller, W. and Prehn, J. (2003). The amyloid precursor protein protects PC12 cells against endoplasmic reticulum stress-induced apoptosis. *Journal of Neurochemistry*, 87(1), pp.248-256.

Kosik, K., Joachim, C. and Selkoe, D. (1986). Microtubule-associated protein tau (tau) is a major antigenic component of paired helical filaments in Alzheimer disease. *Proceedings of the National Academy of Sciences*, 83(11), pp.4044-4048.

Kremerskothen, J., Wendholt, D., Teber, I. and Barnekow, A. (2002). Insulin-induced expression of the activity-regulated cytoskeleton-associated gene (ARC) in human neuroblastoma cells requires p21ras, mitogen-activated protein kinase/extracellular regulated kinase and src tyrosine kinases but is protein kinase C-independent. *Neuroscience Letters*, 321(3), pp.153-156.

Lajtha, A. and Banik, N. (2011). *Role of proteases in the pathophysiology of neurodegenerative diseases*. New York: Springer.

Li, Y., Duffy, K., Ottinger, M., Ray, B., Bailey, J., Holloway, H., Tweedie, D., Perry, T., Mattson, M., Kapogiannis, D., Sambamurti, K., Lahiri, D. and Greig, N. (2010). GLP-1 Receptor Stimulation Reduces Amyloid-β Peptide Accumulation and Cytotoxicity in Cellular and Animal Models of Alzheimer's Disease. *Journal of Alzheimer's Disease*, 19(4), pp.1205-1219.

Li, Y., Perry, T., Kindy, M., Harvey, B., Tweedie, D., Holloway, H., Powers, K., Shen, H., Egan, J., Sambamurti, K., Brossi, A., Lahiri, D., Mattson, M., Hoffer, B., Wang, Y. and Greig, N. (2009). GLP-1 receptor stimulation preserves primary cortical and dopaminergic neurons in cellular and rodent models of stroke and Parkinsonism. *Proceedings of the National Academy of Sciences*, 106(4), pp.1285-1290.

Li, Z., Zhang, W. and Sima, A. (2007). Alzheimer-Like Changes in Rat Models of Spontaneous Diabetes. *Diabetes*, 56(7), pp.1817-1824.

Lichtenthaler, S. (2010). Alpha-secretase in Alzheimer's disease: molecular identity, regulation and therapeutic potential. *Journal of Neurochemistry*, 116(1), pp.10-21.

Lisé, M. and El-Husseini, A. (2006). The neuroligin and neurexin families: from structure to function at the synapse. *Cellular and Molecular Life Sciences*, 63(16), pp.1833-1849.

Lytton, J., Westlin, M. and Hanley, M. R. (1991). Thapsigargin inhibits the sarcoplasmic or endoplasmic reticulum Ca-ATPase family of calcium pumps. Journal of Biological Chemistry, 266(26), pp.17067-17071.

Mayeda, E., Glymour, M., Quesenberry, C. and Whitmer, R. (2016). Inequalities in dementia incidence between six racial and ethnic groups over 14 years. *Alzheimer's & Dementia*, 12(3), pp.216-224.

McClean, P., Parthsarathy, V., Faivre, E. and Holscher, C. (2011). The Diabetes Drug Liraglutide Prevents Degenerative Processes in a Mouse Model of Alzheimer's Disease. *Journal of Neuroscience*, 31(17), pp.6587-6594.

Mohandas, E., Rajmohan, V. and Raghunath, B. (2009). Neurobiology ofAlzheimer's disease. *Indian Journal of Psychiatry*, 51(1), p.55.

Murray, F., Landsberg, J., Williams, R., Esiri, M. and Watt, F. (2007). Elemental Analysis of Neurofibrillary Tangles in Alzheimer's Disease Using Proton-Induced X-ray Analysis. *Novartis Foundation Symposia*, pp.201-216.

Nalivaevaa, N., Fisk, L., Kochkina, E., Plesneva, S., Zhuravin, I., Babusikova, E., Dobrota, D. and Turner, A. (2004). Effect of Hypoxia/Ischemia and Hypoxic Preconditioning/Reperfusion on Expression of Some Amyloid-Degrading Enzymes. *Annals of the New York Academy of Sciences*, 1035(1), pp.21-33.

Nalivaeva, N. and Turner, A. (2013). The amyloid precursor protein: A biochemical enigma in brain development, function and disease. *FEBS Letters*, 587(13), pp.2046-2054.

Noy, P., Yang, J., Reyat, J., Matthews, A., Charlton, A., Furmston, J., Rogers, D., Rainger, G. and Tomlinson, M. (2015). TspanC8 Tetraspanins and A Disintegrin and Metalloprotease 10 (ADAM10) Interact via Their Extracellular Regions. *Journal of Biological Chemistry*, 291(7), pp.3145-3157.

Ohtake, N., Saito, M., Eto, M. and Seki, K. (2014). Exendin-4 promotes the membrane trafficking of the AMPA receptor GluR1 subunit and ADAM10 in the mouse neocortex. *Regulatory Peptides*, 190-191, pp.1-11.

Orsi, A., Fioriti, L., Chiesa, R. and Sitia, R. (2006). Conditions of Endoplasmic Reticulum Stress Favor the Accumulation of Cytosolic Prion Protein. *Journal of Biological Chemistry*, 281(41), pp.30431-30438.

Palsamy, P., Bidasee, K., Ayaki, M., Augusteyn, R., Chan, J. and Shinohara, T. (2014). Methylglyoxal induces endoplasmic reticulum stress and DNA demethylation in the Keap1 promoter of human lens epithelial cells and age-related cataracts. *Free Radical Biology and Medicine*, 72, pp.134-148.

Parkin, E. and Harris, B. (2009). A disintegrin and metalloproteinase (ADAM)-mediated ectodomain shedding of ADAM10. *Journal of Neurochemistry*, 108(6), pp.1464-1479.

Parkin, E., Watt, N., Hussain, I., Eckman, E., Eckman, C., Manson, J., Baybutt, H., Turner, A. and Hooper, N. (2007). Cellular prion protein regulates beta-secretase cleavage of the Alzheimer's amyloid precursor protein. *Proceedings of the National Academy of Sciences*, 104(26), pp.11062-11067.

Parkin, E., Watt, N., Turner, A. and Hooper, N. (2004). Dual Mechanisms for Shedding of the Cellular Prion Protein. *Journal of Biological Chemistry*, 279(12), pp.11170-11178.

Parthsarathy, V. and Hölscher, C. (2013). Chronic Treatment with the GLP1 Analogue Liraglutide Increases Cell Proliferation and Differentiation into Neurons in an AD Mouse Model. *PLoS ONE*, 8(3), p.e58784.

Peila, R., Rodriguez, B. and Launer, L. (2002). Type 2 Diabetes, APOE Gene, and the Risk for Dementia and Related Pathologies: The Honolulu-Asia Aging Study. *Diabetes*, 51(4), pp.1256-1262.

Perry, E. K., Curtis, M., Dick, D. J., Candy, J. M., Atack, J. R., Bloxham, C. A., … Perry, R. H. (1985). Cholinergic correlates of cognitive impairment in Parkinson's disease: comparisons with Alzheimer's disease. *Journal of Neurology, Neurosurgery, and Psychiatry*, *48*(5), 413–421.

Perry, T., Haughey, N., Mattson, M., Egan, J. and Greig, N. (2002). Protection and Reversal of Excitotoxic Neuronal Damage by Glucagon-Like Peptide-1 and Exendin-4. *Journal of Pharmacology and Experimental Therapeutics*, 302(3), pp.881-888.

Peixoto, R., Kunz, P., Kwon, H., Mabb, A., Sabatini, B., Philpot, B. and Ehlers, M. (2012). Transsynaptic Signaling by Activity-Dependent Cleavage of Neuroligin-1. *Neuron*, 76(3), p.667.

Plácido, A., Pereira, C., Duarte, A., Candeias, E., Correia, S., Santos, R., Carvalho, C., Cardoso, S., Oliveira, C. and Moreira, P. (2014). The role of endoplasmic reticulum in amyloid preclichtursor protein processing and trafficking: Implications for Alzheimer's disease. *Biochimica et Biophysica Acta (BBA) - Molecular Basis of Disease*, 1842(9), pp.1444-1453.

Postina, R., Schroeder, A., Dewachter, I., Bohl, J., Schmitt, U., Kojro, E., Prinzen, C., Endres, K., Hiemke, C., Blessing, M., Flamez, P., Dequenne, A., Godaux, E., van Leuven, F. and Fahrenholz, F. (2004). A disintegrin-metalloproteinase prevents amyloid plaque formation and hippocampal defects in an Alzheimer disease mouse model. *Journal of Clinical Investigation*, 113(10), pp.1456-1464.

Prince, M., Wimo, A., Guerchet, M., Ali, G. and Wu, Y. (2015). *World Alzheimer Report 2015 The Global Impact of Dementia An analysis of prevalence, incidence, cost and trends*. London: Alzheimer's Disease International.

Pruessmeyer, J. and Ludwig, A. (2009). The good, the bad and the ugly substrates for ADAM10 and ADAM17 in brain pathology, inflammation and cancer. *Seminars in Cell & Developmental Biology*, 20(2), pp.164-174.

Prusiner, S., McKinley, M., Bowman, K., Bolton, D., Bendheim, P., Groth, D. and Glenner, G. (1983). Scrapie prions aggregate to form amyloid-like birefringent rods. *Cell*, 35(2), pp.349-358.

Qiu, W. and Folstein, M. (2006). Insulin, insulin-degrading enzyme and amyloid-β peptide in Alzheimer's disease: review and hypothesis. *Neurobiology of Aging*, 27(2), pp.190-198.

Reinhard, C., Hébert, S. and De Strooper, B. (2005). The amyloid-β precursor protein: integrating structure with biological function. *The EMBO Journal*, 24(23), pp.3996-4006.

Riesner, D. (2003). Biochemistry and structure of PrPC and PrPSc. *British Medical Bulletin*, 66(1), pp.21-33.

Ring, S., Weyer, S., Kilian, S., Waldron, E., Pietrzik, C., Filippov, M., Herms, J., Buchholz, C., Eckman, C., Korte, M., Wolfer, D. and Muller, U. (2007). The Secreted -Amyloid Precursor Protein Ectodomain APPs Is Sufficient to Rescue the Anatomical, Behavioral, and Electrophysiological Abnormalities of APP-Deficient Mice. *Journal of Neuroscience*, 27(29), pp.7817-7826.

Saftig, P. and Reiss, K. (2011). The "A Disintegrin And Metalloproteases" ADAM10 and ADAM17: Novel drug targets with therapeutic potential?. *European Journal of Cell Biology*, 90(6-7), pp.527-535.

Salminen, A., Kaarniranta, K., Kauppinen, A., Ojala, J., Haapasalo, A., Soininen, H. and Hiltunen, M. (2013). Impaired autophagy and APP processing in Alzheimer's disease:

The potential role of Beclin 1 interactome. *Progress in Neurobiology*, 106-107, pp.33-54.

Salminen, A., Kauppinen, A., Suuronen, T., Kaarniranta, K. and Ojala, J. (2009). ER stress in Alzheimer's disease: a novel neuronal trigger for inflammation and Alzheimer's pathology. *Journal of Neuroinflammation*, 6(1), p.41.

Schedin-Weiss, S., Winblad, B. and Tjernberg, L. (2013). The role of protein glycosylation in Alzheimer disease. *FEBS Journal*, 281(1), pp.46-62.

Schwartz, M., Figlewicz, D., Kahn, S., Baskin, D., Greenwood, M. and Porte, D. (1990). Insulin binding to brain capillaries is reduced in genetically obese, hyperinsulinemic Zucker rats. *Peptides*, 11(3), pp.467-472.

Shimoda, M., Kanda, Y., Hamamoto, S., Tawaramoto, K., Hashiramoto, M., Matsuki, M. and Kaku, K. (2011). The human glucagon-like peptide-1 analogue liraglutide preserves pancreatic beta cells via regulation of cell kinetics and suppression of oxidative and endoplasmic reticulum stress in a mouse model of diabetes. *Diabetologia*, 54(5), pp.1098-1108.

Skovronsky, D., Moore, D., Milla, M., Doms, R. and Lee, V. (2000). Protein Kinase C-dependent α-Secretase Competes with β-Secretase for Cleavage of Amyloid-β Precursor Protein in the Trans-Golgi Network. *Journal of Biological Chemistry*, 275(4), pp.2568-2575.

Smith, D., Roberts, J., Gage, F. and Tuszynski, M. (1999). Age-associated neuronal atrophy occurs in the primate brain and is reversible by growth factor gene therapy. *Proceedings of the National Academy of Sciences*, 96(19), pp.10893-10898.

Smith, M., Rottkamp, C., Nunomura, A., Raina, A. and Perry, G. (2000). Oxidative stress in Alzheimer's disease. *Biochimica et Biophysica Acta (BBA) - Molecular Basis of Disease*, 1502(1), pp.139-144.

Song, J., Ichtchenko, K., Sudhof, T. and Brose, N. (1999). Neuroligin 1 is a postsynaptic cell-adhesion molecule of excitatory synapses. *Proceedings of the National Academy of Sciences*, 96(3), pp.1100-1105.

Stone, J. (2011). Glutamatergic antipsychotic drugs: a new dawn in the treatment of schizophrenia?. *Therapeutic Advances in Psychopharmacology*, 1(1), pp.5-18.

Stoothoff, W. and Johnson, G. (2005). Tau phosphorylation: physiological and pathological consequences. *Biochimica et Biophysica Acta (BBA) - Molecular Basis of Disease*, 1739(2-3), pp.280-297.

Sun, X., He, G., Qing, H., Zhou, W., Dobie, F., Cai, F., Staufenbiel, M., Huang, L. and Song, W. (2006). Hypoxia facilitates Alzheimer's disease pathogenesis by up-regulating BACE1 gene expression. *Proceedings of the National Academy of Sciences*, 103(49), pp.18727-18732.

Suzuki, K., Hayashi, Y., Nakahara, S., Kumazaki, H., Prox, J., Horiuchi, K., Zeng, M., Tanimura, S., Nishiyama, Y., Osawa, S., Sehara-Fujisawa, A., Saftig, P., Yokoshima, S., Fukuyama, T., Matsuki, N., Koyama, R., Tomita, T. and Iwatsubo, T. (2012). Activity-Dependent Proteolytic Cleavage of Neuroligin-1. *Neuron*, 76(2), pp.410-422.

Tamagno, E., Guglielmotto, M., Aragno, M., Borghi, R., Autelli, R., Giliberto, L., Muraca, G., Danni, O., Zhu, X., Smith, M., Perry, G., Jo, D., Mattson, M. and Tabaton, M. (2008). Oxidative stress activates a positive feedback between the γ- and β-secretase cleavages of the β-amyloid precursor protein. *Journal of Neurochemistry*, 0(0), p.071115163316002

Tanaka, M., Sawada, M., Yoshida, S., Hanaoka, F. and Marunouchi, T. (1995). Insulin prevents apoptosis of external granular layer neurons in rat cerebellar slice cultures. *Neuroscience Letters*, 199(1), pp.37-40.

Taylor, D., Parkin, E., Cocklin, S., Ault, J., Ashcroft, A., Turner, A. and Hooper, N. (2009). Role of ADAMs in the Ectodomain Shedding and Conformational Conversion of the Prion Protein. *Journal of Biological Chemistry*, 284(34), pp.22590-22600.

Théberge, J., Bartha, R., Drost, D., Menon, R., Malla, A., Takhar, J., Neufeld, R., Rogers, J., Pavlosky, W., Schaefer, B., Densmore, M., Al-Semaan, Y. and Williamson, P. (2002). Glutamate and Glutamine Measured With 4.0 T Proton MRS in Never-Treated Patients With Schizophrenia and Healthy Volunteers. *American Journal of Psychiatry*, 159(11), pp.1944-1946.

Thinakaran, G. and Koo, E. (2008). Amyloid Precursor Protein Trafficking, Processing, and Function. *Journal of Biological Chemistry*, 283(44), pp.29615-29619.

Tong, Y., Zhou, W., Fung, V., Christensen, M., Qing, H., Sun, X. and Song, W. (2004). Oxidative stress potentiates BACE1 gene expression and A? generation. *Journal of Neural Transmission*, 112(3), pp.455-469.

Tousseyn, T., Jorissen, E., Reiss, K. and Hartmann, D. (2006). (Make) Stick and cut loose—Disintegrin metalloproteases in development and disease. *Birth Defects Research Part C: Embryo Today: Reviews*, 78(1), pp.24-46.

Tousseyn, T., Thathiah, A., Jorissen, E., Raemaekers, T., Konietzko, U., Reiss, K., Maes, E., Snellinx, A., Serneels, L., Nyabi, O., Annaert, W., Saftig, P., Hartmann, D. and De Strooper, B. (2009). ADAM10, the Rate-limiting Protease of Regulated Intramembrane Proteolysis of Notch and Other Proteins, Is Processed by ADAMS-9, ADAMS-15, and the γ-Secretase. *Journal of Biological Chemistry*, 284(17), pp.11738-11747.

Venugopal, C., Demos, C., Jagannatha Rao, K., Pappolla, M. and Sambamurti, K. (2008). Beta-Secretase: Structure, Function, and Evolution. *CNS & Neurological Disorders - Drug Targets*, 7(3), pp.278-294.

Vincent, A., Mclean, L., Backus, C. and Feldman, E. (2005). Short-term hyperglycemia produces oxidative damage and apoptosis in neurons. *The FASEB Journal*, 19(6), pp.638-640.

WARTENBERG, M., LING, F., MÜSCHEN, M., KLEIN, F., ACKER, H., GASSMANN, M., PETRAT, K., PÜTZ, V., HESCHELER, J. and SAUER, H. (2003). Regulation of the multidrug resistance transporter P-glycoprotein in multicellular tumor spheroids by hypoxia-inducible factor (HIF-1) and reactive oxygen species. *The FASEB Journal*, 17(3), pp.503-505.

Webster, N., Green, K., Peers, C. and Vaughan, P. (2002). Altered processing of amyloid precursor protein in the human neuroblastoma SH-SY5Y by chronic hypoxia. *Journal of Neurochemistry*, 83(6), pp.1262-1271.

Westergard, L., Christensen, H. and Harris, D. (2007). The cellular prion protein (PrPC): Its physiological function and role in disease. *Biochimica et Biophysica Acta (BBA) - Molecular Basis of Disease*, 1772(6), pp.629-644.

Yiannopoulou, K. and Papageorgiou, S. (2012). Current and future treatments for Alzheimer's disease. *Therapeutic Advances in Neurological Disorders*, 6(1), pp.19-33.

Younce, C., Burmeister, M. and Ayala, J. (2013). Exendin-4 attenuates high glucose-induced cardiomyocyte apoptosis via inhibition of endoplasmic reticulum stress and activation of SERCA2a. *American Journal of Physiology-Cell Physiology*, 304(6), pp.C508-C518.

Yoshikai, S., Sasaki, H., Doh-ura, K., Furuya, H. and Sakaki, Y. (1991). Genomic organization of the human-amyloid beta-protein precursor gene. *Gene*, 102(2), pp.291-292.

Zhang, Z., Yu, H., Jiang, S., Liao, J., Lu, T., Wang, L., Zhang, D. and Yue, W. (2015). Evidence for Association of Cell Adhesion Molecules Pathway and NLGN1 Polymorphisms with Schizophrenia in Chinese Han Population. *PLOS ONE*, 10(12), p.e0144719.

Zheng, H. and Koo, E. (2011). Biology and pathophysiology of the amyloid precursor protein. *Molecular Neurodegeneration*, 6(1), p.27.

Books:

Lauffer, R. (1992). *Iron and human disease*. Boca Raton, Flo.: CRC Press, p.26.

Weidner, N., Cote, R., Suster, S. and Weiss, L. (2009). *Modern surgical pathology*. Philadelphia, PA: Saunders/Elsevier.

Reports:

Alzheimer's Association (2016). *2016 Alzheimer's Disease Facts And Figures*. Alzheimer's Association.

Prince, M., Wimo, A., Guerchet, M., Ali, G. and Wu, Y. (2015). *World Alzheimer Report 2015 The Global Impact of Dementia An analysis of prevalence, incidence, cost and trends*. London: Alzheimer's Disease International.

Websites:

Alzheimer's Association. (2017). *Current Treatments, Alzheimer's & Dementia | Research Center | Alzheimer's Association*. [online] Available at: http://www.alz.org/research/science/alzheimers_disease_treatments.asp [Accessed 6 Aug. 2017].

Clinicaltrials.gov. (2018). *Evaluating Liraglutide in Alzheimer's Disease - Full Text View - ClinicalTrials.gov*. [online] Available at: https://clinicaltrials.gov/ct2/show/NCT01843075?term=liraglutide&cond=Alzheimer+Disease&rank=1 [Accessed 25 Jan. 2018].

Diabetes.co.uk. (2017). *Incretin Mimetics (GLP-1 Agonists) - Suitability, Benefits & Side Effects*. [online] Available at: http://www.diabetes.co.uk/diabetes-medication/incretin-mimetics.html [Accessed 16 Sep. 2017].

HHMI.org. (2017). *Structure of Synaptic Connectors Solved*. [online] Available at: http://www.hhmi.org/news/structure-synaptic-connectors-solved [Accessed 1 Sep. 2017].

nhs.uk. (2018). *About dementia*. [online] Available at: https://www.nhs.uk/conditions/dementia/about/?tabname=symptoms-and-diagnosis.

Omim.org. (2017). *OMIM Entry - * 104760 - AMYLOID BETA A4 PRECURSOR PROTEIN; APP*. [online] Available at: https://www.omim.org/entry/104760?search=human%20app%20gene&highlight=app%20gene%20human [Accessed 6 Aug. 2017].

Vce.bioninja.com.au. (2017). *Pathogens | Brent Cornell*. [online] Available at: http://www.vce.bioninja.com.au/aos-2-detecting-and-respond/defence-against-disease/pathogens.html [Accessed 27 Aug. 2017].

World Health Organization. (2017). *Dementia*. [online] Available at: http://www.who.int/mediacentre/factsheets/fs362/en/ [Accessed 30 May 2017].

World Health Organization. (2017). *The top 10 causes of death*. [online] Available at: http://www.who.int/mediacentre/factsheets/fs310/en/index1.html [Accessed 16 May 2017].

Www-ssrl.slac.stanford.edu. (2018). [online] Available at: https://www-ssrl.slac.stanford.edu/research/highlights_archive/neuroligin_hires.pdf [Accessed 5 Mar. 2018].